DOCTORAL THESIS

THERMAL STUDY OF THE GLASSY STATES IN SIMPLE HYDROCARBONS

by

Kiyoshi Takeda

Department of Chemistry

Faculty of Science

Osaka University

1991

Doctoral Committee

Professor Hiroshi Suga

Professor Fumikazu Kanamaru

Professor Michio Sorai

ACKNOWLEDGMENTS

I would like to express my sincere thanks to Professor Hiroshi Suga for his advice and encouragement throughout the course of this work as well as illuminating assistance in refining the expression of this thesis. I am also grateful to Associate Professor Takasuke Matsuo for his useful advice and discussions. I am deeply indebted to Associate Professor Masaharu Oguni of Tokyo Institute of Technology for his collaboration and convincing directions of the experiment. I was not a little affected by his enthusiasm on the scientific investigation. I wish to express my great thanks to Dr. Osamu Yamamuro for his cooperation in the experiment, very useful discussions and much pain taken in the refinement of this thesis. I also would like to thank Professor Michio Sorai very much for his fruitful discussions.

Thanks are extended to Mr. Katsumi Mishima, Mr. Shozo Katayama, Mr. Masayoshi Nishiyama, Mr. Masahiro Shiomi and other staffs of the Central Workshop of Osaka University, for their great help in the construction and maintenance of the apparatus. I thank Mr. Osamu Asai and Mr. Kiyotsugu Kabu of the Low Temperature Center of Osaka University for their supply of cryogenic liquids on demand. I gratefully acknowledges to the fellows of Suga's Laboratory and the Microcalorimetery Research Center for their heartwarming encouragements and assistance.

Finally, most thanks are expressed to my parents.

ABSTRACT

Calorimetric and thermoanalytical studies of the glass transition and related structural relaxation were carried out by use of simple straight-chain hydrocarbons as samples. The results are summarized as follows.

A new apparatus of the differential thermal analysis (DTA) for vapor-deposited samples was constructed in order to measure the simple molecular substances which readily crystallize on liquid quenching. This apparatus made it possible to deposit sample vapor at liquid helium temperature (4.2 K). It possesses a high performance to detect small thermal anomaly such as glass transitions by using eight pairs of (Au+0.7%Fe)-(Chromel-P) thermopile connected in series.

DTA measurements of the vapor-deposited samples were carried out for some *n*-alkanes and 1-alkenes of carbon number 2 to 6. A glass transition was observed for propane and for all of 1-alkene studied here. For propane and 1-pentene, glass transitions were found out for the first time at 45.5 K and 71.7 K, respectively. Vapor-deposited ethene and ethane crystallized during the deposition at 4.2 K. For all *n*-alkanes but ethane and propane, the glass transition was not observed ahead of the crystallization. A study of the binary system of (*n*-butane)$_x$(1-butene)$_{1-x}$ elucidated that the crystallization took place below T_g in pure *n*-butane. It is supposed that the crystallization took place below T_g also in other *n*-alkanes for which the glass transition was not observed. Thus it is clear that the crystallization rates of *n*-alkanes are much faster than those of 1-alkenes. A possible

reason was discussed from the viewpoint of the symmetry of the molecular structure. By comparing the temperatures of the previous radiothermoluminescence (RTL) peaks with those of the present thermal anomalies, the RTL peaks in the vapor-deposited hydrocarbons were concluded not to be due to the glass transition but to the phase transition.

The glass transitions in binary systems of propene-propane, propene-1-butene, propene-1-pentene and 1-butene-1-pentene were studied by means of DTA techniques. The composition dependence of T_g was analyzed in terms of the entropy theory (GRGR theory) based on the regular solution model. The theoretical prediction could not fully reproduce the experimental results other than 1-butene-1-pentene system. This disagreement is considered to be due to slight deviation of the real system from the model. The excess configurational entropy S_c^E of the real system was evaluated inversely from the GRGR theory. For propene-propane system, an extremely large S_c^E (= 2.2 J K^{-1} mol^{-1}) was obtained at medium composition range, whereas those of propene-1-butene and 1-butene-1-pentene were nearly zero. Possible reason of the large S_c^E was discussed.

Enthalpy relaxation process of the vapor-quenched (VQ) and the liquid-quenched (LQ) glasses was studied by using an adiabatic calorimeter. The enthalpy relaxation was observed far below T_g for the VQ glass of 1-pentene. Such a low-temperature enthalpy relaxation was confirmed to be a common feature of the glass formed by an extremely high cooling rate. The enthalpy relaxation processes were pursued in the same temperature region (around 69 K). The enthalpy relaxation function ϕ was fitted to

the Kohlrausch-Williams-Watts (KWW) function. The parameter β of the KWW function is determined to be 0.64 and 0.45 for the VQ and LQ samples, respectively. The deviation of β from unity indicates clearly the non-exponential nature of the structural relaxation process. Plot of $\log(\tau_{eff})$ against $(S_c T)^{-1}$ (Adam-Gibbs plot) showed a good linearity for every relaxation process. The successful application of the AG equation clarified the importance of configurational entropy for the structural relaxation processes. The AG plot for the VQ glass showed smaller slope than that of the LQ glass. This difference in the slope was qualitatively explained based on possible dissimilar microscopic structures of the glass.

Thermodynamic study of 1-butene has revealed the existence of a metastable crystalline phase for the first time. The enthalpy and entropy of fusion of the fully stabilized crystalline sample were 3.959 kJ mol^{-1} and 45.09 J K^{-1} mol^{-1}, respectively. Standard thermodynamic functions were calculated by using the new heat capacity data of the stable crystal. Endothermic and exothermic enthalpy relaxation processes were pursued at the same temperature. By fitting the relaxation functions to the KWW function, the non-exponential nature of both processes was found out (β = 0.56 and 0.84 for the exothermic and endothermic processes, respectively). The slope of the AG plot for the exothermic process was positive, whereas that of endothermic process was negative. The negative slope is not acceptable from the physical meanings of the parameters $\Delta\mu$ and s_c^* of the Adam-Gibbs equation. Some factors other that the configurational entropy might be important in the structural relaxation of liquid near the

equilibrium state.

CONTENTS

Chapter 1

GENERAL INTRODUCTION

1-1 Historical Background

Glass is one of the most familiar materials in our life. Mankind has been using it since the era of ancient Egypt as practical materials of tableware, windows, jewels, *etc.* Many of scientific instruments including chemical appliance, Dewar flask and optical glass were also made of glass. Characteristic properties of glass such as its transparency, poor thermal conductivity, and amorphism are effectively utilized for various purposes.

In spite of its familiarity, however, the nature of the glass had not been investigated until the middle of 19th century, when a drastic heat capacity jump in undercooled selenium was first discovered by Regnault. This phenomenon was referred to as glass transition later. Thereafter, investigations on the nature of the glass started at the beginning of this century, as the X-ray diffraction technique was developed. The structural analyses of glasses revealed a very important feature that the glass does not have a structure of the crystal but one of the liquid. This is apparently contrary to the solid-like mechanical property of the glass. Zachariasen suggested a famous structural model for covalent systems known as the random network structure [1,2], which involves ingeniously the directional properties of the covalent bond. This model is still available with slight modifi-

cation for most of the covalent systems. However, the model cannot be applied to the metallic and van der Waals systems because of the non-directional nature of the intermolecular binding forces in these systems. A well-recognized structural model for the metallic and molecular glasses is the dense random packing model of hard spheres proposed by Bernal [3,4]. He classified local structure of the glass into five types by considering the manner by which the hard spheres are packed randomly.

Earnest thermodynamic investigations on the glass and glass transition were also started in the first half of this century. Gibson *et al.* [5] found calorimetrically the existence of a finite amount of entropy at zero kelvin that could not been removed in the glassy glycerol. This phenomenon could not be understood in the framework of classical thermodynamics. Thus the discovery of the existence of residual entropy was the first experimental access to the non-equilibrium character of the glass. Most investigations on condensed systems in those days were made in relation to the confirmation of the third law of thermodynamics.

The development of polymer science and technology in early 1950's accelerated the research activity in glass science. There was a heated discussion as to whether the glass transition is the second order transition in the truly thermodynamic meaning. After all, scientists have recognized firmly that the glass transition is a time-dependent phenomenon. Volume or enthalpy recovery phenomenon was regarded as a relaxation process from a non-equilibrium to the equilibrium state. Dynamical processes of

many synthetic polymers were investigated through mechanical and dielectric relaxations as responses to applied external fields that change sinusoidally with time. The polymer dynamics is very complicated because of the superposition of many intramolecular modes of the polymer chain, and the resultant broad distribution of relaxation times. Nevertheless, some theories of the polymer dynamics in the liquid phase were also developed, *e.g.* ones developed by Rouse *et al.* [6] and Doi and Edwards [7]. They succeeded to some extent in describing semi-quantitatively such complicated dynamics.

Several theories describing the glass transition were also developed. The free volume theory and the entropy theory were the most significant ones. These theories are important because they paid attention to the thermodynamic properties of the glasses. The non-equilibrium state can be defined only in terms of thermodynamics. A brief description of these two concepts will be made in the next section.

Current activity in the research of amorphous state was directed to the metallic glasses. This is relatively new trend because the formation of metallic glasses requires extraordinarily high quenching rate with special techniques. Metallic glasses have been developed mainly for the industrial products of semiconducting and magnetic materials. Therefore, the structural relaxation and crystallization phenomena were very important subjects from the viewpoint of quality control of the products.

In the last decade, non-linear nature governing the dynamics of glasses and undercooled liquids has become a main interest in the field of amorphous physics. Many theories on this subject

have been proposed by Ngai *et al* [8], Palmer *et al* [9], Goetze *et al* [10], Loucheusser *et al* [11], *etc.* In the present stage, however, no theory can give a satisfactory description about the glass transition and dynamics of viscous liquids.

1-2 Formation of Glassy State

In order to clarify the concept of the glass formation, the entropy of a system as a function of temperature is schematically illustrated in Fig. 1-1. The volume vs. temperature diagram is also available for this purpose. As shown in Fig. 1-1, the entropy of the equilibrium liquid decreases on cooling, and its gradient becomes smaller at a certain temperature. This is the glass transition temperature T_g, below which the sample is in glassy state. The entropy of liquid consists of vibrational and configurational parts, while that of crystal consist of only the vibrational part. The departure of entropy from the equilibrium line is caused by freezing of the configurational mode, and occurs at T_g at which the configurational motion becomes slower than the cooling rate. The temperature dependence of the entropy of the glassy state is similar to that of crystal, though, to be exact, a slight difference exists between them. This means that the configurational part is frozen in at the glass transition temperature. The frozen configurational entropy of liquid, therefore, remains down to zero kelvin, and the corresponding entropy associated with the frozen-in disorder is called residual entropy S_{res}. The existence of the residual entropy which is commonly observed for glasses is a manifestation of the non-ergodicity.

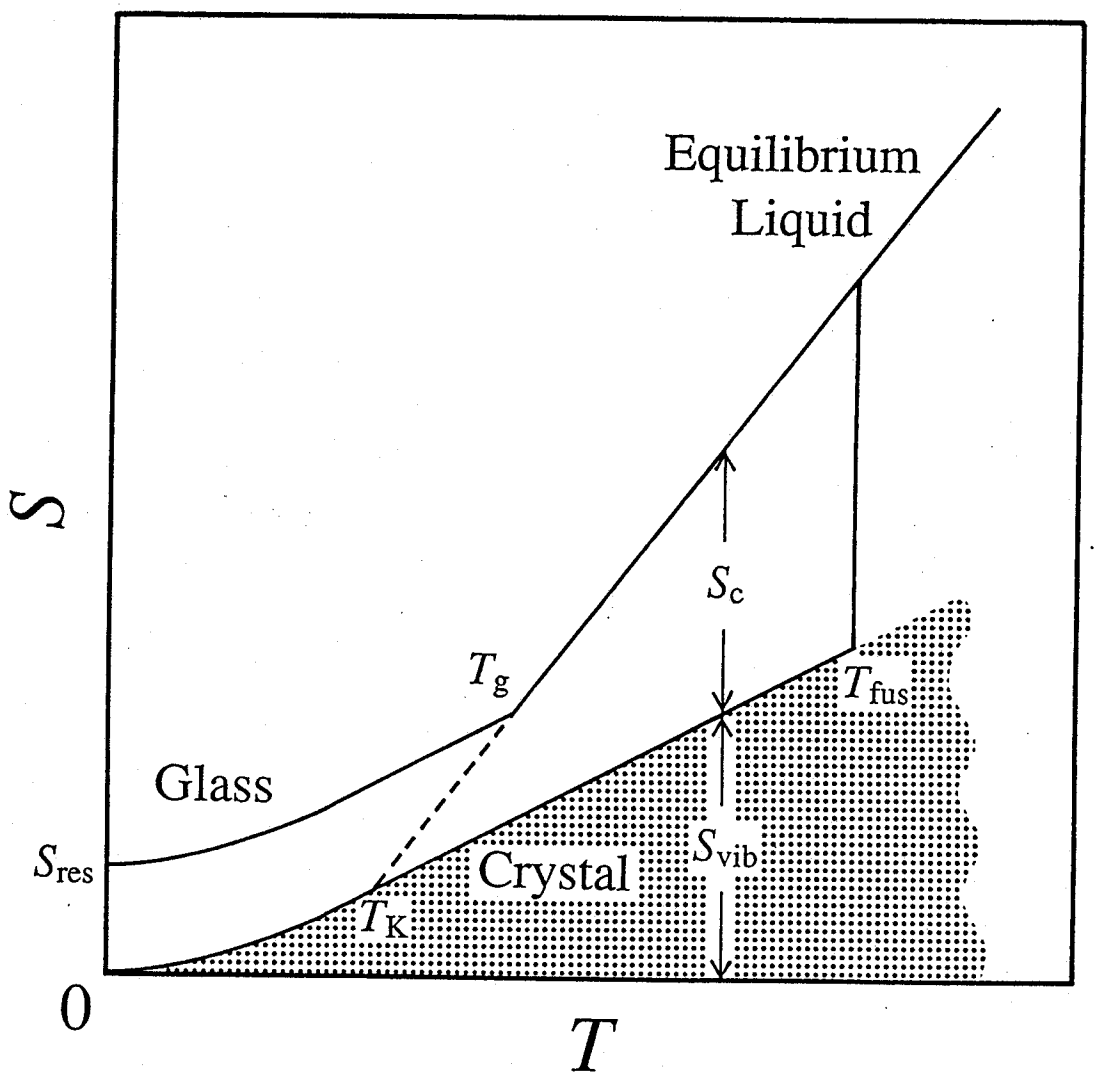

Fig. 1-1. The entropy vs. temperature diagram around the glass transition temperature.

It was pointed out by Kauzmann [12] that, unless the glass transition could occur, the extrapolation of the entropy of equilibrium liquid would reach that of crystal at a finite temperature T_K which is called the Kauzmann temperature. Below this temperature, a strange situation occurs: the entropy of liquid is smaller than that of crystal. What is the structure of a liquid with no configurational disorder? This question is known as the Kauzmann paradox which remains still unresolved.

Formation of glass is a synonym for a process of avoiding the crystallization for classical liquids. Therefore, the glassy state is usually realized by quenching the liquid by evading the crystallization. In this classical technique, some substances are easily undercooled to give their glassy states, whereas the others, such as water and simple molecular liquids crystallize readily above T_g. Especially in the case of water, it is believed that there exists a critical point of undercooled liquid at about 230 K at which crystallization occurs by homogeneous nucleation. This means that we can not vitrify bulk water through the path of the equilibrium liquid.

In order to obtain the glassy state of such readily crystallizable material, special hyper-quenching techniques have been developed. They are, for example vapor-deposition, sputtering, melt spinning, *etc.* The sputtering and melt spinning are relatively new techniques which are usually employed for the formation of metallic glasses. Although the vapor-deposition technique is rather old-fashioned method, it is very powerful and convenient for simple substances. Cooling rate of vapor-deposition reaches 10^{14} K s^{-1} according to the estimation used by

Kouchi *et al.* [13], whereas the melt spinning is at most 10^8 K s^{-1} [4]. The high performance in cooling rate makes it possible to vitrify very simple molecular substances. Actually, Kouchi *et al.* [13] succeeded in vitrifying argon by means of a very slow (3×10^{-11} m s^{-1} in the rate of growth of sample thickness) vapor-deposition onto a substrate kept at 10 K. The glassy argon is quite an important material as a model of theoretical and computer simulation study. The accumulation of the experimental data of such simple molecules must be necessary for the development of the amorphous science.

Here, I will refer to the terminology. The terms *non-crystalline solid* and *amorphous solid* are general designations representing the solid which lacks the three-dimensional periodicity of the constituents with respect to their center of mass. On the other hand, the term *glass* has been conventionally used for the solid formed by undercooling a liquid below the glass transition temperature. The glass definitely shows the glass transition phenomenon. Nowadays, however, the concept of glass has been extended to more general cases. The non-equilibrium solids with frozen-in disordered configurations, such as glassy crystals and glassy liquid crystals, are given adjective *glassy* irrespective of the existence of liquid-like structure. It has been established that the glass transition phenomenon is widely observed for samples prepared by other glass-forming techniques. The word *glassy* is, therefore, synonymous to *non-equilibrium* in the thermodynamic sense. Taking these situations into consideration, the term *glassy state* will be used in this thesis independently of the vitrification technique unless otherwise noted.

1-3 Kinetic Theories of Viscous Liquids and Glasses

A typical non-equilibrium property of glassy state is found out in the glass transition region, where the rate of the molecular motions required for the establishment of new equilibrium liquid becomes comparable with our experimental time scale. In this temperature region, we can observe relaxation phenomena in various thermodynamic quantities, such as enthalpy and volume. This relaxation phenomenon is interesting in the sense that they reflects the molecular rearrangement in the viscous liquid. Therefore, this relaxation phenomena is referred to as *structural relaxation.*

One of the important characters of the structural relaxation is its non-linearity and non-exponentiality. The non-linearity of the viscous flow of the undercooled liquid was already noticed in the 19th century [14]. There are two classical kinetic theories which can describe the non-linear relaxation of the viscous liquid and the glass. They are termed the *free volume theory* [15] and the *entropy theory* [16,17]. These are rather phenomenological, but intuitively take the features of glass into consideration. The free volume theory asserts that the decrease of excess volume in the liquid, which is termed free volume, provokes the slowing down of molecular rearrangement. It is supposed that the transition probability of a molecular orientation and position is proportional to the free volume v_f and the distribution of free volume is proportional to $(1/\bar{v}_f)\exp(-v_f/\bar{v}_f)$. In addition, the transition of a molecule is assumed to happen only when the free volume is larger than some critical value v_c. Then the transition probability of molecule in the supercooled

liquid is [18]

$$W = (1/\bar{v}_f) \exp(-v_c/\bar{v}_f). \qquad (1\text{-}1)$$

This relation implies that the transition probability vanishes under the condition that v_c tends to infinity.

In the liquid phase, the orientation and position of a molecule are correlated closely with those of neighboring molecules and so the molecular rearrangement can take place in a highly cooperative manner. These characters become remarkable especially near the glass transition region. The configurational entropy is a measure of the correlation between molecules in the liquid. The entropy theory formulates the molecular dynamics in the liquid by means of the configurational entropy.

According to the discussion made by Adam and Gibbs, the molecular rearrangement is possible to occur cooperatively in a subsystem containing an appropriate number of molecules. The transition probability of a subsystem is proportional to $\exp(-\Delta G/k_B T)$, where ΔG denotes the activation free energy of the subsystem, and is proportional to the number of constituent molecules z. There is a critical lower limit z^* to the size of the cooperative unit that can yield non-zero probability. Then, the average probability of the rearrangement is obtained by summing up the terms $\exp(-\Delta \mu z/k_B T)$ for z from z^* to infinity. Here, $\Delta \mu$ is the free energy of activation per molecule and k_B the Boltzmann constant. After an appropriate approximation, the probability is

$$W = A \exp(-\Delta \mu \quad z^* / k_B T), \qquad (1\text{-}2)$$

where A is a constant. From the assumption of equivalence and independence of the subsystems, the parameter z^* can be connected to the molar configurational entropy S_c of the system as

$$z^* = N_A \, s_c^* / S_c, \qquad (1\text{-}3)$$

where N_A is the Avogadro constant and s_c^* the entropy of the critical-sized subsystem. Substituting this expression for z^* into Eq. (1-2), the final form of the transition probability for the structural relaxation can be given as

$$W = A \exp(-\Delta \mu \quad s_c^* / k_B T S_c). \qquad (1\text{-}4)$$

Equation (1-4), known as the Adam-Gibbs (AG) equation, is the most important result derived from the entropy theory.

The entropy theory contains less unjustified assumptions than the free volume theory. Moreover, the AG equation predicts the Vogel-Tammann-Fulcher (VTF) type temperature dependence of the relaxation time in the form which can avoid the Kauzmann paradox [12] described above. Above all, the numerical value of the configurational entropy can be calculated from the enthalpy data obtained by means of the adiabatic calorimetry. Because of these reasons, the entropy theory will play a principal role of the analysis in the present study.

1-4 Purposes of the Present Study

In the present experiments, enthalpy of a system was chosen as a probe for the relaxation phenomena. The enthalpy can be measured precisely and sensitively by a low-temperature adiabatic calorimetry. The method provides valuable information on the ultra-slow aspect of the relaxation dynamics. This is because of its long time-scale of the measurement compared with other physico-chemical techniques which usually use an alternating external fields in the range 10^{-1} to 10^{6} Hz. The enthalpy can be related to the entropy of the system. The adiabatic calorimetry has long been improved to a highly sophisticated level and has nowadays a long-term stability of the adiabatic condition and high resolution of the temperature measurement. The high quality of the calorimetry enables us to follow, with high fidelity, the enthalpy relaxation process that takes generally over days or months.

To understand the mechanism of the glass transition with a microscopic model, the experiment should be done for substances as simple as possible. So far, however, the experimental studies of the glass transition and the structural relaxation have been done mainly for polymer, metallic and silicate glasses from practical purpose. Such substances possess rather complex structures and/or interaction to be modeled theoretically. There have been a few numbers of research for simple molecular glasses possessing low glass transition temperature and readily crystallizing property. In the present study, a series of straight-chain hydrocarbons were chosen as the samples. The vapor-deposition technique was used for the samples which are crystallizable

readily. The hydrocarbons belong to one group of simple compounds whose intermolecular interactions are just the dispersion energy, and the similarity of molecular structures would make a systematical discussion possible.

The purposes of the present study are roughly divided into two parts. The first is to determine the glass transition temperatures of some simple hydrocarbons that have not been reported so far. The second, which is the main purpose of this study, is to investigate the structural relaxation phenomena from the thermodynamic point of view, focusing attention to its non-linearity and cooperativity. The entropy theory was utilized to analyze the experimental data, and the verification of the validity of the theory is included in the second purpose.

For the first purpose, the glass transition temperatures were determined for the vapor-deposited samples of several simple hydrocarbons. The interrelation between the crystallization and the glass transition is examined as well. These experiments and discussions are described in Chapter 3. For the second purpose, calorimetric measurements of the enthalpy relaxation processes were carried out for 1-pentene (Chapter 5) and 1-butene (Chapter 6) on the basis of the following two interests. One is to clarify any possible differences in the relaxation phenomena between the vapor-deposited and liquid-quenched glasses. The other is whether the configurational entropy of glass is really a physical property governing the enthalpy relaxation processes. To investigate the significance of the configurational entropy in the mixing process, the composition dependence of the glass transition temperature was studied for several binary systems of hydro-

carbons (Chapter 4).

References to Chapter 1

[1] W. J. Zachariasen, *J Am. Ceram. Soc.*, 54, 3841 (1932).

[2] W. Vogel, *Chemistry of Glass*, Am. Ceram. Soc., Colombus (1985).

[3] J. D. Bernal, *Proc. Roy. Soc.*, A280, 299 (1964).

[4] S. R. Elliot, *Physics of Amorphous Materials*, Longman, New York (1984).

[5] G. N. Lewis and G. E. Gibson, *J. Am. Chem. Soc.*, 42, 1529 (1920); G. E. Gibson and W. F. Giauque, *J. Am. Chem. Soc*, 45, 93 (1923).

[6] P. E. Rouse Jr., *J. Chem. Phys.*, 21, 1272 (1953); B. R. Zimm, *J. Chem. Phys.*, 24, 269 (1956)

[7] M. Doi and S. F. Eswards, *J. Chem. Soc. Faraday Trans.*, 2, 74, 1789, 1802, 1818 (1978).

[8] K. L. Ngai, R. W. Rendell, A. K. Rajagopal and S. Teitler, *Dynamic Aspects of Structural Change in Liquids and Glasses*, p. 150, Edited by C. A. Angell and M. Goldstein, N. Y. Acad. Sci., New York (1986).

[9] R. G. Palmer, D. L. Stein, E. Abrahams and P. W. Anderson, *Phys. Rev. Lett.*, 53, 958 (1984).

[10] W. Goetze, *Z. Phys. B*, 56, 139 (1984); W. Goetze and L. Sjoegren, *J. Phys. C: Solid State Phys.*, 20, 879 (1987).

[11] Leutheusser, *Phys. Rev. A*, 29, 2765 (1984); S. P. Das and G. F. Mazenko, *Phys. Rev. A*, 34, 2265 (1986).

[12] W. Kauzmann, *Chem. Rev.*, 43, 219 (1948).

[13] A. Kouchi and T. Kuroda, *Jpn. J. Appl. Phys.*, 29, L807

(1990).

[14] Kohlrausch, *Ann. Phys. (Leipzig)*, 12, 393 (1847).

[15] H. S. Cohen and D. Turnbull, *J. Chem. Phys.*, 31, 1164 (1959); D. Turnbull and H. S. Cohen, *J. Chem. Phys.*, 34, 120 (1961).

[16] J. H. Gibbs and E. A. Dimarzio, *J. Chem. Phys.*, 28,373 (1958); E. A. Dimarzio and J. H. Gibbs, *J. Chem. Phys.*, 28, 807 (1958); J. H. Gibbs, *Modern Aspects of the Vitreous States*, Vol. 1 p. 152, Edited by J. D. Mackinzie, Butterworth, London (1960).

[17] G. Adam, J. H. Gibbs, *J. Chem. Phys.*, 43, 139 (1965).

[18] M. I. Klinger, *Phys. Rep.*, 165, 275 (1988).

Chapter 2

APPARATUSES USED IN THE PRESENT STUDY

2-1 Introduction

Thermal behavior of material at low temperature is one of the principal interests in solid state science, and many thermal techniques have been developed since the previous century [1]. For the study of the glassy state, especially, thermodynamic investigations seem to be the most significant because the glass is in thermodynamically non-equilibrium state. The study on relaxation phenomena of thermodynamic quantities, such as enthalpy and volume, directly provides us with the non-equilibrium nature of the glassy state and the rate of approaching towards the equilibrium values. Thermal methods to investigate the properties of materials can be divided into two classes. The first one is of the calorimetry, for example, heat capacity calorimetry and reaction calorimetry. The calorimetric methods provide *quantitative* information on the thermodynamic properties of the materials. Especially, the adiabatic calorimetry, which gives accurate entropy and heat capacity data, enables us to discuss about the microscopic mechanisms of the interesting phenomena in solid state physics such as phase transition and structural relaxations. However, they have some shortcoming: they usually require long time for measurements, and complex and large-scaled apparatuses. The second class is of the thermal analyses, such as differential thermal analysis (DTA) and thermo-

gravimetry (TG). Although these are *qualitative* methods in comparison to those belonging to the first class, they have simple operations of measurement and often come to quite convenient techniques for the purposes such as the determination of the temperatures of phase transition and glass transition.

In the present study, the techniques of both classes were properly used, so as to make the most of their advantage of each technique. The determination of glass transition temperatures in Chapter 3 and 4 was carried out by means of DTA technique. On the other hand, low temperature adiabatic calorimetry was applied to the quantitative analysis of the enthalpy relaxation processes in Chapter 5 and 6. In this chapter, the structure of the DTA apparatus for vapor-deposited sample, which is constructed for the present study, will be described in section 2-2, and the outlines of the other apparatuses used in this study will be given in 2-3.

2-2 DTA Apparatus for Vapor-deposited Samples (Type I DTA)

The experimental study of simple molecular compounds is significant for the glass transition and related structural relaxation phenomena because they have not been understood completely even for the rare gases. The simpler the molecular structure and interaction are, the easier the theoretical treatment becomes. On the other hand, the vitrification of a simple molecular compound is very difficult, because they are easy to crystallize. The vapor-deposition is a powerful method to vitrify such materials, owing to its prominent ability in cooling rate (10^6 - 10^{14} K s^{-1}) [2,3]. The former value was estimated from the geometry

of the present apparatus described below, and the latter from the interaction between the substrate and a molecule.

In the present study, a new DTA apparatus for vapor-deposited sample was constructed. This apparatus is aiming at the determination of T_g of simple compounds. Nearly twenty years ago, Haida *et al.* reported thermal analyses of the simple molecular glasses formed by the vapor-deposition at liquid hydrogen temperature (20 K) [4]. The present apparatus made it possible to deposit sample vapor at liquid helium temperature (4.2 K). It is expected that the vitrification would be easier as the deposition temperature is lowered. This apparatus is called *type I DTA* hereafter.

A schematic cross section of the cryostat is shown in Fig. 2-1. The cryostat is divided into two portions with different roles. The upper portion, of doubly reentrant shape, is a Pyrex Dewar used for producing and maintaining cryogenic temperatures. The outer reentrant space (E) is filled with liquid nitrogen, and the inner space (D) with liquid helium or hydrogen depending on the desired temperature of vapor deposition of sample. Temperatures as low as 10 K can be produced by pumping on liquid hydrogen through the outlet tube (B). The glass Dewar has a complex structure so that it may be broken by a rapid temperature variation during transfer of the refrigerant. In order to relax such potential strain, a thin copper plate (H), 0.1 mm in thickness, was used as the bottom of the outer refrigerant vessel and a glass-bellows (F) was incorporated at the center of the Dewar. The connection between the copper plate and the glass tubes was realized by soldering through Kovar-Pyrex seals.

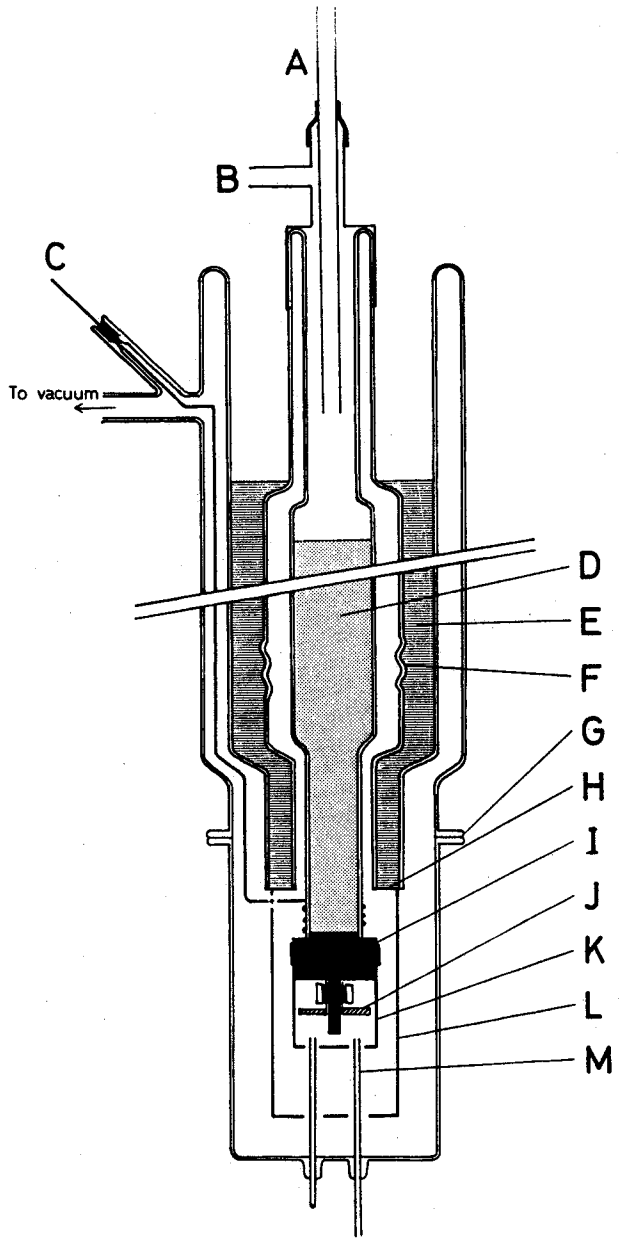

Fig. 2-1. Schematic cross section of a cryostat of the DTA apparatus for vapor-deposited samples. A:refrigerant inlet, B:refrigerant outlet, C:electrical wire, D:inner refrigerant vessel, E:outer refrigerant vessel, F:glass-bellows, G:ground glass joint, H:copper plate, I:copper block, J:sample-depositing substrate, K:adiabatic shield, L:radiation shield, M:sample inlet.

The lower portion, (I) - (M), is for sample deposition and measurement. A copper block (I), which is fixed with Wood's alloy to the bottom of the inner vessel of Dewar through another Kovar-Pyrex seal, is kept at the temperature of the refrigerant (D). Two cold substrates (J), each for sample deposition and reference, are attached on the copper block. A thermal shield (K) is mechanically fixed to the copper block. An outer shield (L) is pinned with screws at the bottom of the outer vessel of Dewar through the Kovar seal. Both of the shields provide stable conditions for the deposition and subsequent DTA experiment. Fig. 2-2 illustrates the details around the sample plate on an enlarged scale. A pair of 1 × 1 cm^2 copper substrates, 0.1 mm thick, were fixed symmetrically on both sides of the copper block (B) by pressing them with brass pieces (G) and thin mica plates (H) for electrical isolation. One is used for vapor-deposition and the other is for reference without any deposited material. The sample vapor is introduced through the sample inlet (I) and condensed in vacuo on the substrate (E), which is cooled down in advance to a desired low temperature. The sample inlet is made of copper tube of 2 mm outer diameter and its tip is around 1 cm away from the substrate. The entire inner space is evacuated to about 0.1 mPa by an oil diffusion pump.

The absolute value of temperature of the reference plate is monitored by a Chromel-P-(Au+0.07%Fe) thermocouple in conjunction with a digital multimeter (Model 195; Keithley Instruments, Inc.). Its thermoelectromotive force (EMF) against the ice point installed outside the cryostat was calibrated at five fixed points; the melting point of ice, the boiling points of helium

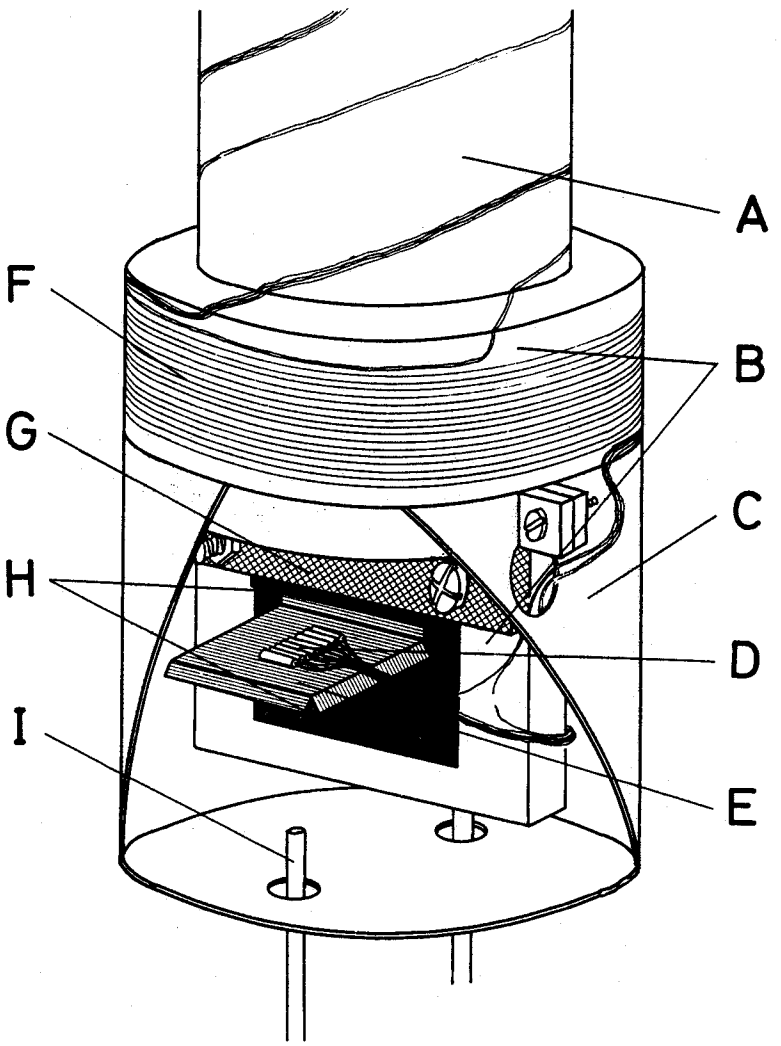

Fig. 2-2. Magnified sketch around the measurement part. A:inner refrigerant vessel, B:copper block, C:adiabatic shield, D:thermopile and thermocouple, E:sample-depositing substrate, F:heater wire, G:brass-fixer, H:mica plate, I:sample inlet.

and hydrogen, and the triple points of hydrogen and nitrogen. These data were used to correct the EMF table previously reported by the NBS [5]. Eight pairs of Chromel-P-(Au+0.07%Fe) thermocouples arranged in series are spanning the reference and sample substrates in order to detect sensitively the temperature differences between them. Each junction of the thermocouples was inserted into a copper tube (0.6 mm O.D., 0.4 mm I.D., 2 mm L) with epoxy resin (Stycast; Grace Japan) for electrical isolation. The copper tubes were then fixed with Wood's alloy onto the substrates. The thermocouple signals are amplified with a microvolt meter (Model AM-1001; Ohkura Electric Co. Ltd.) and recorded on a strip chart.

The rate of vapor deposition is controlled with a microvalve installed on the way of the sample inlet, in such a way to keep the temperature difference between the sample and reference substrates in the range 0.01 to 0.05 K which corresponds to 2 - 10 μV in EMF. The volume of sample deposited over a few hours is 0.001 - 0.01 cm^3. After the deposition, the refrigerant remaining in the inner Dewar vessel (D in Fig. 2-1) is evaporated by a heater wound around the copper block (F in Fig. 2-2) and the DTA experiment is started.

2-3 Other Apparatuses

2-3-1 Conventional Type of DTA (Type II DTA)

Conventional type of DTA apparatus for low temperature was used for the samples which can be vitrified by liquid quenching. This DTA apparatus will be called *type II DTA* apparatus. The sample liquid of about 1 cm^3 was charged into a conventional DTA

tube made of Pyrex glass along with helium gas of 3 kPa at 77 K. This DTA tube and the reference DTA tube with benzene were embedded into wells drilled in a copper block around which heater wire is wound. The block was suspended inside a brass vessel into which 3 kPa of helium gas was introduced as heat transmitting medium. The lowest temperature, 20 K, was achieved by immersing the brass vessel in liquid hydrogen. The temperature difference between the sample and the reference and the absolute value of temperature were monitored with Chromel-P-Constantan thermocouples inserted in the reentrant wells of the DTA tubes. Further description of this apparatus is given elsewhere [6].

The sensitivities and base-line stabilities of the two DTA apparatuses described above will be shown in Chapter 4. Both apparatuses were sensitive enough to determine glass transition temperatures with the error of 0.1 - 0.3 K.

2-3-2 Adiabatic Calorimeter for Vapor-deposited Samples (VD)

In Chapter 5, the enthalpy relaxation process in the glassy state prepared by the vapor-deposition was measured by means of a special type of adiabatic calorimeter [7]. In this section, the feature of this apparatus will be outlined. Henceforth, it will be called *VD calorimeter*.

The VD calorimeter is essentially filling-tube type [8]. The sample vapor is introduced from the outside of the cryostat into the calorimeter cell set in advance inside the cryostat. In the present case, a copper tube of 1 mm O.D. is connected to the cell through which the sample vapor is deposited onto the wall of the cell kept at a temperature lower than T_g. Multifold reen-

trant-structured stainless tube incorporates the tube and the cell in order to reduce the heat flow from the tube into the cell during the vapor deposition. Adiabatic condition of the cell can be achieved by controlling the temperatures of the copper tube and the inner adiabatic shields at the same temperature of the cell with thermocouples and heater wires as usual.

The low temperature down to 10 K is realized by a built-in cryorefrigerator manufactured by Cryo-Mech. Co. Ltd. On depositing the sample, the calorimeter cell is mechanically brought into contact with the refrigerant tank, in which liquid hydrogen is stored. The sample transfer tube has to be kept at higher temperature than the cell, typically at 150 - 200 K, so that the sample vapor does not condense on the way. The lowest temperature available for the vapor-deposition is around 40 - 50 K. It takes about 1 week to deposit the sample of 1 g. Such a slow rate of the deposition is required to prevent a possible crystallization or structural relaxation by the temperature increase arising from the heat of condensation of the sample vapor. After the deposition, the mechanical contact between the cell and the refrigerant tank is switched off and the heat capacity and enthalpy relaxation measurements are started from 10 K.

A Rh-Fe resistance thermometer was used for the temperature measurement. The precision and accuracy of temperature measurement are 0.1 mK and 10 mK, respectively. Heat capacities of empty cell are shown in Fig. 2-3. The precision of heat capacity measurement is estimated within 0.5 % [7] for the sample of about 1 g. The large imprecision compared with that of usual calorimeter is due to the small amount of the sample and the heat leakage

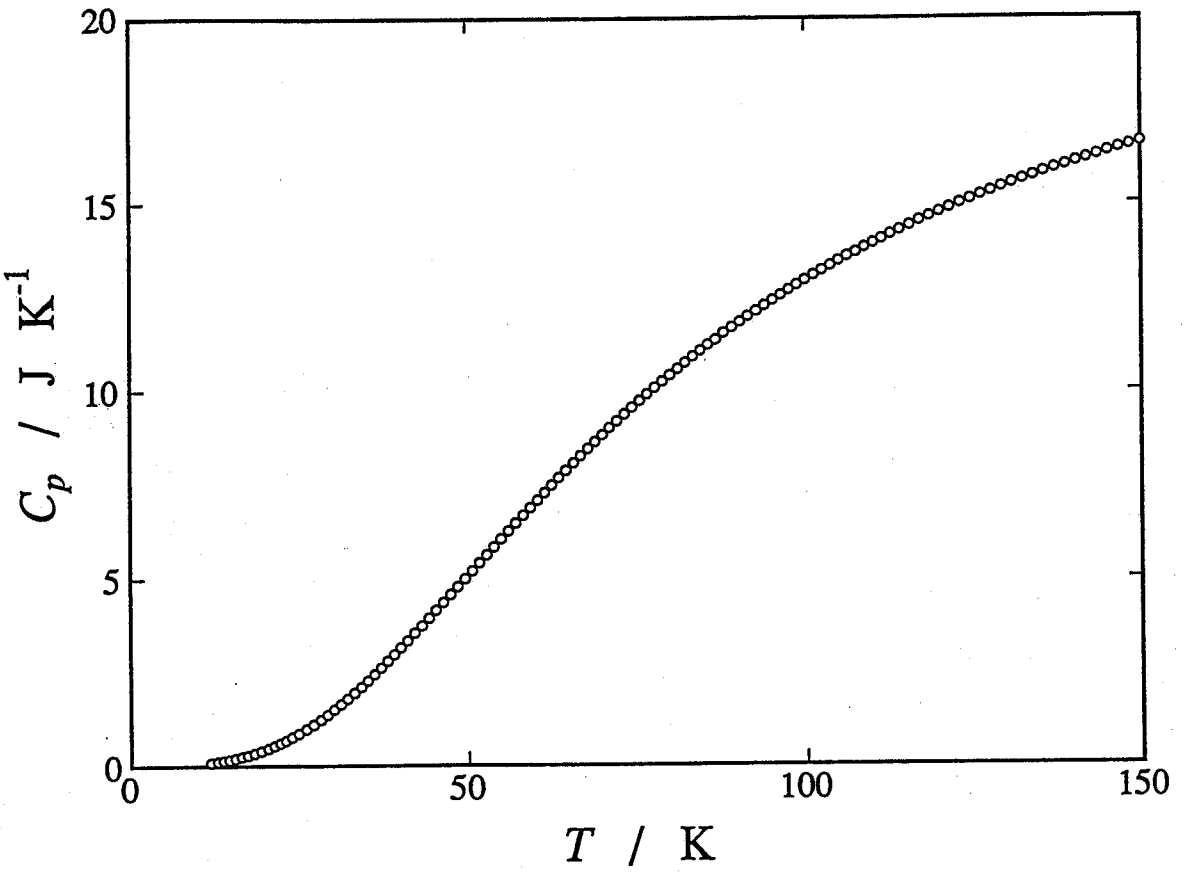

Fig. 2-3. Heat capacity of the empty cell for VD calorimeter.

through the sample transfer tube. For the measurement of enthalpy relaxation, however, this precision was sufficient enough because the amount of enthalpy relaxed was very large for the vapor-deposited samples.

2-3-3 Adiabatic Calorimeters for Bulk Samples (BS I, BS II)

The VD calorimeter is not useful for the liquid quenched samples since the enthalpy relaxation of liquid-quenched sample is much smaller than that of vapor-deposited sample [7]. Hence, the liquid-quenched sample was measured with two types of adiabatic calorimeters for bulk samples, *BS I* and *BS II*.

The BS I calorimeter has a built-in cryorefrigerator of Cryo-Mech Co. Ltd. similar to the VD calorimeter. It is unique that this calorimeter can liquefy hydrogen gas, which is supplied from the hydrogen storage, in the refrigerant tank. The low temperature experiment from about 10 K can be achieved by the forced evaporation of liquefied hydrogen.

The BS II calorimeter can provide low temperature down to 5 K with liquid helium as coolant. This make it possible to determine the residual entropy of vitreous sample with high precision as described in Chapter 6.

With these instruments, heat capacity measurement can be performed with the imprecision and inaccuracy of 0.1 % and 0.2 %, respectively. More detailed descriptions about these calorimeters are described in Refs. [9,10].

2-3-4 Calorimetric Sample Cell for Bulk Samples

To measure heat capacity of 1-butene (Chapter 6) and pentene

(Chapter 5) which have rather high vapor-pressure at room temperature, the sample cell of the high pressure calorimeter was used with slight modification. Fig. 2-4 shows the cross section of the modified calorimeter cell. The original version of the cell is connected to the high pressure generator through the pressure transmitting tube [11], while the present version is suspended with Nylon strings attached at the screw cap (D). The sample liquid is distilled into the cell through a copper tube of 1.2 mm O.D. (C), which is pinched off with soldering after the distillation. This sample cell is made of Cu-Be alloy, and designed to bear the pressure of 10 MPa. The inside volume is 12.3 cm^3 and the mass was 50.8 g. The temperature of the cell is measured with the same type of Rh-Fe resistance thermometer as used in the VD calorimeter.

The heat capacity of the empty cell is shown in Fig. 2-5. The larger heat capacity data measured by the BS I calorimeter compared to those of BS II are derived from an extra copper belt used for the fixing of the thermocouple. The relatively large heat capacity, which is 2 - 3 times of the usual cell for the same amount of sample (ca. 10 cm^3), is disadvantageous in the sense that it reduces the precision of the measurement, but is rather advantageous in the sense that it represses too much temperature variation due to the enthalpy relaxation at glass transition region. Isothermal measurement is ideal to investigate time-dependence of the enthalpy relaxation rate though it is, in principle, impossible in the adiabatic calorimetry.

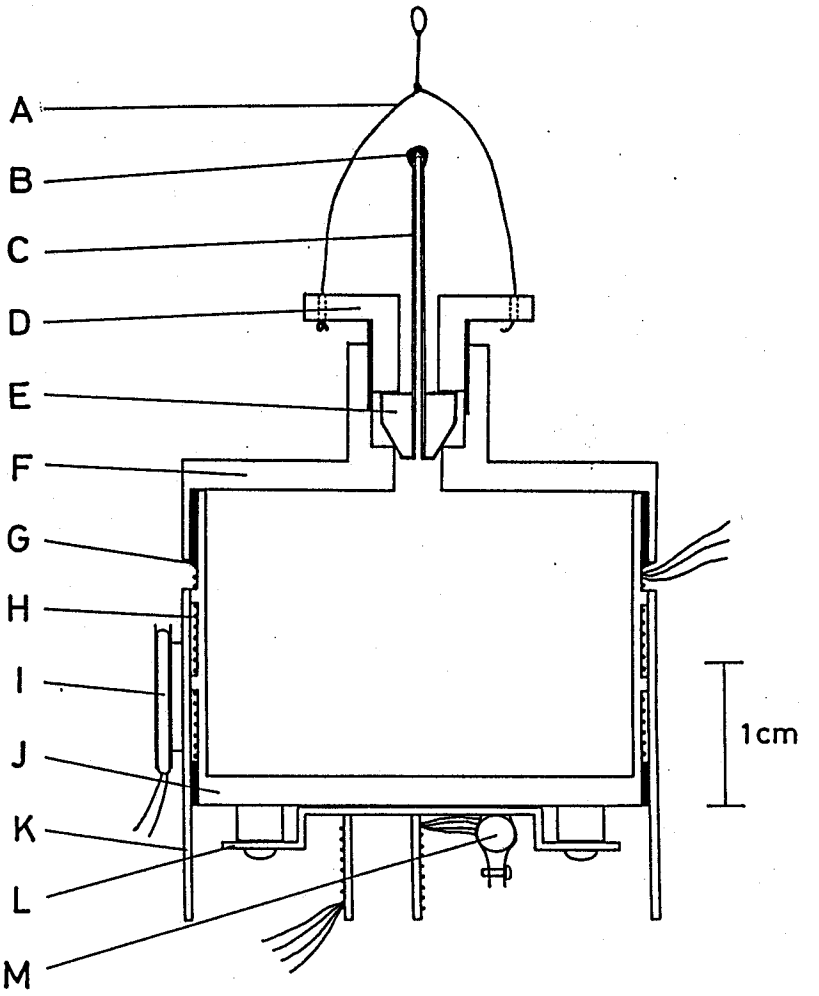

Fig. 2-4. Schematic cross section of the calorimeter cell.
A:Suspending Nylon string, B:soldered seal, C:sample inlet copper tube, D:screw cap, E:plug, F:body (upper), G:silver solder, H:heater wire, I:thermocouple, J:body (upper), K:cell cover, L:thermometer holder, M:Rh-Fe resistance thermometer.

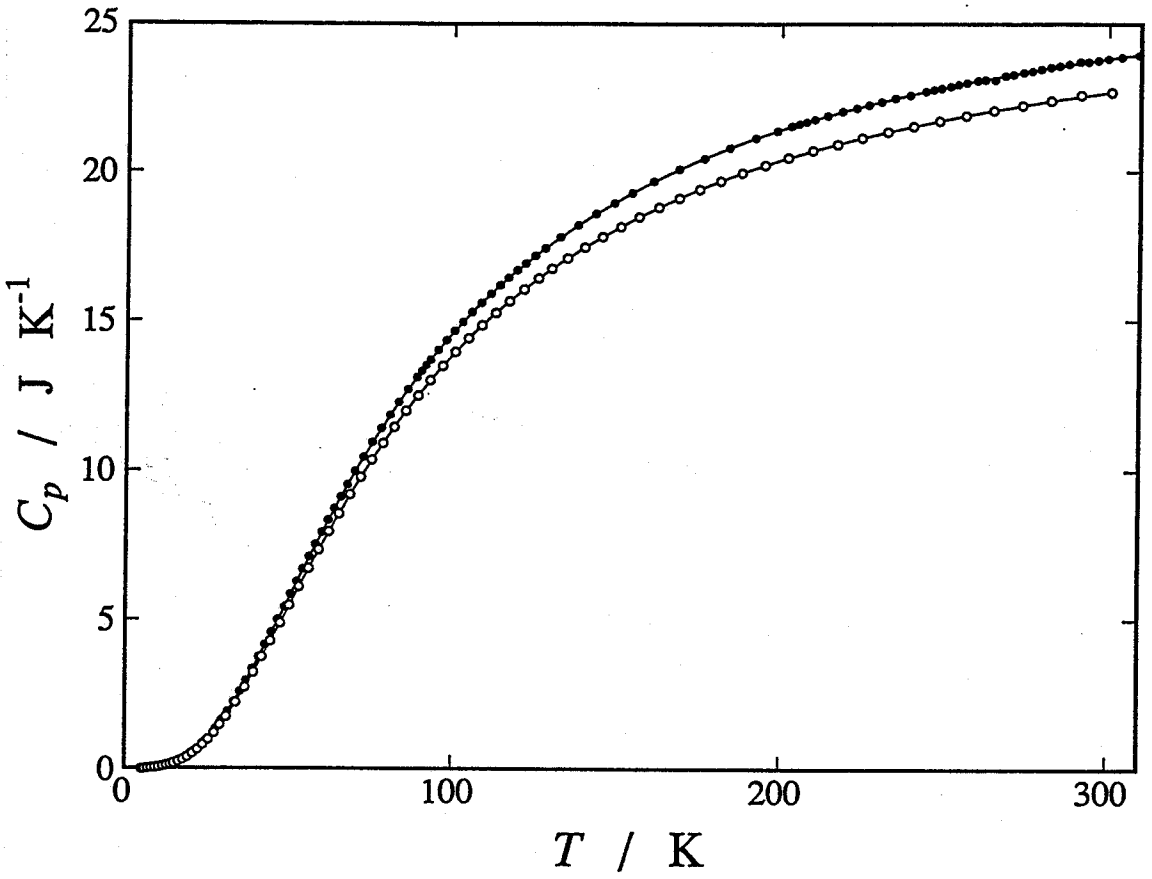

Fig. 2-5. Heat capacities of the empty cell for the bulk sample measured by BS I (filled circle) and BS II (open circle) calorimeters. Solid lines denote the calculated curves optimized to polynomial function.

References to Chapter 2

[1] S. Seki, in "*Netsu. Ondosokutei to Shisanetsubunseki*", Nankoudou Press., Eds. S. Seki and R. Fujishiro (1978).

[2] K. Takeda, M. Oguni and H. Suga, *J. Phys. Chem. Solids*, accepted.

[3] A. Kouchi and T. Kuroda, *Jpn. J. Appl. Phys.*, 29, L807 (1990).

[4] O. Haida, H. Suga and S. Seki, *Thermochim. Acta*, 3, 177 (1972).

[5] L. L. Sparks, R. L. Powell and J. Hall, Cryogenic Thermocouple Table, NBS report 9712 (1968).

[6] M. Oguni, N. Okamoto, O. Yamamuro, T. Matsuo and H. Suga, *Thermochim. Acta*, 121, 323 (1987).

[7] H. Hikawa, M. Oguni and H. Suga, *J. Non-Cryst. Solids*, 101, 90 (1988).

[8] E. F. Westrum Jr., G. T. Furukawa and J. P. McCullough, *Experimental Thermodynamics*, Vol. 1, Edited by J. P. McCullough and D. W. Scott, Butterworths, London (1968).

[9] O. Yamamuro, M. Oguni, T. Matsuo and H. Suga, *Bull. Chem. Soc. Jpn.*, 60, 1269 (1987).

[10] K. Moriya, T. Matsuo and H. Suga, *J. Chem. Thermodyn.*, 14, 1143, (1982).

[11] Y. P. Handa, O. Yamamuro, M. Oguni and H. Suga, *J. Chem. Thermodyn.*, 21, 1249 (1989).

Chapter 3

GLASS TRANSITION AND CRYSTALLIZATION OF SOME SIMPLE HYDROCARBONS

3-1 Introduction

The formation of glass by the liquid-undercooling method is always a process accompanied by potential crystallization. If the crystallization could be by-passed successfully, a glass transition will be observed on the way of cooling at a finite temperature. On the other hand, behavior of a substance once vitrified is not universal. Most of them show both the glass transition and the crystallization successively. However, some good glass formers such as glycerol and 3-methylpentane do not exhibit any anomaly other than a glass transition. For some inorganic materials such as $Fe_xNi_{80-x}P_{14}B_6$ [1] and $Ca(PO_3)_2$ [2], crystallization can be observed even below their glass transition temperatures.

n-Alkanes are one of the compound groups whose glassy states have been rarely studied so far. Aside from rare gases, they are the simplest class of compounds whose intermolecular interaction is just the dispersion energy. Actually, simple *n*-alkanes crystallize very quickly on cooling, because of the simplicity of their intermolecular interaction. This is the reason why very little study of glass transition has been carried out for *n*-alkanes so far. In contrast, some of 1-alkenes can be easily vitrified. For example, 1-butene is known as one of the best glass former among the molecular liquids, whereas *n*-butane is a

very hard glass former. It is expected from the structural resemblance of these two substances that the manner and strength of molecular interaction are also similar and the physical properties resemble each other. What is a significant factor which induces large difference in glass-forming ability (or crystallization tendency) between *n*-alkanes and 1-alkenes ? This question awakes our interest.

In the present chapter, the vapor-deposition technique was used to vitrify *n*-alkanes and 1-alkenes, and thermal characterization of their amorphous state was carried out by using differential thermal analysis (DTA). Principal interest here is on the glass transition and crystallization phenomena, and interrelation of them.

The vapor-deposition technique has already been applied to some simple hydrocarbons by Sugawara and Tabata [3]. They reported some correlations between T_g and radiothermoluminescence (RTL) peaks of the vapor-deposited samples. The present results were compared with their data, and the origin of RTL peaks will be discussed.

3-2 Experimental

The commercial materials of ethene, ethane, propene, propane (> 99.5%), *n*-butane, *n*-pentane (> 99.0%), *n*-hexane (> 99.9%), 1-butene (> 98.5%) and 1-pentene (> 99.8%) were used as samples. The first four material are from Gasukuro Kogyo Inc. and the others from Tokyo Kasei Kogyo Co. Ltd. The value in bracket behind each sample denotes purities claimed by them. The first four substances, *n*-pentane and *n*-hexane were used after degassing

without further purification. 1-Pentene and *n*-butane were purified by the fractional distillation under reduced pressure. Each sample was stored in a glass container (nearly 150 cm^3) with a polytetrafluoroethylene (PTFE) cock and a glass joint through which the sample is transferred into the cryostat. The deposition temperatures were 4.2 K for ethene and ethane, 63.1 K for 1-pentene and 20.4 K for the remaining samples, respectively. The mass of sample deposited during a few hours was about 10 mg.

The DTA experiment was carried out with the type I apparatus at the heating rate of 1.5 - 2.5 K min^{-1} in the range from the deposition temperature to the temperature at which the sample was completely vaporized. The vapor deposition was performed twice for propane, propene, *n*-butane and *n*-pentane to examine the effect of thermal histories as described later. For the first deposit, the temperature was raised continuously over the whole temperature range to examine the overall thermal anomalies (Run 1). For the second, the sample was cooled to the lowest temperature from just above or below the temperature at which some anomalies were observed in Run 1, and the next heating experiment was started (Run 2, 3, ...). For 1-pentene, DTA was made also with the type II DTA apparatus using the sample of 0.5 cm^3 in the temperature range above 63.5 K.

A binary mixture between *n*-butane and 1-butene was also studied with the type I DTA. The samples were prepared in the following manner. First, the *n*-butane gas of known pressure was filled in a specified space on a hand-made vacuum-line with a pressure gauge at room temperature, and the gas was condensed in the sample container kept at liquid nitrogen temperature. Next,

the same space was filled with the 1-butene gas of desired pressure, and the gas was again condensed in the same container. Since the pressures of sample gases were low enough to be regarded as the ideal gas at room temperature and the vapor pressures of the condensed substances were negligibly small at liquid nitrogen temperature, it is believed that the ratio of the initial pressures give the correct composition of the mixture.

3-3 Results of Measurement

3-3-1 Ethene and Ethane

The upper portion of Fig. 3-1 schematically shows the DTA signal observed during the vapor deposition of ethene at 4.2 K. The temperature was kept constant and the base line of the signal also showed good stability throughout the deposition process. Many spike-like exothermic peaks, however, appeared in the case of this substance. The lower portion of Fig. 3-1 shows the DTA signal observed in the heating run. Any anomaly was not observed below 70 K, above which a large endothermic peak due to vaporization was observed. This leads to the conclusion that the above mentioned peaks observed during the deposition originated from intermittent crystallization. Accumulation of the condensation heat at the deposited surface of the sample is considered to induce quasi-periodically local devitrification even at the substrate temperature of 4.2 K.

The result of DTA experiment for ethane is reproduced in Fig. 3-2. Exothermic peaks appeared above 23.9 K. These would not, however, be due to crystallization but to stabilization between some crystalline modifications, because spike-like peaks

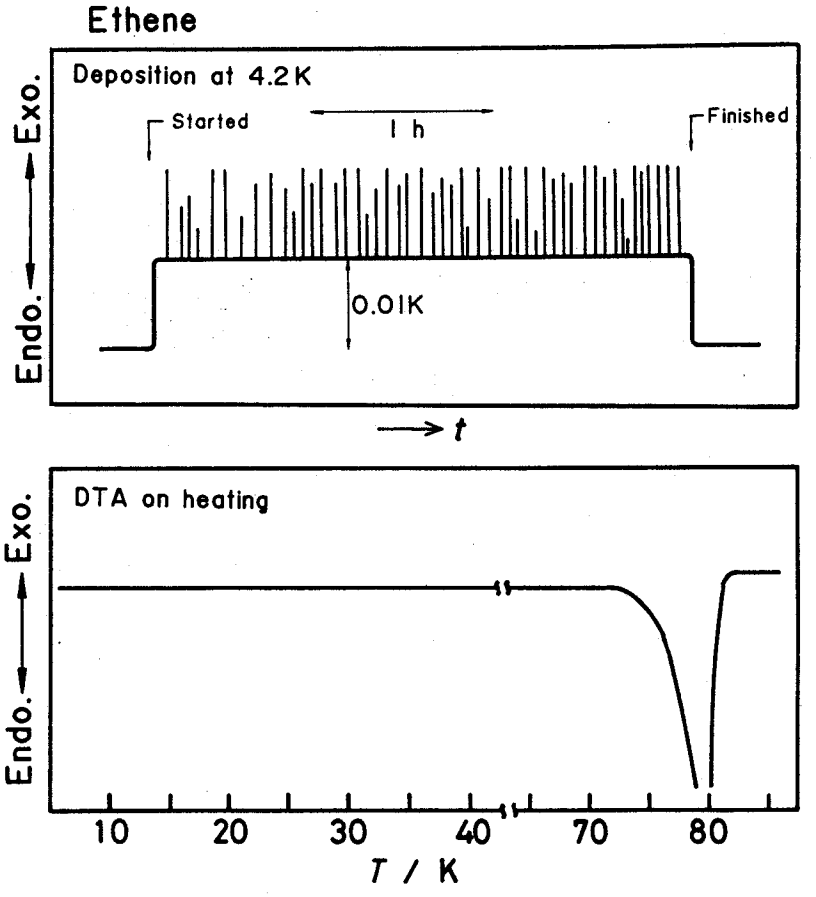

Fig. 3-1. Schematic DTA signals of ethene detected in the vapor-deposition procedure at 4.2 K (upper portion) and heating run (lower portion).

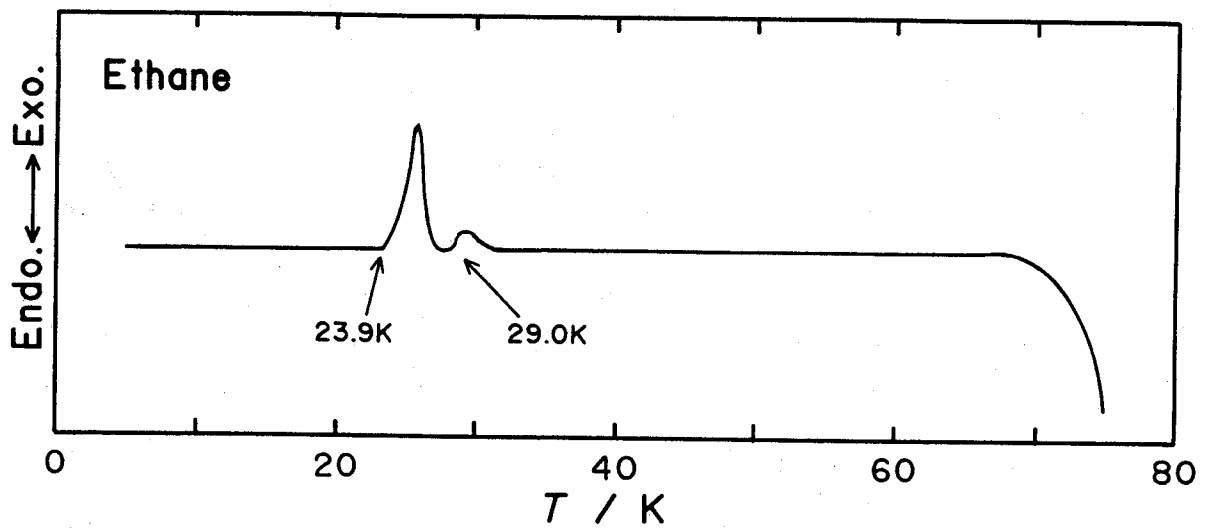

Fig. 3-2. Schematic DTA signal of vapor-deposited ethane.

similar to those observed for ethene were observed during the deposition. It is considered that the sample crystallised during the deposition.

For other substances studied here, no peaks were observed during the deposition process.

3-3-2 1-Pentene

The results of the DTA experiments of 1-pentene are summarized in Fig. 3-3. The upper curve was obtained for the liquid-quenched sample by using the type II DTA apparatus, and the lower one for the vapor-deposited sample using the type I apparatus. The exothermic and subsequent endothermic peaks around 100 K correspond to crystallization and fusion, respectively. Apparent partition of the crystallization into two peaks in the vapor-deposited sample would be caused by the difference in the homogeneous and heterogeneous nucleation rates in various parts of the sample. The nucleation rate of the sample near the substrate may be affected more or less by the nature and quality of the material. Examination of the crystallization behavior with different substrate deserves further study. Base-line shifts due to the glass transitions were observed at 71.2 and 71.7 K for the liquid-quenched and vapor-deposited samples, respectively. It is the first time that the glass transition was observed in this substance. The glass transition temperatures in the two experiments can be regarded as coincident values in view of the difference in the employed apparatuses. This gives another example of the fact that the glass transition takes place at essentially the same temperature irrespective of the method of the glass forma-

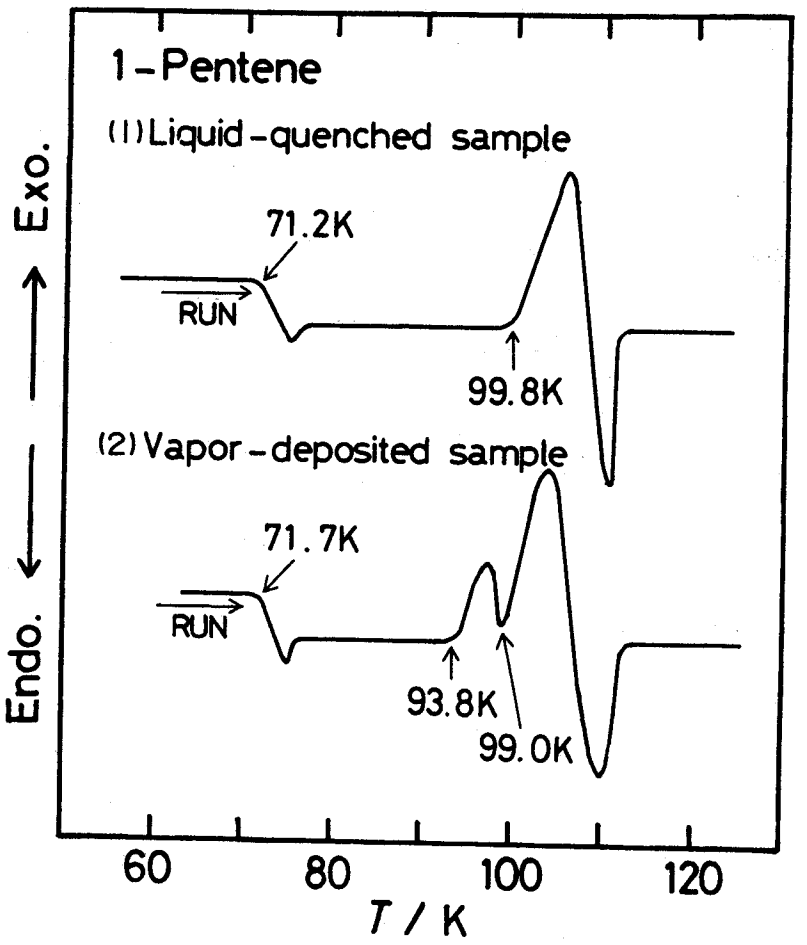

Fig. 3-3. Schematic DTA curve of glassy 1-pentene. Liquid-quenched sample was measured with the type II DTA apparatus, and vapor-deposited one with the type I apparatus.

tion for the same substance.

3-3-3 Propane and Propene

DTA curves of vapor-deposited propane are shown in Fig. 3-4. The glass transition was found at 45.5 K and the crystallization at 48.7 K. Another exothermic peak at 63.5 K would be due to irreversible transformation from an unidentified to the stable crystalline modifications. An endothermic peak at 85.4 K is due to fusion, which agrees with the literature value [4]. The broad exothermic peak at the initial stage of heating in Run 1 would result from an exothermic relaxation phenomenon characteristic of the vapor-deposited glasses [5]. The observation of this effect shows a successful vitrification of the sample on deposition. This kind of low-temperature enthalpy stabilization was not observed by the previous DTA apparatus [6]. Improvement of thermal stability and sensitivity made it possible to observe clearly, in agreement with the observation by an adiabatic calorimeter for vapor-deposited sample. Non-existence of the low temperature enthalpy relaxation for the vapor-deposited 1-pentene described in the previous section is due to the deposition temperature which is high enough to terminate the relaxation during the deposition process.

Runs 2, 3 and 4 are the reheating curves obtained after thermal treatments indicated by the broken lines. The glass transition was observed at the same temperature of 45.5 K for the samples that had not experienced crystallization at 48.7 K (Runs 2 and 3).

Figure 3-5 shows the results for propene. A broad exother-

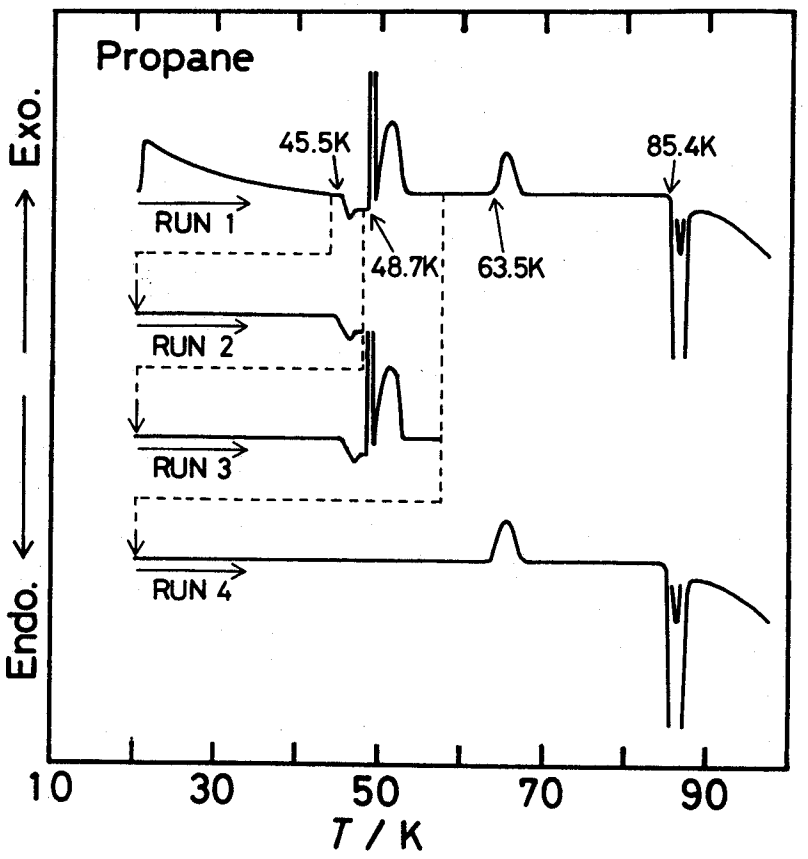

Fig. 3-4. Schematic DTA curves of vapor-deposited propane. Broken lines represent the thermal history of each sample.

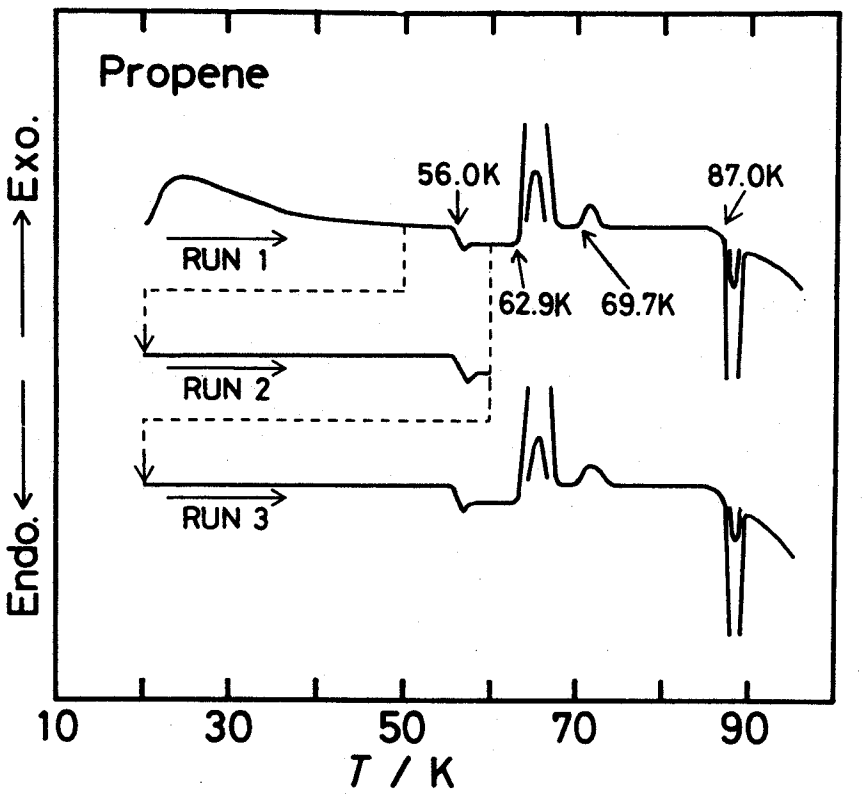

Fig. 3-5. Schematic DTA curves of vapor-deposited propene. Broken lines represent the thermal history of each sample.

mic effect due to the low-temperature relaxation was observed just above the vapor-deposition temperature. The glass transition at 56.0 K and crystallization at 62.9 K can be seen as in the case of propane. The endothermic effect around 87 K is a superposition of the fusion and evaporation. The glass transition temperature of this substance roughly agreed with previous value 55 K which was reported by Haida *et al* [6].

3-3-4 Other *n*-Alkanes

DTA curves of *n*-butane, *n*-pentane and *n*-hexane are shown in Figs. 3-6 to 3-8, respectively. All the samples exhibited the following common features. The first is a low-temperature exothermic effect which could be observed only in the initial period of the first heating experiment of the deposit. These phenomena are the same kind of effects as what was observed for propane or propene, and therefore, they confirm that the samples were successfully deposited to be glassy states as described before.

The second is that no indications of the glass transitions were observed on heating before the crystallization. Since most of *n*-alkanes belong to the fragile liquid [7], the heat capacity differences between their liquid and crystal at the melting point of the present *n*-alkanes are as large as that of propane, for which the glass transition was observed as described before. This means that the present DTA apparatus has enough sensitivity to detect the glass transitions of the present *n*-alkanes if ever. Therefore, we can conclude that the crystallization took place before the deposits reached hypothetical glass-transition temperatures for *n*-butane, *n*-pentane and *n*-hexane.

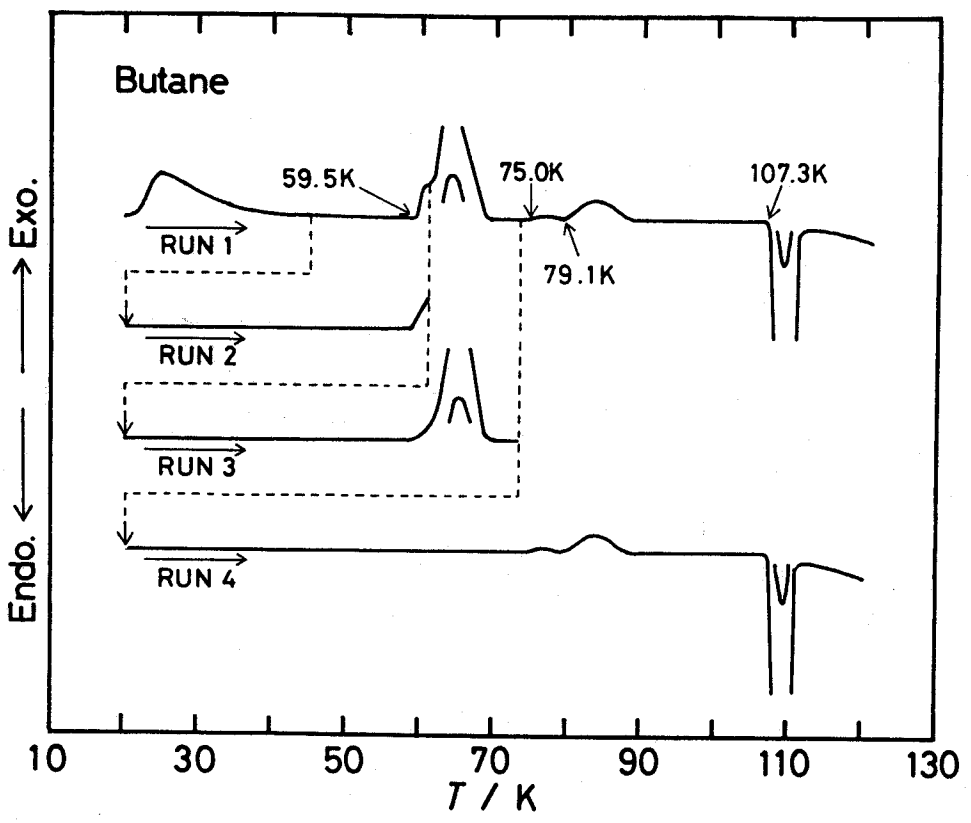

Fig. 3-6. DTA curves of vapor-deposited *n*-butane. Broken curves denote thermal histories experienced before runs 2, 3 and 4. The endothermic peak observed at 107.3 K is due to a solid-solid phase transition [4].

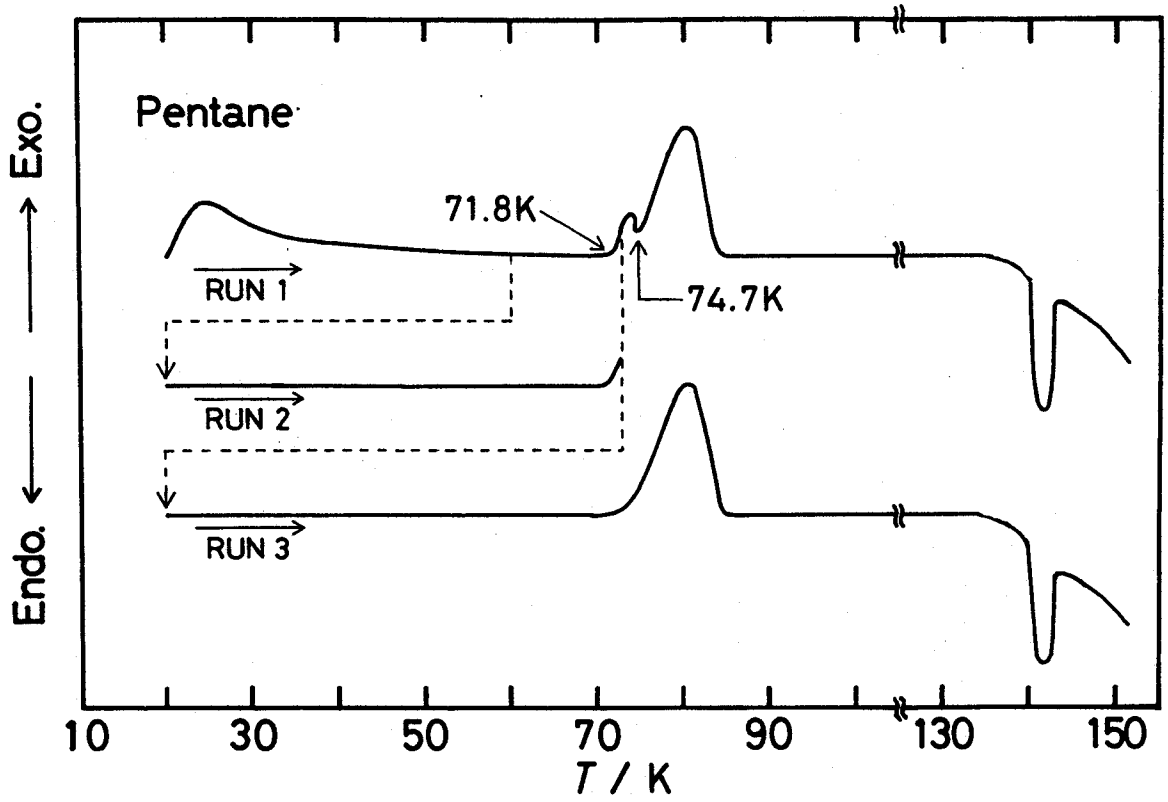

Fig. 3-7. DTA curves of vapor-deposited *n*-pentane. Broken curves denote thermal histories experienced before runs 2 and 3.

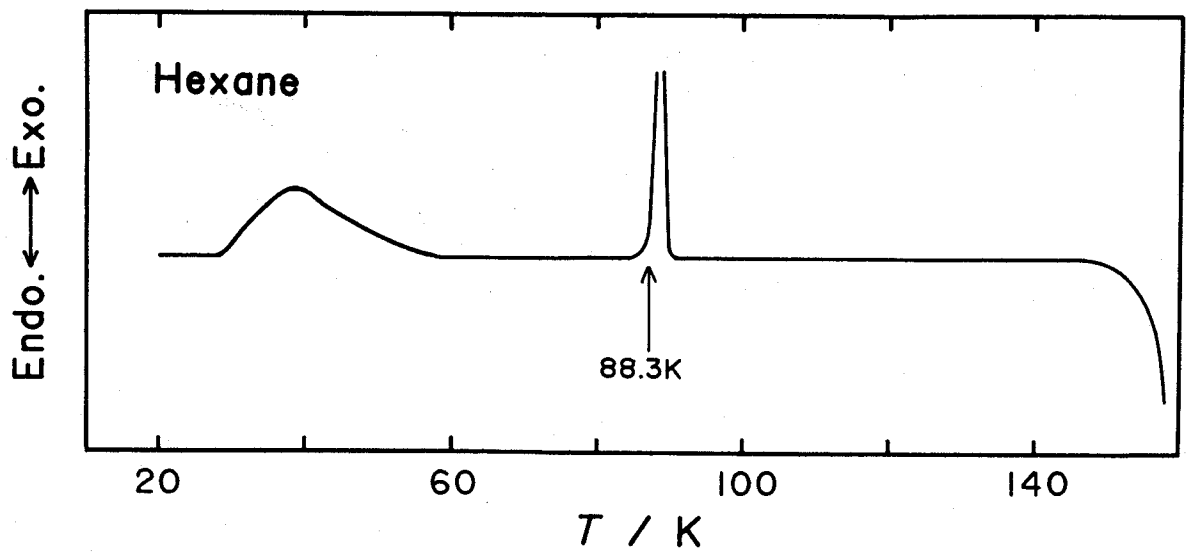

Fig. 3-8. DTA curve of vapor-deposited *n*-hexane.

3-3-5 Binary System Between *n*-Butane and 1-Butene

Figure 3-9 shows schematically DTA results for the binary systems $(C_4H_{10})_x(C_4H_8)_{1-x}$ with several values of x in the range $x > 0.5$. The glass transition phenomena were observed for all the samples of x = 0.50, 0.74 and 0.84 at 59.5, 62.0 and 61.9 K, respectively. Large exothermic anomalies above the glass transitions were due to crystallization. What should be noted here is that small exothermic effects were observed just below the glass transition points for x = 0.74 and 0.84. More detailed discussion will be given in the next section.

3-4 Discussion

3-4-1 Crystallization below Glass Transition Temperature

The glass transition is usually considered to be a freezing-in phenomenon of molecular configurations in the liquid state. According to this understanding, it is difficult to imagine the occurrence of microscopic molecular rearrangement below the glass transition temperature T_g, and still more difficult to expect there the crystallization which requires grand-scale molecular-ordering. The conclusion by Sugawara and Tabata as described later seems to be drawn based on such understanding. Confirmation of polymerization reaction of a γ-ray irradiated vinyl acetate [8] occurring just above its glass transition temperature supports also such a classical view.

On the other hand, there is an increased number of evidences which show the existence of residual atomic or molecular mobility within the overall frozen structure. The residual mobility in metallic glasses leads to some peculiar properties in these

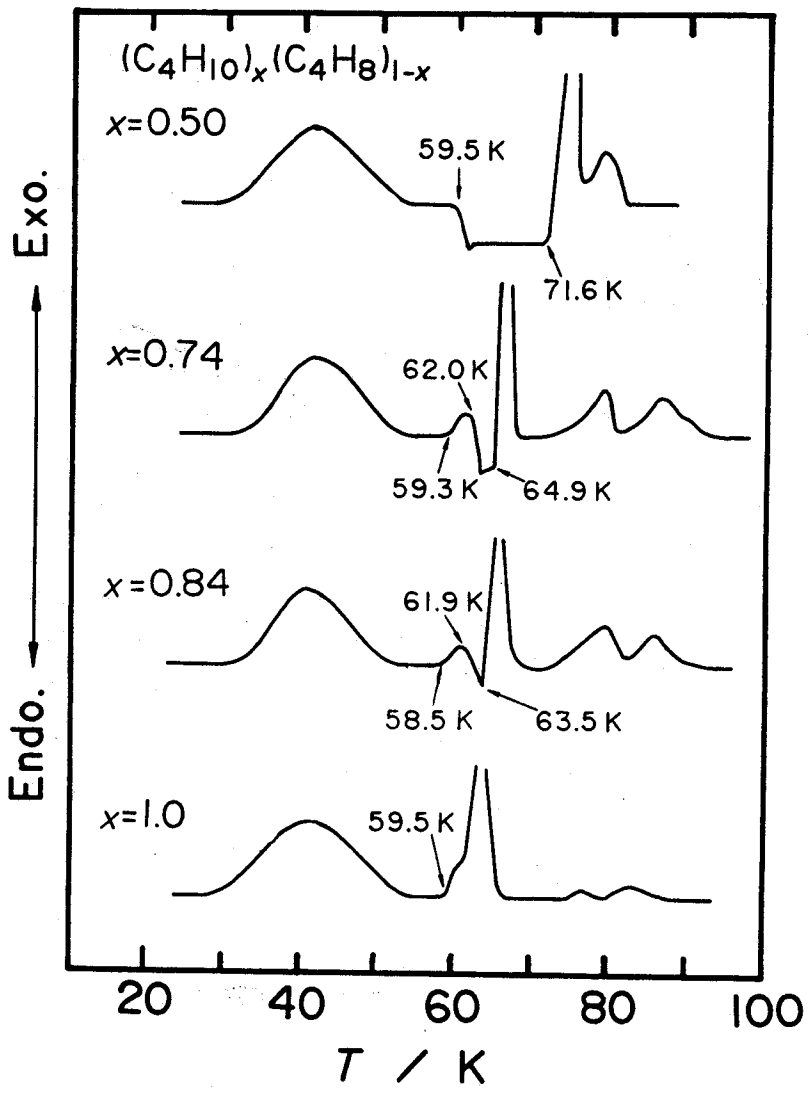

Fig. 3-9. DTA curves of the binary system of *n*-butane and 1-butene. Mole fraction of butane is indicated by *x*.

materials far below their T_g [9]. Certain alkali oxide glasses exhibit high mobility of ions within the frozen matrix [10]. Change in structure of some chalcogenide glasses induced by light irradiation arises from mobility of certain constituting elements below their T_g [11]. These observations can give an appropriate interpretation to the present result that there was no anomalous base-line shift due to glass transition in every DTA curve of the present *n*-alkanes before the crystallization took place. The classical view that the molecules in the glassy state are firmly immobilized is clearly inconsistent with present results.

The results of DTA experiments on $(C_4H_{10})_x(C_4H_8)_{1-x}$ with x = 0.74 and 0.84 could be interpreted in two ways. One is that the small exothermic phenomena below the glass transitions are due to a partial crystallization or a kind of its precursor. In this case, we would conclude that the vapor-deposited sample is able to crystallize even below the glass transition point. Another is that, neglecting the exothermic phenomena ahead of the glass transitions, the large anomalies above the glass transition points are regarded as due to the global crystallization. In this case, it can be seen from Fig. 3-9 that the crystallization temperature decreased with the mole fraction x of *n*-butane. The observed glass-transition and crystallization temperatures were plotted against x in Fig. 3-10. The crystallization temperature decreased linearly and intersects the glass-transition line around x = 0.87. Extrapolating T_g line to x = 1.0, we obtain the hypothetical T_g for *n*-butane to be 63.5 K, which is definitely higher than its crystallization temperature T_{cryst} = 59.5 K. This allows us to conclude that the vapor-deposited *n*-butane

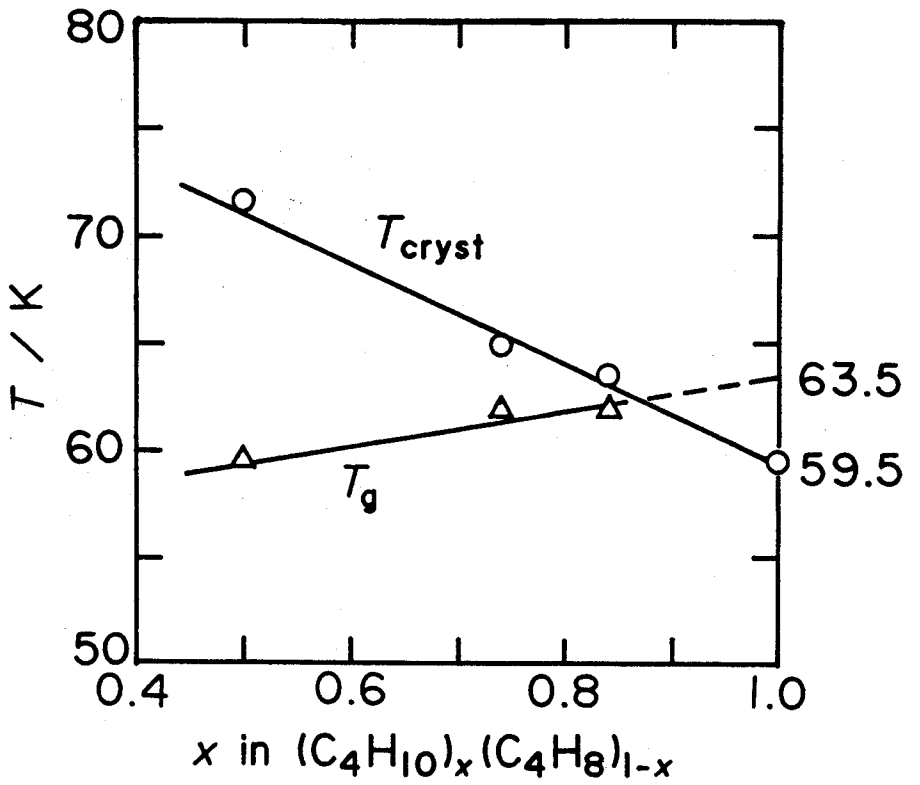

Fig. 3-10. Temperatures of crystallization T_{cryst} and glass-transition T_g plotted against mole fraction of *n*-butane.

crystallized below T_g. In both cases, anyway, we reached the same conclusion that some vapor-deposited samples may crystallize even below T_g. In this way, the present binary system provides an interesting example in that the vapor-deposited mixture crystallizes before or after the glass transition temperature depending on the composition. The threshold composition may depend on the experimental time scale.

Angell [10] has reviewed the competition problem between the glass transition and crystallization process in terms of two time scales, τ_{in} and τ_{out}. The former is a characteristic time for the structural relaxation in the metastable phase and the latter a kinetic parameter governing the crystallization into the stable phase. He cited an interesting binary system Na_2O-B_2O_3 in which the compositional change produced partial masking of endothermic glass transition by the immediately-followed exothermic crystallization in otherwise well-separated peaks. This phenomenon can be interpreted by the intersection of temperature dependence of τ_{in} and τ_{out}. The thermal behavior will be controlled delicately by a complex combination of nucleation at low temperature and crystal growth at high temperature. There is an analogy between the system cited above and the present system of $(C_4H_{10})_x(C_4H_8)_{1-x}$. In the case of crystallization below T_g, however, the effect of the enthalpy relaxation should be taken into consideration. The vapor-deposited sample shows the low-temperature enthalpy relaxation associated with the lowering of the fictive temperature which characterizes a non-equilibrium structure of glass. Since these characteristic times might be determined by the fluctuational change of the structure, their

values would be governed more or less by the fictive temperature. Therefore, we can conclude that the crystallization will occur even below T_g if the fictive temperature of the system happens to reach some value at which τ_{in} and τ_{out} intersect with each other.

This kind of crystallization below the glass transition has been observed in metallic glasses and $Ca(PO_3)_2$ as mentioned in the introduction of this chapter. The classical view that the crystallization of liquid-cooled glass is not likely to take place below the glass transition comes from the Einstein-Stokes relation,

$$\eta D = k_B T / 6\pi r, \qquad (3\text{-}1)$$

where η, D and r are viscosity of liquid, diffusion constant and radius of constituent molecules, respectively. With the increase in η up to the order of 10^{13} Pa s, all the diffusional motions of molecules in liquid are virtually still. The physical basis of this equation is that the force hindering the motion of a molecule in liquid is a viscous drag due to coupling of the molecular motion to that of other molecules. The residual and massive mobility below the glass transition therefore implies a substantial breakdown of the Einstein-Stokes relation as the temperature approaches the glass transition region.

It was pointed out that decoupling between self-diffusion of constituent molecules and viscous flow of liquid took place far below T_g [12] and that the above relation was valid above T_g but not below T_g [13]. In addition, self-diffusional molecular-

motion played an important role in the crystallization process below T_g, although viscous flow was important above T_g. In the case that the constituent of the glass possesses enough diffusivity crystallization would be able to occur even below T_g. For the metallic glasses, ultra-fast quenching with the rate ranging at least 10^6 - 10^8 K s^{-1} was necessary for avoiding the nucleation and growth in the undercooled liquid region. For the molecular glasses, vapor-condensation technique was efficient for rapid extraction of the thermal energy during the transformation from the original liquid to the final non-crystalline state. In addition to the diffusional process, overall and internal rotational degrees of freedom must take into account in the micromechanism of the crystallization of the present molecular glass. These additional motions will give better glass-forming ability to the *n*-alkanes compared to the metallic liquids.

Since the glass transition is a kinematic phenomenon characterized by the interrelation of time scales between molecular motions and experimental observation, the behavior of glass in the glass transition region is strongly dependent on the cooling and/or heating rate. For instance, the molecular-dynamics simulation of the Lennard-Jones liquids showed that the microscopic structure of the glass is conspicuously dependent on the cooling rate [14]. Namely, the lower the cooling rate becomes, the larger the scale of short- and/or medium-range order is developed in the glass. In such situation, the molecular diffusivity would be decreased. In the present vapor-deposition technique, the kinetic energy of the depositing molecules was dissipated so rapidly that the molecules did not have sufficient opportunity to

organize themselves into ordered array before the kinetic energy has decreased below a threshold value for that. Consideration of geometry of the present DTA apparatus gives an estimate of the corresponding quench rate at higher than 10^6 K s^{-1}. Thus, constituents of the vapor-deposited glasses would possess considerably high molecular diffusivity in its nature. On the other hand, the heating rate in the present study was less than 0.05 K s^{-1}. Under such a low heating rate, crystallization would be able to start and proceed in some substances. Generally speaking, if the glass was prepared under extremely high cooling rate and heated at much lower rate, crystallization may take place below the temperature of glass transition which depends on the heating rate. In the case reported by Luborsky, the glassy state was prepared by melt-spinning technique in which the cooling rate achieves 10^6 - 10^8 K s^{-1}, and therefore the above-mentioned condition is still held.

According to this understanding, it is supposed that crystallization is not likely to occur below T_g in the ordinary experimental time scale for the glassy sample which is prepared by the conventional liquid-cooling method. But if annealed for an extraordinary long time, a liquid-cooled sample would crystallize as well even below T_g. This is naturally consistent with the fact that the glass is a metastable state. The liquid-cooled glass would have a possibility to crystallize below the conventionally determined glass transition temperature, provided the ratio of cooling to heating rates, nearly 10^8 as in the present study, could be hold. The heating rate in this case comes to around 10^{-8} K s^{-1}, which corresponds to 10^3 days anneal-

ing during the traverse of temperature interval of 1 K.

These considerations remind us the argument by Kauzmann [15] concerning the way avoiding possible entropy catastrophe in an equilibrium liquid that occurs below a critical temperature, referred to as the Kauzmann temperature T_K or the ideal glass-transition temperature [16]. In order to keep the equilibrium liquid structure at a temperature below its T_g conventionally defined, we must wait a long time by the prolonged relaxation time for reorganization of the molecular arrangement. The lower the temperature to which equilibrium is maintained, the longer it takes to reach the state. Kauzmann pointed out the possibility of instability for the liquid phase in the sense that relaxation out of the glassy state to the corresponding crystalline phase occurs likely during waiting for the internal equilibrium within it. However, Angell *et al.* negatively discussed the possibility of the equilibrium instability in supercooled liquid below T_g [17]. From the calculation of nucleation induction time for $Li_2O \cdot 2SiO_2$, they concluded that, at least in the equilibrium state, the nucleation induction time of this substance does not necessarily shorten with decreasing temperature, and thus the instability of liquid would not occur above T_K. According to this conclusion, it seems valid that crystallization does not proceed by fluctuation within the equilibrium structure but by that under the non-equilibrium structure. Namely, the fundamental processes of structural relaxation may promote the crystallization.

3-4-2 Tendencies of Glass Formation and Crystallization

Figure 3-11 shows the experimental results of the T_g, T_{cryst} and T_b/T_{fus} plotted against carbon number n for n-alkanes and 1-alkenes, where T_b and T_{fus} denotes the normal boiling and fusion temperatures, respectively. With failure in the vitrification of ethane and ethene, n = 2, the following discussion will be limited to $n \geq 3$. The glass transition was observed for propane and all the 1-alkenes, whose T_b/T_{fus} values are 2.5 or larger, but not for the substances with T_b/T_{fus} around 2.0. The latter ones are considered to have crystallized below T_g, as described above. Such a correlation between observability of glass transition and the ratio is just the same as has been pointed out in relation to the ability of glass formation by the liquid-cooling method [18]. Thus the ratio of T_b/T_{fus} can be regarded as a measure of appearance of the glass transition phenomenon irrespective of the method for glass formation, though there exists no definite value of the critical ratio. In other words, the substance with poor glass-forming ability has likely a tendency to crystallize below the glass transition temperature during warming of the vapor-deposited state. This is interpreted in terms of the concept of fictive temperature T_f as follows. The glass formed by the vapor deposition at lower temperature has higher fictive temperature in the molecular configuration, and short- or medium-range order develops with increasing the temperature of vapor deposition, resulting in the decrease of the fictive temperature. Namely, the effect of heating of vapor-deposited glass corresponds more or less to that of decreasing the fictive temperature of the equilibrium liquid down to the so-called *crystallization-danger-*

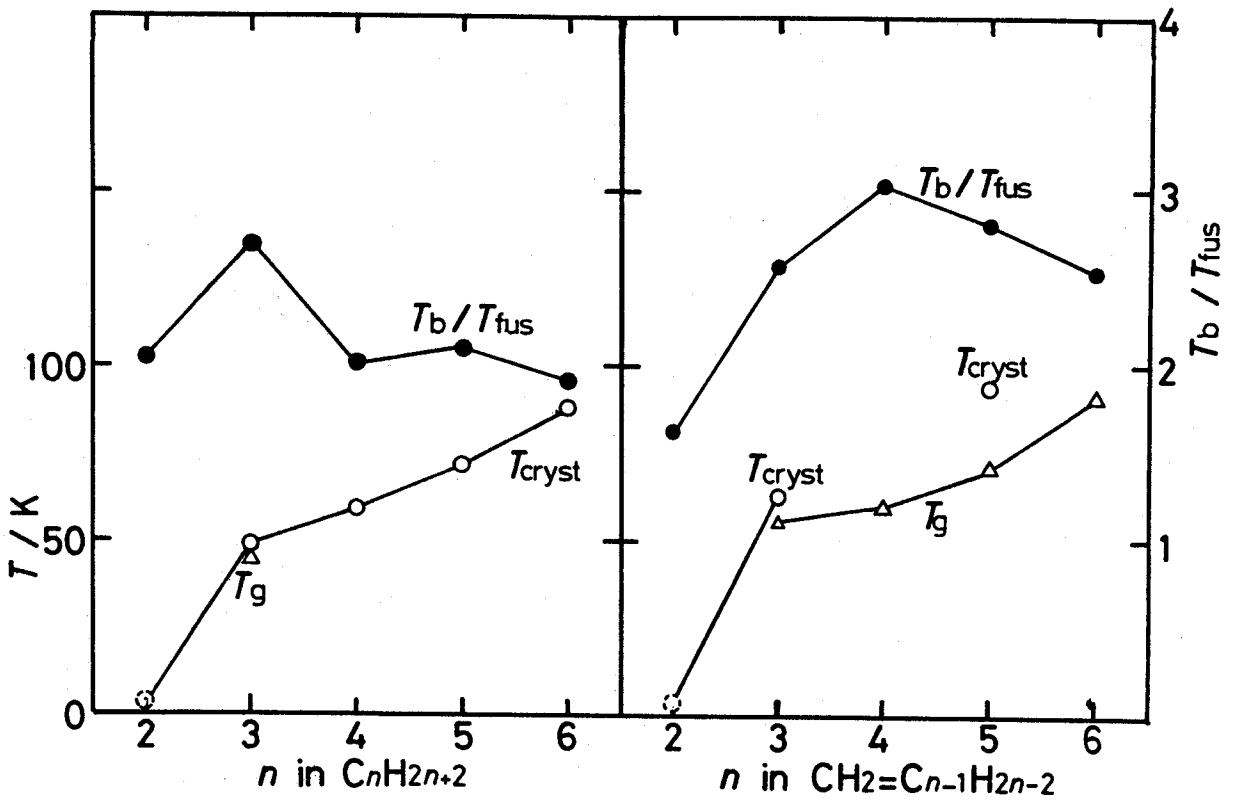

Fig. 3-11. Variations of glass transition temperature T_g, crystallization temperature T_{cryst} and ratio T_b/T_{fus} with carbon number of aliphatic hydrocarbons.

ous region.

The difference in crystallization tendency between *n*-alkanes and 1-alkenes is noted in the present study. This demonstrates an important role of the presence of a double C=C bond in the molecule for the hindrance to crystallization. The replacement of the single with the double bond at a molecular end seems to bring into the properties of molecule the following two main effects; loss of the rotational degree of freedom about the bond axis and asymmetrization of the molecule as a whole. These two factors would not cause significant Gibbs energy change in their liquid states at high temperatures, as implied by the similar values of their boiling temperatures of the corresponding *n*-alkanes and 1-alkenes. However nucleation and growth processes require additional head-to-tail ordering of 1-alkene molecules compared to the case of *n*-alkanes. The fluctuational reorientation of the 1-alkene molecules required for the head-to-tail ordering is not believed to happen easily in a viscous state. In addition, Gibbs energy of 1-alkene would be affected largely by poor molecular packing in the crystal arising from the above factors. The last problem has discussed quantitatively by Wong and Angell [19] from the thermodynamic point of view in the case of fluorotoluene isomers. Both the kinetic and thermodynamic aspects will enhance much the glass-forming ability of 1-alkenes.

Figure 3-12 shows the carbon number dependence of the ratios of T_g and T_{cryst} to T_{fus}. The ratios T_g/T_{fus} for 1-alkenes are all distributed around 2/3 indicated by the broken line. This agrees quite well with the empirical relation which has been observed in other systems [20], although there exists no rigorous

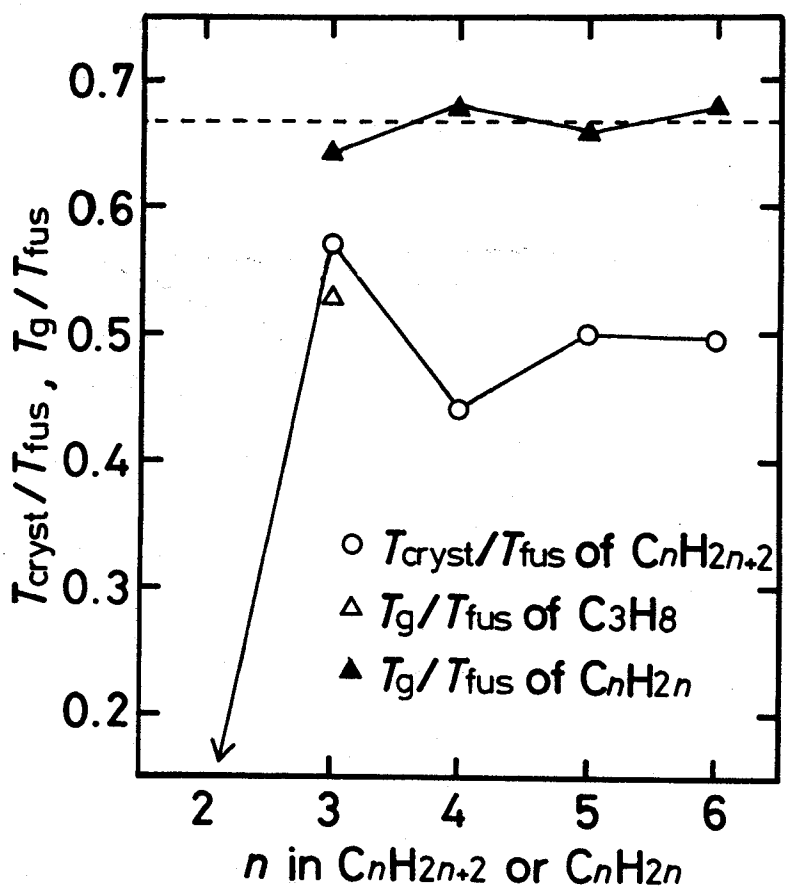

Fig. 3-12. Variations of ratios T_g/T_{fus} and T_{cryst}/T_{fus} with carbon number of aliphatic hydrocarbons.

theoretical basis. But values of the ratio for some simple substances become much smaller than that value, e.g. that of propane, for which the glass transition was observed uniquely among *n*-alkanes, is 0.53, and that of tetrachloromethane CCl_4 is 0.24 [21]. On the other hand, the values of T_{cryst}/T_{fus} of vapor-deposited *n*-alkanes are found to be around 0.5 except for ethane. Although the real temperatures of the sample during the crystallization might be higher than 4.2 K owing to the heat of condensation, their T_{cryst}/T_{fus} values should be smaller than 0.5 which corresponds to about 35 K of T_{cryst}. Thus the properties of such simple substances can not be easily predicted from those of larger molecules.

3-4-3 Comparison with RTL Data

A study on the low temperature property of vapor-deposited hydrocarbons has been carried out by Sugawara and Tabata [3] by using the RTL technique. They observed two types of spectrum peaks which they called *unstable* and *stable* peaks. They emphasized the existence of correlation between phase transitions and RTL peaks, and concluded that the unstable peak temperature $T_{unstable}$ is related to T_g in the manner that T_g is a few Kelvin lower than $T_{unstable}$. In Table 3-1, RTL peak temperatures were summarized with our results of T_g, T_{cryst} and so on. They observed unstable peaks for all substances except for ethene, and estimated T_g for each substance. In the present work, however, all alkanes but for propane did not exhibit the glass transition phenomena. In particular, in the case of ethane the vitrification was failed and only the stabilizations between crystalline

Table 3-1. Comparison of temperatures at which some anomalies were observed in DTA and RTL experiments.

* : present work; ** : after Sugawara and Tabata [3].

Compounds	DTA*			RTL**	
	T_g/K	T_{cryst}/K	T_{trs}/K	$T_{unstable}$/K	T_{stable}/K
ethane	-	-	23.9 29.0	30.6	
propane	45.5	48.7	63.5	48.6	85.9
n-butane	-	59.5	75.0 79.1	65.1	110
n-pentane	-	71.8	(74.7)	76.2	143.5
propene	56.0	62.9	69.7	61.4	89.7

phases were observed at 23.9 and 29.0 K. Considering the difference in experimental methods, it seems sure that the unstable peak of ethane at 30.6 K corresponds to either of these irreversible transformations. For other substances, $T_{unstable}$ roughly agree with the crystallization temperature observed in the present work. Considering these results, we can conclude as follows. Firstly, the RTL unstable peaks are correlated with irreversible phase changes including crystallization. Secondly, their assertion that T_g is given as the temperature a few Kelvin lower than the $T_{unstable}$ is reasonable only for the substances which can be captured in the vitreous states by the vapor deposition and do not crystallize below the conventionally defined T_g. Thus the correlation would not be observed in general as the substance becomes simpler.

References to Chapter 3

[1] F. E. Luborsky, *Mat. Sci. Eng.*, 28, 139 (1977).

[2] Y. Abe, *Nature*, 282, 55 (1979); Y. Abe, T. Arahori and A. Naruse, *J. Am. Ceram. Soc.*, 59, 487 (1976).

[3] I. Sugawara and Y. Tabata, *Chem. Phys. Lett.*, 41, 357 (1976).

[4] J. Timmermans, *Physico-Chemical Constants of Pure Organic Compounds*, Elsevier, Amsterdam (1950).

[5] H. Hikawa, M. Oguni and H. Suga, *J. Non-Cryst. Solids*, 101 90 (1988).

[6] O. Haida, H. Suga and S. Seki, *J. Non-Cryst. Solids*, 22 219 (1976).

[7] C. A. Angell, *J. Non-cryst. Solids*, 73, 1 (1985).

[8] K. Nakatsuka, K. Adachi, H. Suga and S. Seki, *J. Polym. Sci.*, 6, 779 (1968).

[9] H. S. Chen, *Rep. Prog. Phys.*, 43, 354 (1980).

[10] C. A. Angell, *J. Non-cryst. Solids*, 102, 205 (1988).

[11] S. I. Smedley and C. A. Angell, *Mat. Res. Bull.*, 15, 421 (1980).

[12] U. Koester, *Dynamic Aspects of Structural Change in Liquids and Glasses*, p.39, Edited by C. A. Angell and M. Goldstein, N. Y. Acad. Sci., New York (1986).

[13] A. L. Greer, *J. Non-cryst. Solids*, 61&62, 737 (1987).

[14] F. Yonezawa, S. Nosė and S. Sakamoto, *J. Non-cryst. Solids*, 95&96, 83 (1987).

[15] W. Kauzmann, *Chem. Rev.*, 43, 219 (1948).

[16] C. A. Angell, *J. Am. Ceram. Soc.*, 51, 117 (1968).

[17] C. A. Angell, D. R. MacFarlane and M. Oguni, *Dynamic Aspects of Structural Change in Liquids and Glasses*, p.241, Edited by C. A. Angell and M. Goldstein, N. Y. Acad. Sci., New York (1986).

[18] M. H. Cohen and D. Turnbull, *J. Chem. Phys.*, 34, 120 (1960).

[19] J. Wong and C. A. Angell, *Glass: Structure by Spectroscopy*, Marcel Dekker, New York (1976).

[20] S. Sakka and T. D. Mackenzie, *J. Non-cryst. Solids*, 6, 145 (1971).

[21] O. Haida, H. Suga and S. Seki, *Thermochim. Acta*, 3, 177 (1976).

Chapter 4

GLASS TRANSITIONS OF BINARY MIXTURES OF HYDROCARBONS

4-1 Introduction

One of the most interesting subjects in the solution is the dynamics of the constituent molecules, in which the intramolecular mode-mode coupling and intermolecular correlation are argued along with the local structure around each molecule. The glass transition of binary mixtures can be accounted for as the dynamical property of the molecular motions in the ultra-slow regime. From such interests, some experimental studies on the composition dependence of the glass transition temperatures have been carried out for ionic solutions [1], alcohols [2] and organic halides [3].

The configurational entropy is the thermodynamic quantity related to the correlation between molecules and is expected to play an important role in describing the kinetic properties of liquid near the glass transition temperature. It is also an interesting problem how the entropy of mixing is included in the configurational entropy. Based on the entropy theory, a phenomenological treatment about the glass transition temperatures of binary systems was developed by Gordon *et al.* [4] (GRGR theory). The GRGR theory is interesting in the sense that it has established the method to predict the composition dependence of T_g only from the thermodynamic quantities of both pure components with no adjustable parameter within the framework of their model.

The basic idea is that the glass transition is a kinetic manifestation of the underlying second-order phase transition that may occur at T_K in an equilibrium liquid as suggested by Adam and Gibbs [5].

In this chapter, composition dependence of the glass transition temperatures was investigated for the binary mixtures of simple hydrocarbons. The DTA technique was utilized to determine the glass transition temperatures. Compared with the binary systems previously studied, the present systems have simple molecular structures and intermolecular interactions. The glassy states were obtained by vapor-deposition so as not to allow phase separation and/or crystallization during preparation. The purpose of the present experiment is to understand the composition dependence of the glass transition temperature from the entropic point of view. The GRGR theory was used to analyze the data. The validity of the GRGR theory was argued and sight extension of the theory was made.

4-2 Entropy Theory of Binary Glass

The composition dependence of T_g is known to be reproducible empirically by the hyperbolic form [4]

$$T_g(x) = \frac{x\,T_{g1} + C(1-x)\,T_{g2}}{x + C(1-x)}, \qquad (4\text{-}1)$$

where x is the mole fraction of component 1, and T_{g1} and T_{g2} are the glass transition temperatures of the component 1 and 2, respectively. The constant C is only one adjustable parameter in this expression. It has been theoretically confirmed by Gordon

et al. that the composition dependence of T_K is also reproducible by Eq. (4-1). They supposed that the composition dependence of T_g is similar to that of the Kauzmann temperature T_K. Practically speaking, the composition dependence of T_K was assumed to have the same functional form as Eq. (4-1) with identical value of the parameter C. The composition dependence of T_g is predictable from that of T_K.

The next step is to determine the composition dependence of T_K. Since T_K is the temperature at which the configurational entropy vanishes, the T_K can be evaluated from the data of heat capacity and the entropy of fusion by use of the relation

$$\Delta_{fus}S = \int_{T_K}^{T_{fus}} \frac{C_p^{liq} - C_p^{cr}}{T} dT. \qquad (4\text{-}2)$$

The thermodynamic data of the mixture have seldom been measured so that the T_K value is approximately estimated by means of the thermodynamic data of pure substances as follows.

In general, the entropy of mixing $\Delta_{mix}S$ is given by

$$\Delta_{mix}S = -R[x \ln x + (1-x) \ln (1-x)] + \Delta_{mix}S^E, \qquad (4\text{-}3)$$

where the last term is excess entropy of mixing. Gordon *et al.* treated the mixture as the regular solution in which the excess entropy of mixing $\Delta_{mix}S^E$ is assumed to be zero independently of temperature. Then Eq. (4-3) becomes

$$\Delta_{mix}S = -R[x \ln x + (1-x) \ln (1-x)]. \qquad (4\text{-}4)$$

In the case of binary system, its solid solution is taken as the reference state for the evaluation of the configurational entropy. The entropies of liquid solution (LS) and solid solution (SS) are given by

$$S^{LS}(x, T) = x\, S_1^{liq}(T) + (1-x)\, S_2^{liq}(T) - R\,[\, x \ln x + (1-x) \ln (1-x)\,] \qquad (4\text{-}5)$$

and

$$S^{SS}(x, T) = x\, S_1^{cry}(T) + (1-x)\, S_2^{cry}(T) - R\,[\, x \ln x + (1-x) \ln (1-x)\,], \qquad (4\text{-}6)$$

respectively. Here, the expression S_i^{α} was used for the entropy of pure component i in the phase α. Subtraction of Eq. (4-6) from (4-5) gives simply,

$$S_c(x, T) = x\, S_{c1}(T) + (1-x)\, S_{c2}(T). \qquad (4\text{-}7)$$

This result indicates that the configurational entropy of the regular solution is additive as a function of the mole fraction of pure components.

The Kauzmann temperature T_K at a given mole fraction is obtained by the following equation

$$S_c(x, T_K) = 0, \qquad (4\text{-}8)$$

where $S_c(x, T_K)$ is calculated by using Eqs. (4-5) to (4-7) with

the heat capacities of pure components. Then the parameter C of Eq. (4-1) is determined by fitting (x, T_K) data with the least squares method, and the composition dependence of T_g can be calculated by using Eq. (4-1) and the common value of C.

4-3 Experimental

The commercial materials of propane (Gasukuro Kogyo Inc.; 99.5 %), propene (Gasukuro Kogyo Inc.; 99.5 %), 1-butene (Tokyo Kasei Kogyo Co. Ltd.; 98.5 %) and 1-pentene (Tokyo Kasei Kogyo Co. Ltd.; 98.5 %) were used without further purification. Four binary systems of propene-propane, propene-1-butene, propene-1-pentene, and 1-butene-1-pentene were prepared. Preparation of a mixture was done in the same way as described in chapter 3 for the system between *n*-butane and 1-butene. Special caution was taken so that the sample mixture was not partially on a wall of the sample container in order to guarantee the uniform composition of the sample gas throughout the deposition. The heating rates of subsequent DTA experiments were about 2 K min^{-1} and 1 K min^{-1} in the type I and type II apparatuses, respectively.

The experimental DTA curves of 1-butene obtained by both the apparatuses were shown in Fig. 4-1. The glass transition temperature was determined as an intersection of the extrapolations of base-line and rising part of the base-line shift. The precision of the determined temperature was within $\pm$ 0.3 K.

4-4 Results and Discussion

4-4-1 Results of DTA Experiment

Figures 4-2 to 4-5 show the schematic drawings of the DTA

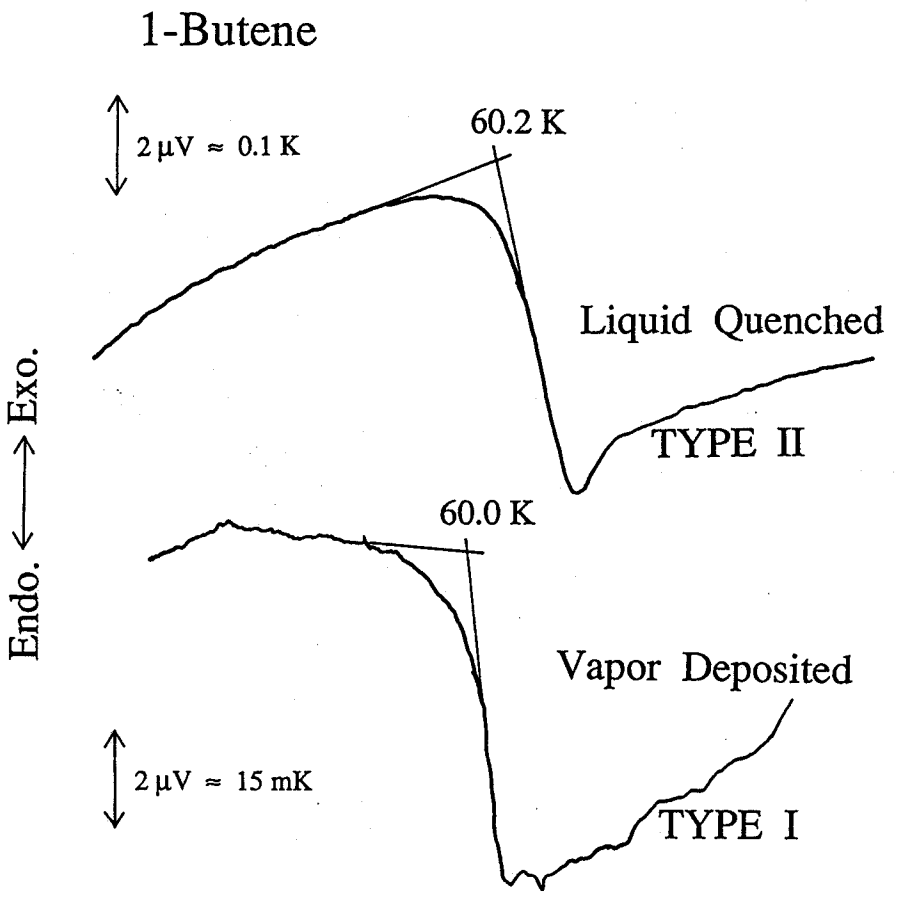

Fig. 4-1. Experimental DTA curves around the glass transition temperature of 1-butene. The upper is for the liquid-quenched sample measurted by the type II apparatus, and the lower the vapor-deposited sample by type I.

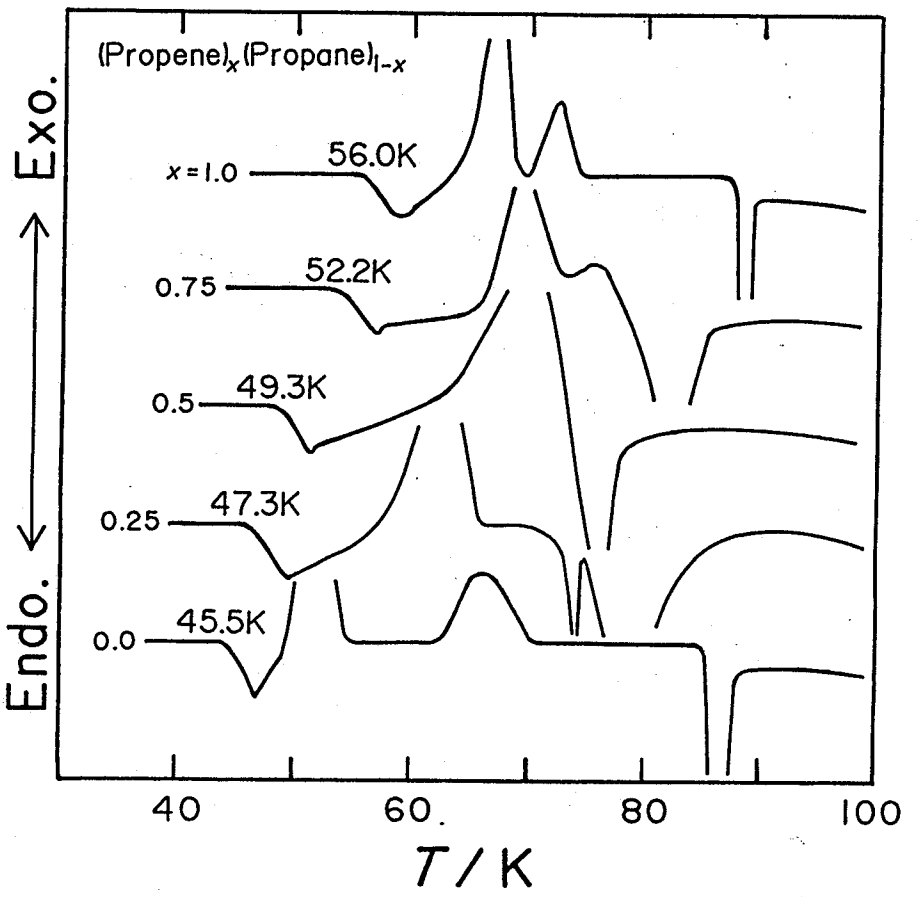

Fig. 4-2. Schematic DTA curves for vapor-deposited samples of (propene)$_x$(propane)$_{1-x}$ system measured by the type I apparatus.

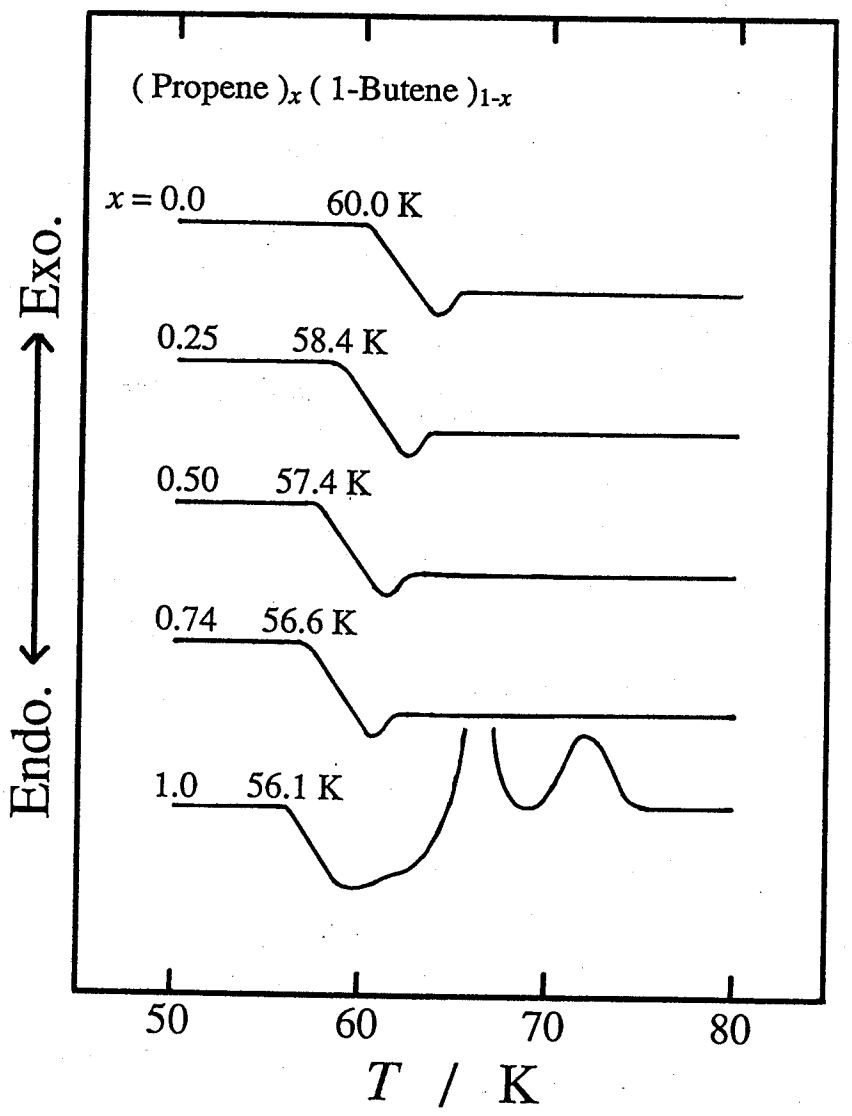

Fig. 4-3. Schematic DTA curves for vapor-deposited samples of (propene)$_x$(1-butene)$_{1-x}$ system measured by the type I apparatus.

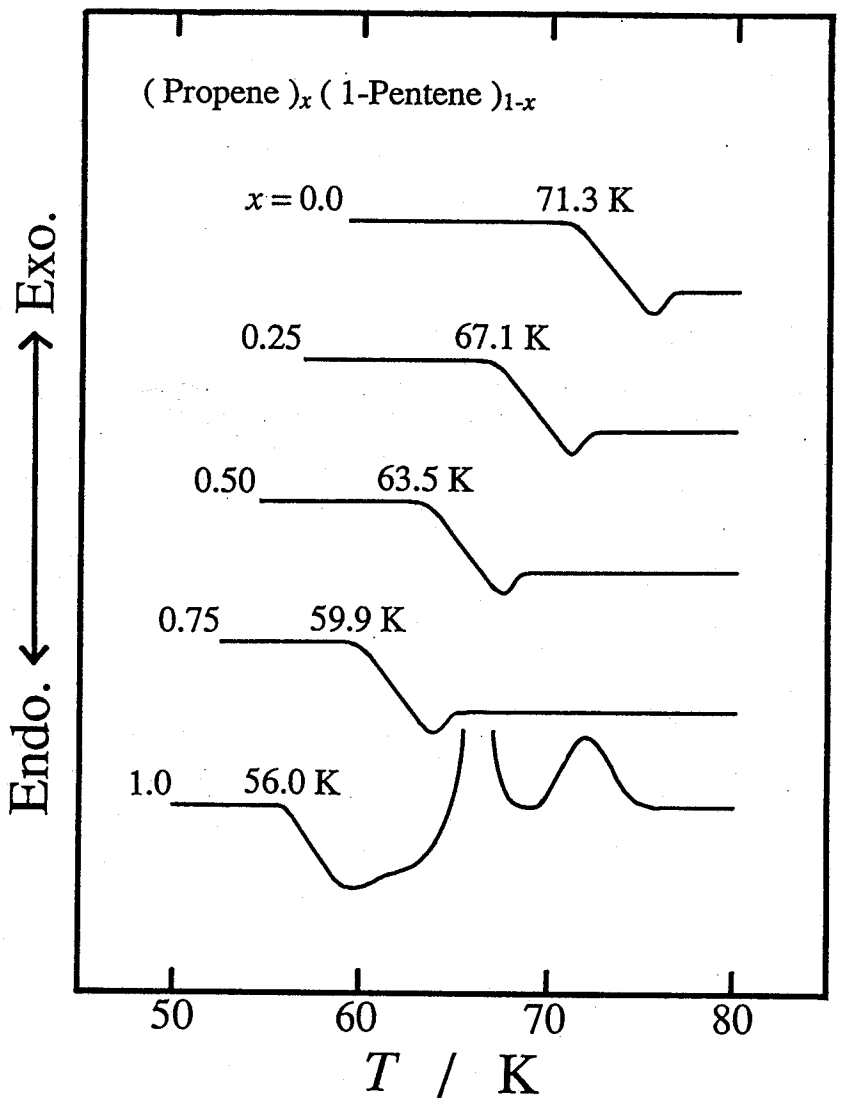

Fig. 4-4. Schematic DTA curves for vapor-deposited samples of (propene)$_X$(1-pentene)$_{1-X}$ system measured by the type I apparatus.

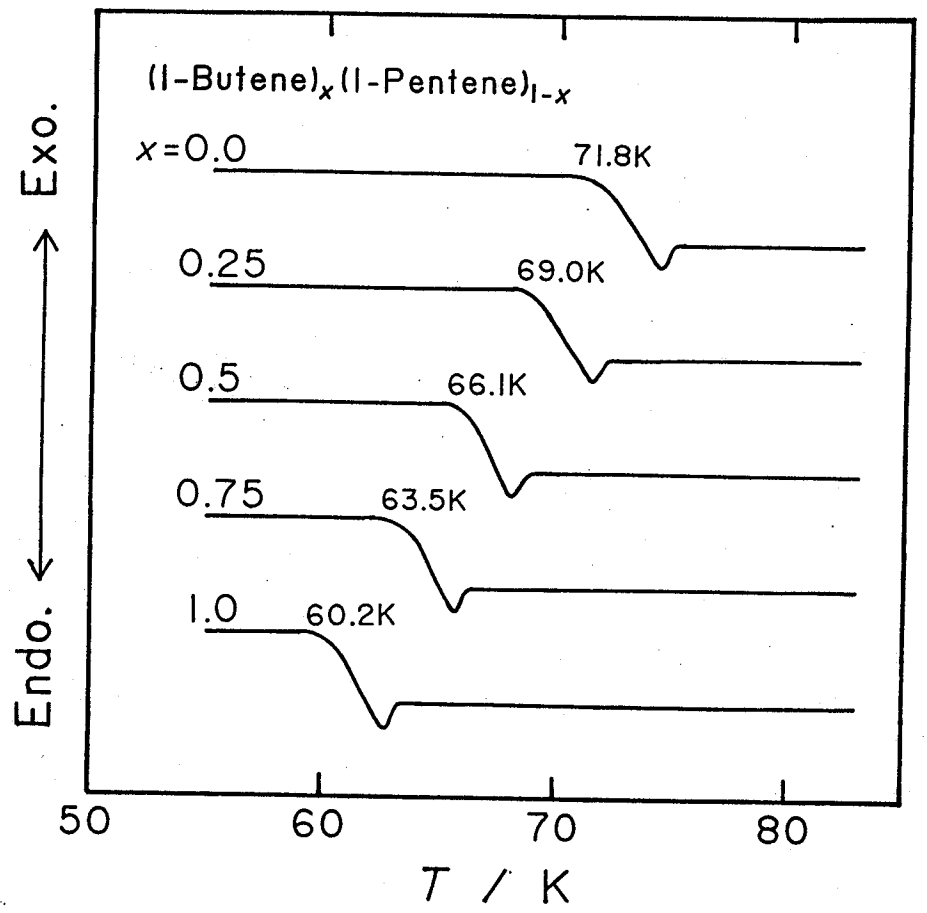

Fig. 4-5. Schematic DTA curves of liquid-quenched samples of (1-butene)$_x$(1-pentene)$_{1-x}$ system measured by the type II apparatus.

curves. For all the systems, a step-like anomaly due to the glass transition was observed. The determined glass transition temperatures were shown in each figure.

In the cases of the pure propene and the propene-propane system, some exothermic peaks were observed following to the glass transition. These effects are due to the crystallization and stabilizations from an unidentified metastable to the stable crystal. The endothermic peak observed in the higher temperature region is due to the fusion process. The fusion for x = 0.25 was clearly split into a sharp and a broad peaks. This type of fusion phenomenon is observed for systems exhibiting a eutectic point. In the present system, the phase separation could take place on crystallization. No indications of the eutectic melting for the x = 0.5 and 0.75 samples are probably due to the fact that temperature difference between the eutectic point and the liquidus line is too small to be detected separately by DTA.

The observed T_g data were plotted against the mole fraction in Figs. 4-6 to 4-9. In all the systems, T_g changed monotonously against the composition. The solid lines are the best curves of T_g fitted to Eq. (4-1). Each value of the parameter C determined by the least squares method is shown in Table 4-1.

4-4-2 Analyses in Terms of the GRGR Theory

The configurational entropies of the pure substances were evaluated from the data of the heat capacity and entropy of fusion by using Eq. (4-2). The extrapolations of the heat capacities of the equilibrium liquid and crystal were carried out by the least squares fitting to polynomial functions. The deter-

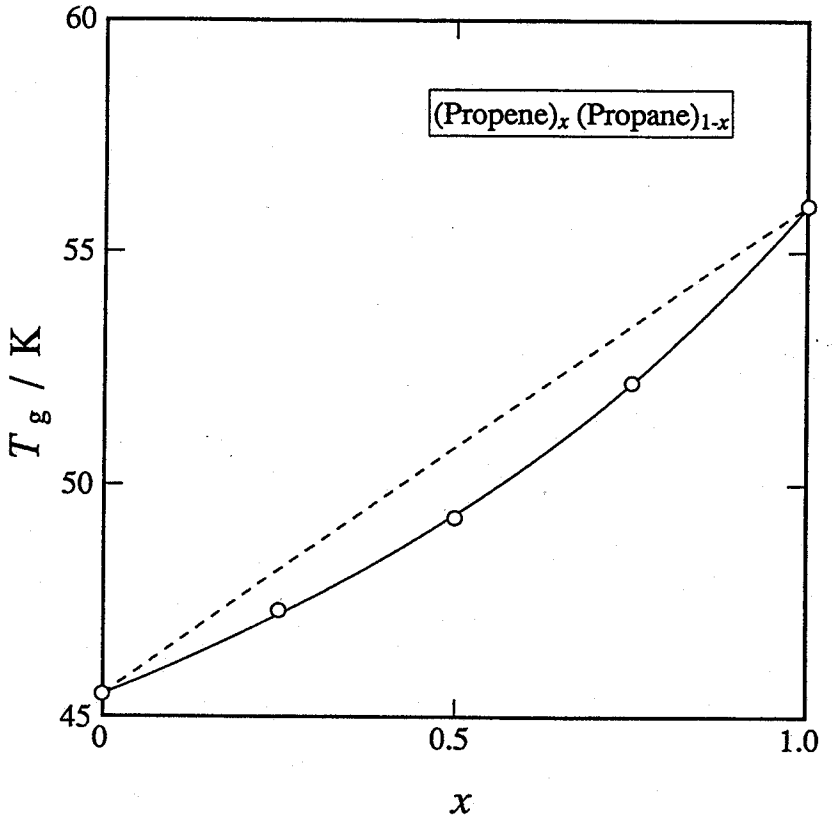

Fig. 4-6. The composition dependence of the glass transition temperature in (propene)$_X$(propane)$_{1-X}$ system. The solid curve denotes the optimized curve fitted to Eq. (4-1), and the broken curve is predicted T_g variation by the GRGR theory.

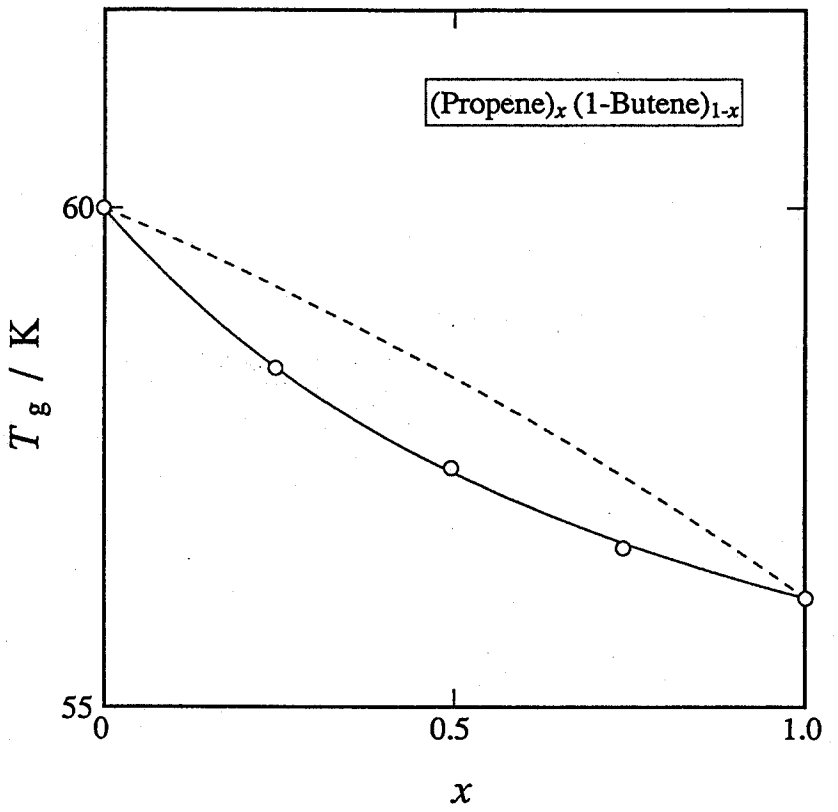

Fig. 4-7. The composition dependence of the glass transition temperature in (propene)$_X$(1-butene)$_{1-X}$ system. The solid curve denotes the optimized curve fitted to Eq. (4-1), and the broken curve is predicted T_g variation by the GRGR theory.

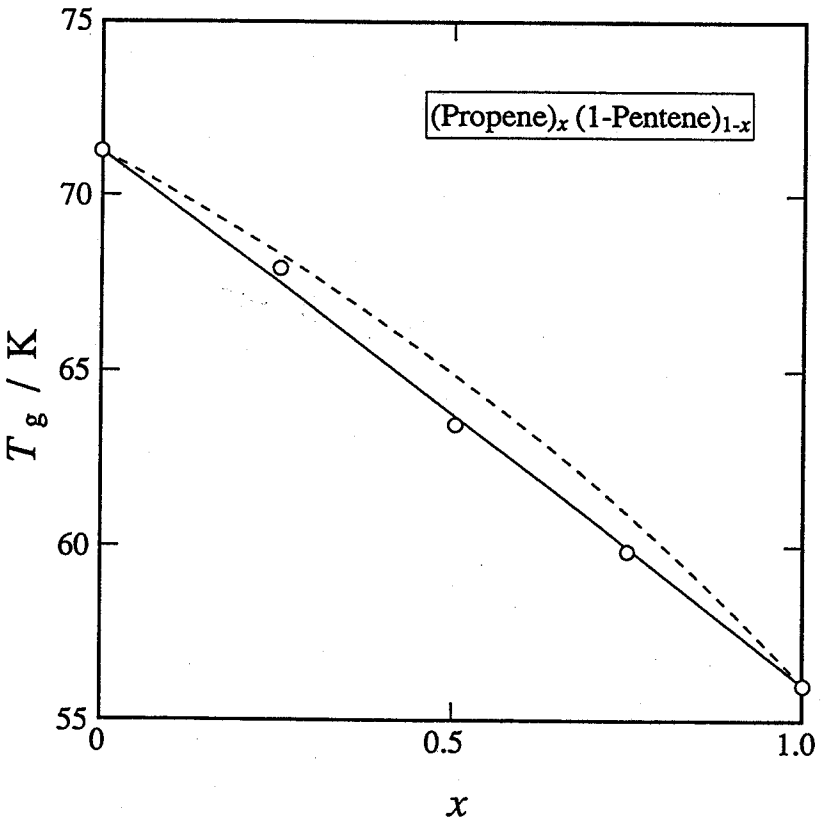

Fig. 4-8. The composition dependence of the glass transition temperature in (propene)$_X$(1-pentene)$_{1-X}$ system. The solid curve denotes the optimized curve fitted to Eq. (4-1), and the broken curve is predicted T_g variation by the GRGR theory.

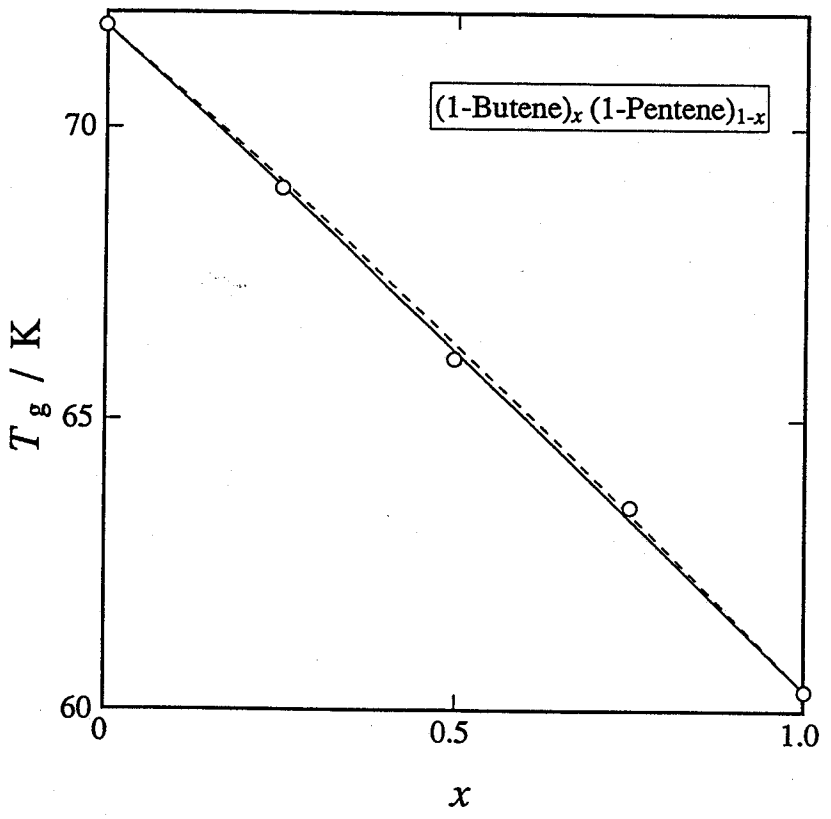

Fig. 4-9. The composition dependence of the glass transition temperature in (1-butene)$_x$(1-pentene)$_{1-x}$ system. The solid curve denotes the optimized curve fitted to Eq. (4-1), and the broken curve is predicted T_g variation by the GRGR theory.

Table 4-1. Determined parameter C of Eq. (4-1).

Systems	C_{exp}	C_{theory}
$(propene)_x(propane)_{1-x}$	1.71	0.976
$(propene)_x(1\text{-butene})_{1-x}$	0.472	1.30
$(propene)_x(1\text{-pentene})_{1-x}$	1.03	1.40
$(1\text{-butene})_x(1\text{-pentene})_{1-x}$	1.04	1.08

C_{exp}: obtained by fitting T_g; C_{theory}: obtained by fitting T_K.

mined coefficients of the polynomials are tabulated in Table 4-2 along with the literature sources of the heat capacity data. The composition dependence of T_K was evaluated for every 10 mole % of composition. The composition dependence of T_g was reproduced by using Eq. (4-1) and the best-fit value of the parameter C obtained for T_K as tabulated in Table 4-1.

The broken curves drawn in Figs. 4-6 to 4-9 are the T_g curves reproduced as described above. For the system of (1-butene)$_x$(1-pentene)$_{1-x}$, the calculated T_g curve gives a good agreement with the experimental data. On the other hand, definite deviations were found for other systems. These deviations indicate probably the invalidity of GRGR model for the present systems. A possible extension of the GRGR theory will be discussed in the following section.

4-4-3 Estimation of Excess Configurational Entropy

In the GRGR theory, both the liquid and solid solutions are assumed to be regular solutions. This assumption makes it easy to estimate the configurational thermodynamic quantities. The disagreement between the theoretical and experimental results can be explained phenomenologically by allowing the existence of excess configurational entropy.

In a real solution, $\Delta_{mix}S^E$ in Eq. (4-3) is not zero. Therefore, the entropy of binary mixture is

$$S^{LS}(x, T) = x\, S_1{}^{liq}(T) + (1-x)\, S_2{}^{liq}(T) - R\,[\, x \ln x + (1-x) \ln (1-x)\,] + \Delta_{mix}S^{E,LS}, \qquad (4\text{-}9)$$

Table 4-2. Coefficients of power series used on the evaluation of T_K.

The heat capacity was expressed in the form

$$C_p/\mathrm{J\ K^{-1}\ mol^{-1}} = \sum_{i=0}^{N} A(i)\ T_S{}^i$$

along with $T_S = [(T/\mathrm{K}) - T_{av}]/F$.

	Propane[1]		Propene[2]		1-Butene[3]		1-Pentene[4]	
	Crystal	Liquid	Crystal	Liquid	Cryatal	Liquid	Crystal	Liquid
T_{av}	49.145	159.835	47.09	155.625	0	0	57.6693	110.556
F	39.8389	77.9611	36.5667	75.3056	1	1	35.17	42.8209
$A(0)$	32.0852	88.902	34.0905	86.9944	-16.9669	149.57	47.5104	129.286
$A(1)$	28.1879	7.44781	24.3353	-0.437641	1.38017	-0.754388	26.3881	-3.15769
$A(2)$	-10.7918	3.08457	-9.58306	6.53027	-6.2018×10^{-3}	3.35523×10^{-3}	-6.8633	3.3751
$A(3)$	6.66491		10.1325				1.27984	-0.655784
$A(4)$	6.24419		4.15262					
$A(5)$	-8.1775		-8.30198					

Heat capacity data were after 1) Ref. [5], 2) Ref. [6], 3) Chap. 6, and 4) Chap. 5.

for the liquid solution, and

$$S^{SS}(x, T) = x\, S_1^{cry}(T) + (1-x)\, S_2^{cry}(T) - R\,[\, x \ln x + (1-x) \ln (1-x)\,] + \Delta_{mix}S^{E,SS}, \qquad (4\text{-}10)$$

for the solid solution. Here, $\Delta_{mix}S^{E,LS}$ and $\Delta_{mix}S^{E,SS}$ are the excess entropies of mixing for the liquid and solid solutions, respectively. Thus the configurational entropy is given by

$$S_c(x, T) = x\, S_{c1}(T) + (1-x)\, S_{c2}(T) + S_c^E, \qquad (4\text{-}11)$$

where $S_c^E = \Delta_{mix}S^{E,LS} - \Delta_{mix}S^{E,SS}$ is the excess configurational entropy. The existence of this term means that the intermolecular correlation of each component is affected more or less by the mixing. This quantity depends on the temperature in general. It is necessary to estimate S_c^E for the determination of T_K by use of Eq. (4-11).

The excess configurational entropy S_c^E is usually obtained from the precise data of heat of mixing and vapor pressure of the mixture in the interested temperature range. In the present case, however, there have been no experimental data probably due to difficulty caused by low temperature problems. Therefore, the inverse operations to obtain T_K and S_c^E were tried from the experimental T_g data. The Kauzmann temperature can be estimated inversely from the composition dependence of T_g by using Eq. (4-1). Assuming that S_c^E is independent of temperature, the quantity can be evaluated as a residual configurational entropy at T_K

obtained by the regular solution model by reversing its sign.

In Fig. 4-10, the estimated excess configurational entropy was shown as a function of the composition. The error of S_c^E value is estimated to be about ± 0.5 J K^{-1} mol^{-1} in the intermediate composition range. This error arises mainly from the inaccuracy inherent in the extrapolation of the liquid heat capacity towards T_K. The S_c^E values of the (1-butene)$_x$(1-pentene)$_{1-x}$ systems were zero within the error of the estimation. However, the S_c^E values beyond the error were found for other two systems. Especially for (propene)$_x$(propane)$_{1-x}$ system, the obtained S_c^E value (2.2 J K^{-1} mol^{-1} at x = 0.5) is almost half of the ideal mixing entropy of R ln2 (= 5.76 J K^{-1} mol^{-1}). The literature value of the excess entropy for the liquid solution of the related system is 0.077 J K^{-1} mol^{-1} at 298.15 K for (n-hexane)$_{0.5}$(n-decane)$_{0.5}$ [8], and 0.032J K^{-1} mol^{-1} at 255.4 K for (ethane)$_{0.5}$(propane)$_{0.5}$ [9]. One idea to explain this unexpectedly large S_c^E in the propene-propane system is to consider the effect of temperature; *i.e.*, in the undercooled liquid at low temperature, the correlation between the molecules is increased and so the configurational entropy S_c of the system will change significantly by the mixing. Actually, the excess entropy of the (ethane)$_{0.5}$(propane)$_{0.5}$ system at 112 K is three times larger than the value at 255.4 K though all of the excess entropy can not be attributed to the configurational part. It is desired to make a direct measurement of the excess entropy at low temperatures. It is also possible to explain the large S_c^E value by the invalidity of the assumptions in the GRGR theory; *e.g.*, the composition dependence of T_g and T_K can be expressed with the

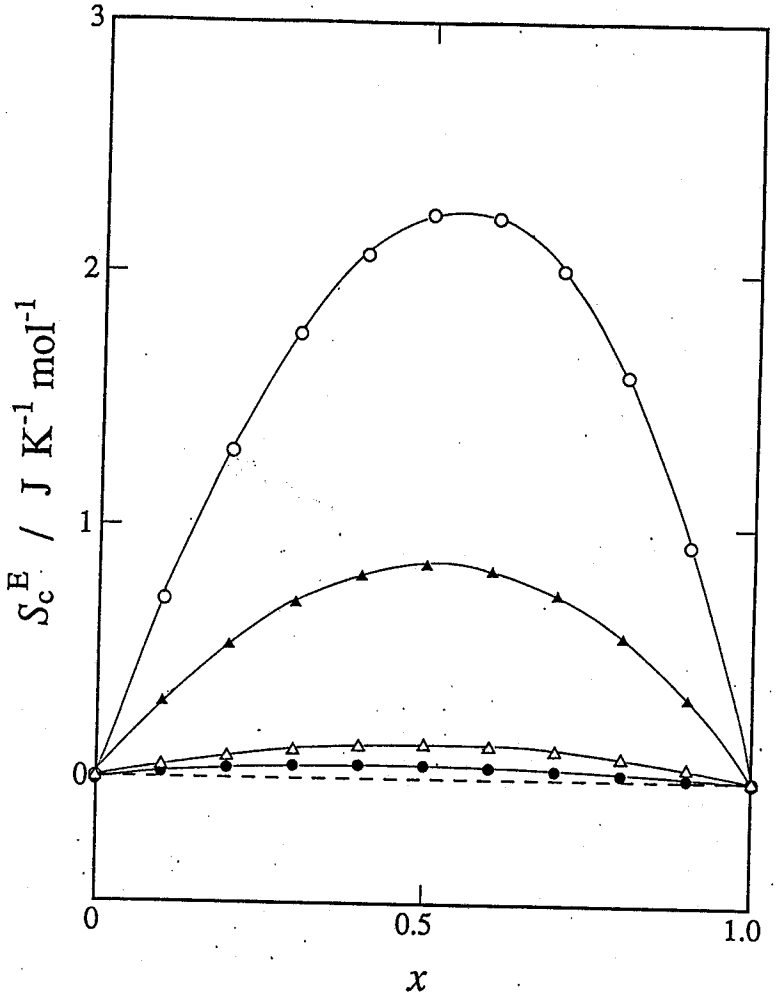

Fig. 4-10. Estimated excess configurational entropy S_c^E.

(propene)$_x$(propane)$_{1-x}$: open circle,

(propene)$_x$(1-butene)$_{1-x}$: solid circle,

(propene)$_x$(1-pentene)$_{1-x}$: solid triangle,

(1-butene)$_x$(1-pentene)$_{1-x}$: open triangle.

identical value of the parameter C in Eq. (4-1). It is also important subject in the future to confirm the validity of the GRGR theory further by both theoretical and experimental approaches.

References to Chapter 4

[1] A. J. Easteal, E. J. Sare, C. T. Moynihan and C. A. Angell, *J. Solution Chem.*, 3, 807 (1974).

[2] A. V. Lesikar, *J. Solution Chem.*, 6, 81 (1977); *J. Chem. Phys.*, 66, 4263 (1977); C. A. Angell, J. M. Sare and E. J. Sare, *J. Phys. Chem.*, 82, 2622 (1978).

[3] A. V. Lesikar, *J. Solution Chem.*, 6, 839 (1977).

[4] J. M. Gordon, G. B. Rouse, J. H. Gibbs and W. M. Risen Jr., *J. Chem. Phys.*, 66, 4971 (1977).

[5] G. Adam, J. H. Gibbs, *J. Chem. Phys.*, 43, 139 (1965).

[6] J. D. Kemp and C. J. Egan, *J. Am. Chem. Soc.*, 60, 1521 (1938).

[7] T. M. Powell and W. F. Giauque, *J. Am. Chem. Soc.*, 61, 2366 (1939).

[8] K. N. Marsh, J. B. Ott and M. J. Costigan, *J. Chem. Thermodyn.*, 12, 343 (1980).

[9] W. R. Adams, P. Gopal, J. A. Zollweg and W. B. Streett, *J. Chem. Thermodyn.*, 19, 39 (1987).

Chapter 5

CALORIMETRIC STUDY OF 1-PENTENE
ENTHALPY RELAXATION IN VAPOR-DEPOSITED AND LIQUID-QUENCHED SAMPLES

5-1 Introduction

It has been confirmed in many cases that an amorphous solid exhibits a glass transition phenomenon at an identical temperature irrespective of the method of preparation. For example, the vapor-deposited (VQ) and liquid-quenched (LQ) glasses of 1-pentene have essentially the same glass transition temperature as described in Chapter 3. This coincidence of T_g indicates that the two glassy states are thermodynamically similar to each other just below T_g, because the equilibrium liquid above T_g should be a unique state defined in terms of minimum Gibbs energy in a metastable phase. However, it is also believed that glasses produced by different methods have different structures at temperatures much lower than T_g. This suggests that the non-equilibrium structures of the VQ and LQ glasses are different from each other, and thus their dynamic properties at low temperatures should not be identical. Actually, it has been sometimes observed that the VQ glasses exhibited structural relaxation phenomena accompanied with large exothermic effects at temperatures far below T_g [1,2].

Recently, Oguni *et al.* have made a calorimetric measurement of the VQ glass of butyronitrile and analyzed its enthalpy relaxation process quantitatively [3,4]. They elucidated that the

relaxation process of the VQ glass bears a non-exponential character and the relaxation time exhibits a non-VTF temperature dependence. Application of the Adam-Gibbs (AG) equation clarified the important role of configurational entropy as a parameter in describing the structural relaxation process in the VQ glass of butyronitrile.

In this chapter, the heat capacities and the enthalpy relaxation processes of the VQ and LQ samples of 1-pentene as studied by an adiabatic calorimetry are described. At temperature by a few kelvin lower than T_g, the enthalpy relaxations of the VQ and LQ glasses were compared quantitatively. Characterizations of the relaxation processes in the VQ and LQ glasses were analyzed in terms of the Kohlrausch-Williams-Watts function and the Adam-Gibbs equation. The present experiments were motivated by the following questions: Is the relaxation phenomenon occurring far below T_g a universal feature of the VQ glass independent of materials? Does the LQ glass relax in the same way as the VQ glass in the same temperature region ? Some difference is expected to be observed because the difference in non-equilibrium structure may influence the relaxation process even just below T_g.

5-2 Theoretical Bases for the Analyses of Relaxation Processes

In the present and next chapters, the experimental data were analyzed in the same way. It is appropriate, therefore, to summarize first the theoretical bases and the practical technique of the analyses of the experimental data.

5-2-1 Evaluation of the Configurational Enthalpy

The molecular motion in liquids will be divided into the vibrational and configurational parts. In response to any fluctuation in the external parameters like temperature and pressure, the vibrational mode can regain its equilibrium immediately while the configurational mode regains its equilibrium with a definite time constant (relaxation time) governed by the external parameters. Slow equilibration in the configurational mode causes temperature difference between the two modes and provokes them to exchange energy. The temperature drift observable in the glass transition region is regarded as the variation of the vibrational temperature. Therefore, the enthalpy relaxed in the recovery process can be evaluated from the observed temperature drift rate in the following procedure. The configurational enthalpy relaxation rate dH_c/dt is given by the product of the spontaneous temperature drift rate dT/dt and the vibrational heat capacity C_{vib} of the system including the sample cell. The spontaneous temperature drift is obtained by subtracting the natural drift rate, due to the slight imperfection of the adiabatic control from the total observed drift rate. Thus the configurational enthalpy H_c relaxed in a period of time Δt is

$$\frac{dH_c}{dt}\Delta t = C_{vib}\frac{dT}{dt}\Delta t. \qquad (5\text{-}1)$$

In the case of long-time relaxation processes (2 - 3 days), the enthalpy at any instance can be obtained by summing up the quantity $(dH_c/dt)\cdot\Delta t$ from the origin of H_c. The values dH_c/dt and

C_{vib} change with time during the relaxation so that Δt is usually taken to be 1 - 10 min. The origin of H_c has been conventionally defined to be the point at which the sample reached the equilibrium value of enthalpy. This point corresponds to the temperature where the spontaneous temperature drift disappears.

5-2-2 Kohlrausch-Williams-Watts Function

Any relaxation process of a physical quantity can be characterized by a functional form of the time evolution of the quantity. The relaxation function ϕ for the enthalpy is defined as

$$\phi(t) = \Delta H_c(t) / |\Delta H_c(0)|, \qquad (5\text{-}2)$$

where ΔH_c denotes the departure of configurational enthalpy from the equilibrium value.

Many physico-chemical phenomena have been described by a linear response relation in which the relaxation rate of a physical quantity is proportional to the departure from its equilibrium value. Using the relaxation function ϕ, this relaxation is described in the following form.

$$\frac{d\phi}{dt} = \frac{\phi}{\tau}, \qquad (5\text{-}3)$$

where τ is a time constant called relaxation time. For a constant τ ($\equiv \tau_D$), the unique solution of Eq. (5-3) is the simple exponential (*Debye type*) relaxation function,

$$\phi(t) = \exp(-t/\tau_D). \qquad (5\text{-}4)$$

However, this relaxation function is usually not applicable to the structural relaxations of undercooled liquids. This is because the structural relaxation takes place in a highly cooperative manner; the constituent molecules are strongly coupled each other in the liquid. It is known that the following Kohlrausch-Williams-Watts (KWW) function (stretched exponential form) is a good empirical expression to reproduce the structural relaxation process in the undercooled liquids [5,6].

$$\phi = \exp\left[-(t/\tau_{KWW})^{\beta}\right], \qquad (5\text{-}5)$$

where τ_{KWW} is a characteristic time constant, roughly corresponding to τ in Eq. (5-4). A new parameter β, ranging between 0 and 1, is introduced here. This parameter β is a measure of the deviation from the simple exponential relaxation, since Eq. (5-5) is identical to Eq. (5-3) when $\beta = 1$. Relaxation functions of the KWW type is drawn in Fig. 5-1 for various values of β. The long-time tail grows up with decreasing value of β. The theoretical basis for the validity of the KWW function has not been established yet, although some authors have tried to derive the KWW function in terms of the statistical mechanics [7,8].

5-2-3 Adam-Gibbs Equation

Gibbs and his co-workers [9,10] developed the concept of configurational entropy in the liquid. Adam and Gibbs [11] then expressed the relaxation time of kinetic property related to the configurational entropy of static one by the following equation

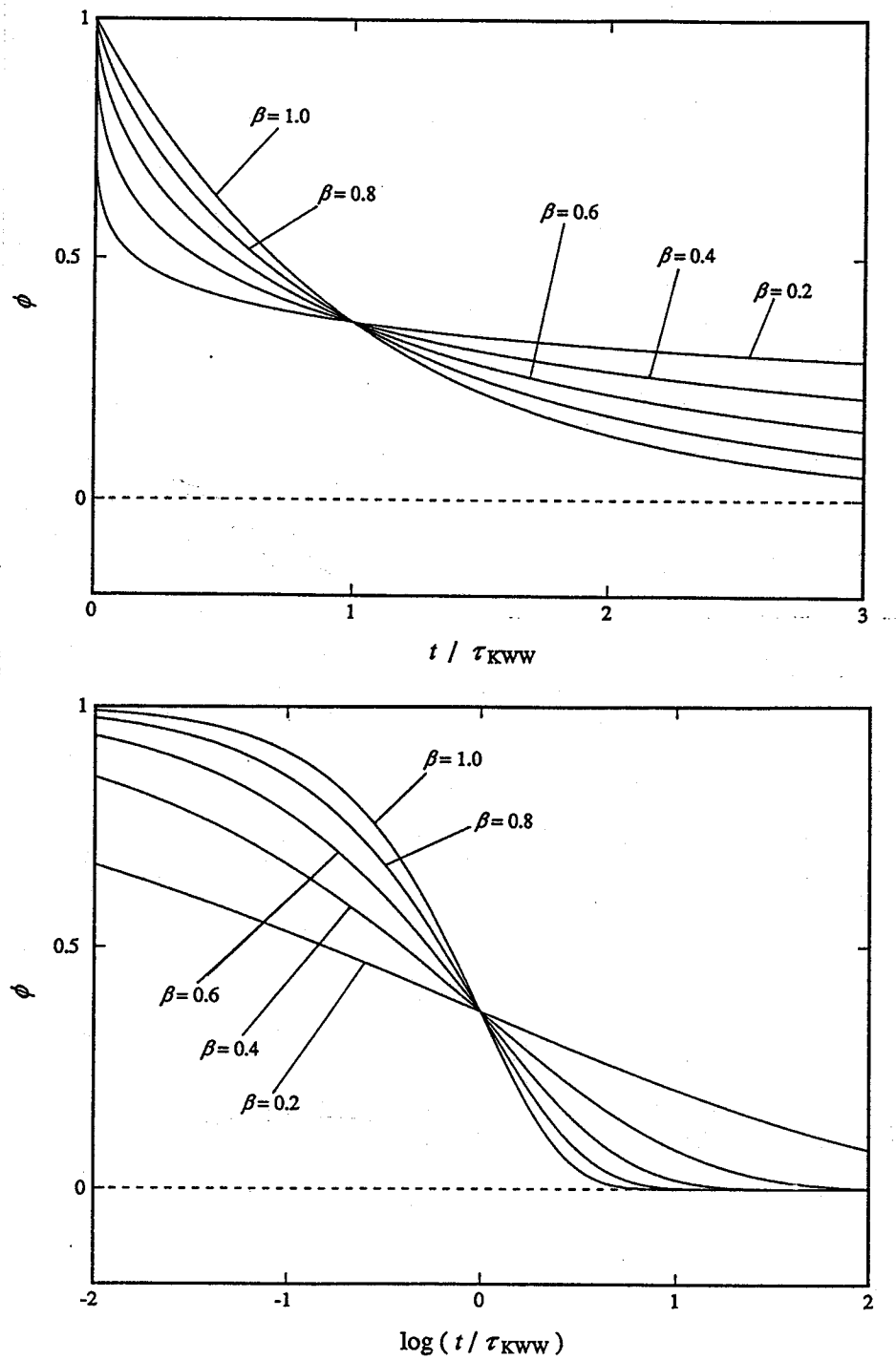

Fig. 5-1. KWW type relaxation functions for various values of β drawn against time (upper) and logarithmic time (lower).

(see Chapter 1).

$$\tau = \tau_0 \exp (\Delta\mu \ s_c^* / k_B \ T \ S_c), \qquad (5\text{-}6)$$

where $\Delta\mu$ denotes the free energy barrier for the activation process of relaxation, s_c^* the configurational entropy of a critical size subsystem that can perform a cooperative molecular rearrangement, k_B the Boltzmann constant and S_c the configurational entropy of the macrosystem. The values $\Delta\mu$ and s_c^* are practically independent of time if the temperature change is small enough during the relaxation. Therefore, a plot of logarithmic relaxation time against reciprocal of the S_c T should give a straight line. We may call hereafter this plot as Adam-Gibbs plot. In the present study, the relaxation time τ is supposed to be evaluated as the effective relaxation time τ_{eff} derived from Eq. (5-3). This quantity is first proposed by Kovacs *et al.* [12].

The configurational entropy S_c can be evaluated from the configurational part of the heat capacity which is given by subtracting the vibrational part from the total heat capacity of the liquid.

$$S_c = \int_{T_K}^{T_f} \frac{C_c}{T} dT, \qquad (5\text{-}7)$$

or equivalently,

$$S_c = S_c(T_{fus}) + \int_{T_{fus}}^{T_f} \frac{C_c}{T} dT. \qquad (5\text{-}8)$$

Here, C_c is the configurational heat capacity. The parameter T_f is the fictive temperature, and T_K the Kauzmann temperature. The former is defined as the temperature at which the equilibrium liquid has the same enthalpy as that of the respective non-equilibrium state [13,14], and the latter is defined as the temperature at which the configurational entropy of the equilibrium liquid disappears [15]. The configurational entropy at the fusion point $S_c(T_{fus})$ is obtained by subtracting the vibrational entropy of the glass at T_{fus} from the third-law entropy of liquid at the fusion point $S(T_{fus})$. This is identical with $\Delta_{fus}H/T_{fus}$ if the vibrational heat capacity of the crystal is the same as that of the glassy state. In the present calculation, Eq. (5-8) was used for the evaluation of the configurational entropy.

5-3 Experimental

5-3-1 Preparation of Samples

In the present study, the heat capacities of VQ and LQ glasses were measured by different calorimeters because the LQ glass requires a large amount of sample to obtain sufficient accuracy of the enthalpy measurement as described in Chapter 2. Hereafter, the samples for the VQ and LQ glasses will be called *VQ sample* and *LQ sample*, respectively.

A commercial sample of 1-pentene, whose purity was claimed to be more than 99.8 mol %, was purchased from Tokyo Kasei Kogyo Inc. For the LQ sample, the sample was purified once by the vacuum distillation technique, and stored in the sample-container which is made of Pyrex glass equipped with a polytetrafluoroethylene (PTFE) cock. The volume capacity of the container is about

150 cm^3. The sample of 0.09715 mol was distilled through a capillary tube into the calorimeter cell with helium gas of about 500 Pa at 78 K and then the transfer tube was pinched off with soldering at the tip. The BS I type cryostat was utilized for the calorimetric measurement as described in Chapter 2.

For the VQ sample, the sample was purified in the same manner as that for the LQ sample. A sample container of 4 cm^3 was connected to the vapor-deposition line of the VD calorimeter. The sample vapor was deposited onto the substrate controlled at a temperature between 38 and 47 K. The amount of the sample deposited within 50 h was 0.01462 mol, which was determined by comparing the values of the heat capacities with those of the LQ sample between 110 and 120 K.

The purities of the samples were determined by the fractional melting method to be 99.2 mol % and 99.1 mol % for the VQ sample and the LQ samples, respectively.

5-3-2 Calorimetric Measurement

Heat capacities of the VQ and LQ samples were measured by means of the adiabatic calorimeters described before in the temperature range of 12 - 120 K for the VQ sample and 12 - 300 K for the LQ sample. The LQ glass was prepared by cooling the supercooled liquid of the LQ sample from 78 K with the rate of 3 K min^{-1}. The crystalline phase was obtained by annealing the LQ sample at several temperatures between the glass transition (T_g = 70 K) and the melting (T_{fus} = 107.8 K) points.

For the VQ glass, exothermic effect due to the enthalpy relaxation was pursued for a long time at 53, 58, 62 and 69 K on

the way of the heat capacity measurement. The enthalpy relaxation of the LQ glass was pursued at 83.5 K in a separate experiment from the heat capacity measurement. The relaxation was observed by heating at 2 K min^{-1} from 20 K to reproduce a condition similar to that of VQ glass.

5-4 Results and Discussion

5-4-1 Heat Capacity

Exothermic effect due to the enthalpy relaxation was observed during the heat capacity measurement for the VQ and LQ samples. The observed enthalpy relaxation rate dH_c/dt was plotted against temperature in Fig. 5-2. For the LQ glass, exothermic followed by endothermic temperature drift was observed as usual. The drift rate gradually increased with increasing temperature and had a maximum just below T_g. On the other hand, for the VQ glass, the exothermic effect started just above the deposition temperature and was accelerated rapidly by warming. Broken lines drawn for the VQ samples represent slowing down of the temperature drift rate at each step of a long-time annealing of the sample. Further heating, however, enhanced the exothermic effect again. This cycle of exothermic effect was repeated up to T_g. This strange exothermic effect is just the same as that observed in butyronitrile [3,4] and is concluded to be a universal property of the vapor-deposited glass.

Since the exothermic rate was nearly constant within a period of temperature measurement, the heat capacity was evaluated by regarding this effect as a sort of heat leakage from surroundings. Therefore, the heat capacities of the VQ and LQ

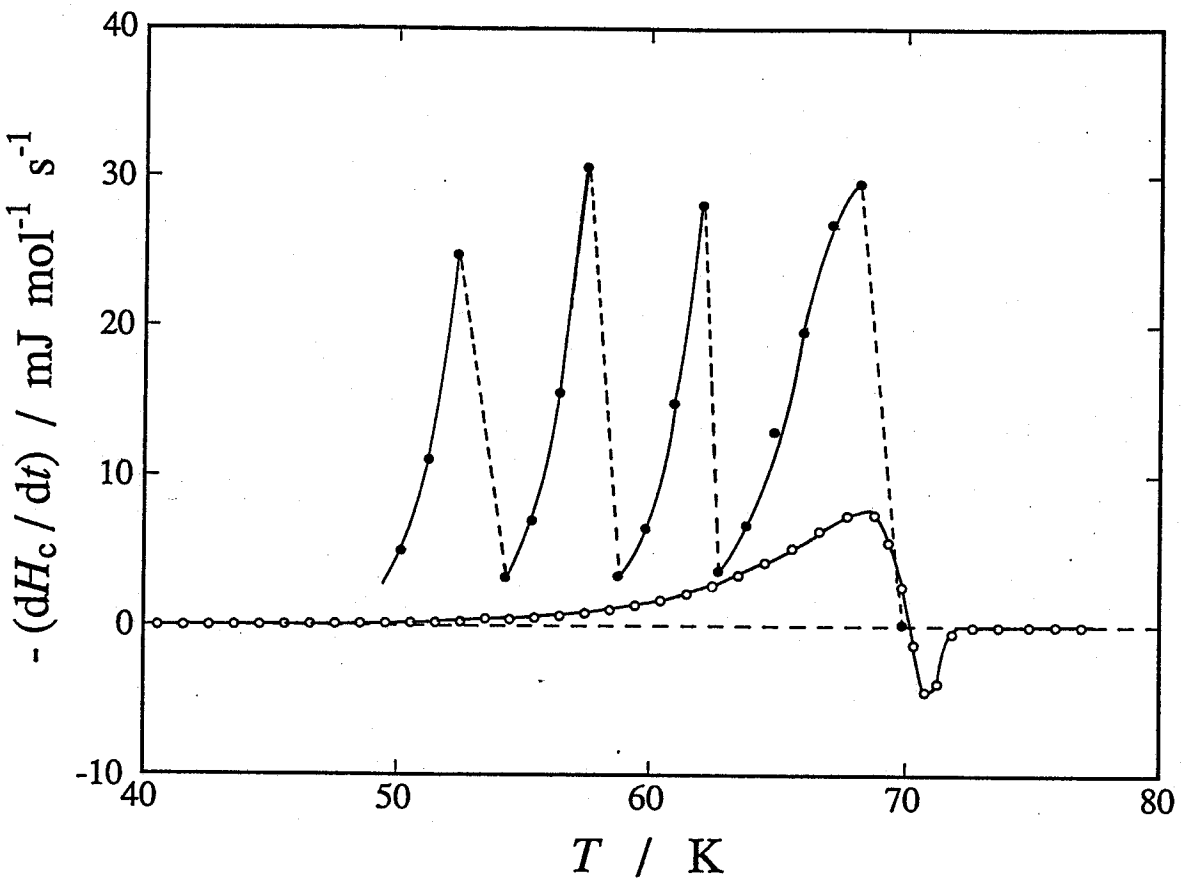

Fig. 5-2. Rate of configurational enthalpy relaxation observed on the way of heat capacity measurement for the VQ (closed circle) and LQ (open circle) samples. Broken lines indicate the slowing down of relaxation rate by a long-time annealing at each particular temperature.

samples below T_g correspond to the instantaneous values due to the vibrational contribution. On the other hand, endothermic effects observed just above T_g are included into the heat capacity, since the sample equilibrated within 30 min or so after each energy supply. Accordingly, the heat capacity obtained in this temperature region is the sum of the vibrational and configurational contributions.

In the high temperature region (T > 250 K), slight heat capacity contribution from the heat of vaporization is not negligible because of high vapor pressure of the sample. By subtracting this effect from the apparent value, the heat capacity under the saturated vapor pressure, C_S, was obtained. The correction for the heat of vaporization amounted nearly 0.3 % of the heat capacity of the sample around 300 K. The molar heat capacities under saturated vapor pressure are plotted in Fig. 5-3 for VQ, LQ and crystalline (CR) samples and tabulated in Table 5-1. For both vitreous samples VQ and LQ, a glass transition was observed at essentially the identical temperature around 70 K. This result is consistent with the observation in DTA study described in Chapter 3.

The crystalline sample fused at 107.8 K. The enthalpy and entropy of fusion were 5.846 kJ mol^{-1} and 54.48 J K^{-1} mol^{-1}, respectively. The enthalpy value was about 0.7 % larger than the literature value 5.807 kJ mol^{-1} [16], and this difference is beyond the experimental error. Since 1-pentene is difficult to crystallize fully, the previous author possibly measured the heat capacity of a mixture of liquid and crystal.

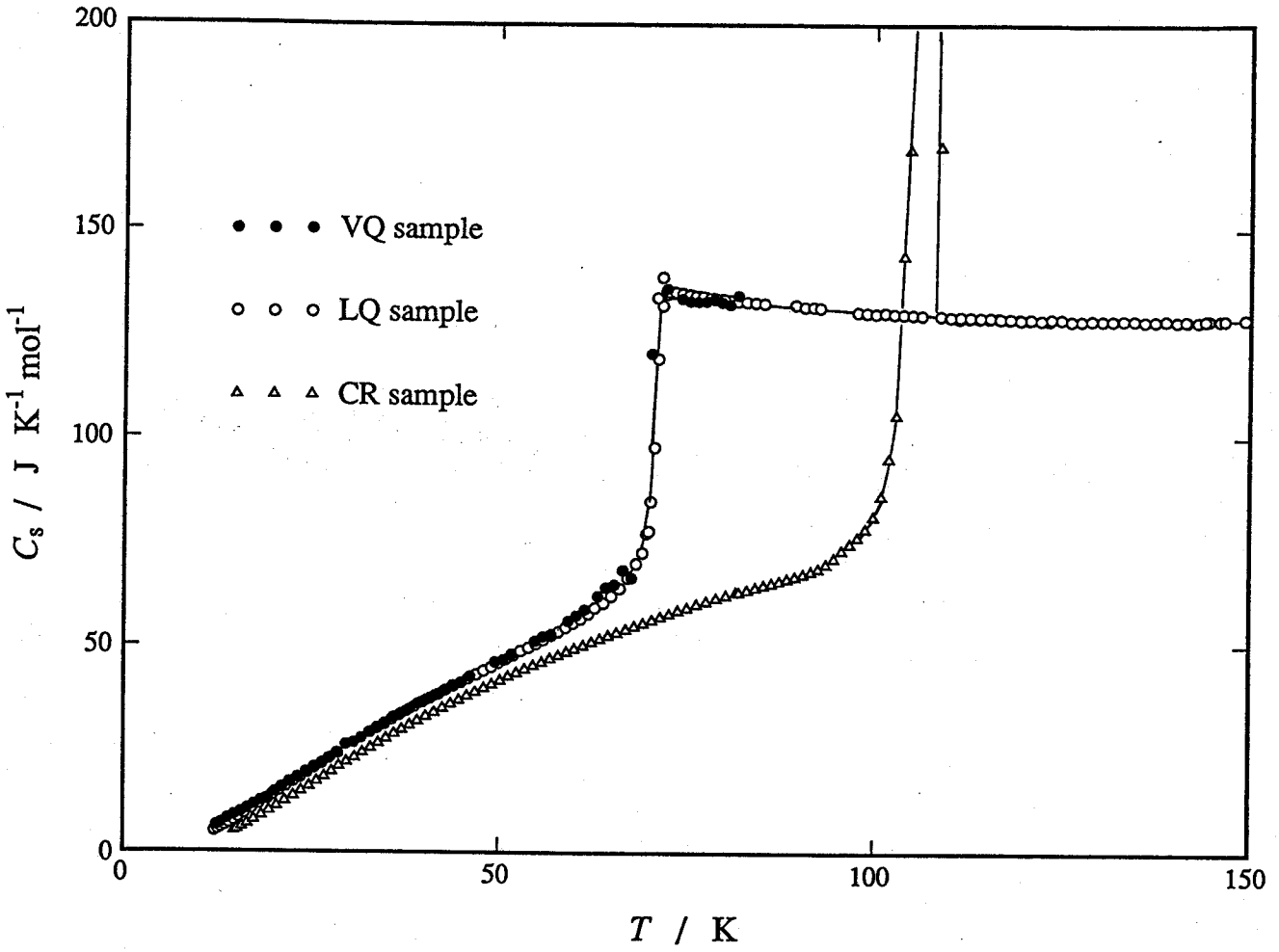

Fig. 5-3. Molar heat capacities of 1-pentene under the saturated vapor pressure.

Table 5-1. Heat capacities of 1-pentene under saturated vapor pressure.

T_{av} / K	C_s / $JK^{-1}mol^{-1}$	T_{av} / K	C_s / $JK^{-1}mol^{-1}$	T_{av} / K	C_s / $JK^{-1}mol^{-1}$	T_{av} / K	C_s / $JK^{-1}mol^{-1}$
CRYSTAL		Series 2		64.63	52.35	107.85	73500
Series 1		15.01	5.306	65.76	53.13	107.87	22260
37.08	29.49	15.46	5.706	66.89	53.85	108.73	170.2
37.84	30.27	16.08	6.291	68.03	54.64	109.99	129.3
38.74	31.16	16.80	7.009	69.17	55.35	110.92	129.2
39.66	32.07	17.69	7.918	70.32	56.12	111.97	129.1
40.57	32.96	18.69	8.967	71.47	56.88	113.02	129.2
41.47	33.80	19.72	10.11	72.62	57.64		
42.42	34.71	20.75	11.28	73.78	58.46	VQ Glass	
43.42	35.65	21.82	12.49	74.98	59.12	12.58	6.679
44.41	36.55	22.89	13.71	76.25	59.94	13.29	7.234
45.44	37.45	23.93	14.89	77.54	60.67	14.15	8.328
46.49	38.40	24.97	16.06	78.84	61.40	15.08	9.178
47.54	39.34	26.02	17.22	80.16	62.13	15.94	9.897
48.58	40.21	27.04	18.38	81.49	62.90	16.81	10.78
49.64	41.11	28.04	19.57			17.73	11.73
50.71	42.04	29.02	20.87	Series 3		18.64	12.64
51.79	42.88	30.03	21.94	81.90	62.84	19.54	12.90
52.87	43.77	31.10	23.04	82.96	63.35	20.48	14.76
53.95	44.64	32.15	24.22	84.03	63.91	21.47	15.90
55.04	45.45	33.20	25.37	85.09	64.46	22.48	17.13
56.13	46.30	34.23	26.49	86.15	64.98	23.52	18.31
57.23	47.14	35.26	27.61	87.21	65.52	24.60	19.58
58.32	47.94	36.30	28.74	88.26	66.05	25.68	20.71
59.43	48.75	37.34	29.76	89.32	66.56	26.76	21.80
60.53	49.50	38.40	30.82	90.37	67.19	27.84	23.00
61.64	50.32	39.45	31.88	91.42	67.90	28.89	24.06
62.75	51.11	40.52	32.91	92.46	68.59	29.93	26.19
63.87	51.84	41.59	33.91	93.52	69.61	30.98	26.68
64.99	52.64	42.66	34.93	94.57	71.02	32.02	27.81
66.11	53.38	43.73	35.95	95.62	72.94	33.05	29.05
67.24	54.10	44.81	36.93	96.68	74.48	34.09	30.25
68.37	54.85	45.89	37.88	97.74	76.08	35.17	31.37
69.51	55.58	46.97	38.85	98.80	78.11	36.21	32.72
70.65	56.39	48.06	39.78	99.85	81.09	37.31	33.72
71.80	57.15	49.15	40.69	100.90	86.04	38.46	34.75
72.95	57.95	50.23	41.63	101.92	95.02	39.57	36.04
74.10	58.70	51.33	42.53	102.90	105.5	40.69	37.04
75.26	59.39	52.42	43.42	103.82	143.8	41.80	38.03
76.42	60.08	53.52	44.31	104.62	169.5	42.92	39.16
77.59	60.74	54.61	45.14	105.68	254.0	44.03	40.46
78.76	61.43	55.71	45.99	106.71	642.8	45.16	41.07
79.94	62.08	56.82	46.85	107.23	1549	46.30	42.63
81.13	62.72	57.92	47.63	107.48	3067	49.58	46.10
82.31	63.45	59.03	48.48	107.62	5218	50.67	46.62
83.51	64.09	60.15	49.29	107.71	7932	51.78	48.08
84.71	64.85	61.26	50.02	107.76	11360	54.84	51.17
85.91	65.58	62.38	50.84	107.81	15780	55.88	52.23
87.12	66.31	63.50	51.58	107.84	24340	56.96	52.85

Table 5-1. Continued.

T_{av} / K	C_s / $JK^{-1}mol^{-1}$
59.30	56.02
60.37	57.37
61.47	58.83
63.22	62.00
64.30	64.16
65.39	64.86
66.49	68.27
67.61	66.47
70.12	120.3
72.11	136.0
74.10	133.6
75.16	133.0
76.22	132.9
77.29	133.0
78.35	133.5
79.43	132.7
80.51	132.2
81.59	134.4
LQ Glass	
Series 1	
12.34	5.284
12.78	5.669
13.25	6.137
13.77	6.682
14.33	7.291
14.95	7.946
15.61	8.650
16.42	9.553
17.40	10.68
18.41	11.85
20.21	13.97
21.07	15.01
21.94	16.07
22.85	17.15
23.80	18.18
24.76	19.36
25.74	20.45
26.72	21.58
27.72	22.83
28.77	24.17
Series 2	
17.35	10.64
17.91	11.27
18.62	12.10
19.39	13.04
20.20	13.98
21.10	15.05
Series 3	
27.90	23.00
28.84	24.24
29.82	25.42
30.78	26.23
31.73	27.42
Series 4	
33.18	29.06
34.12	30.11
35.05	31.11
36.03	32.18
37.05	33.25
38.07	34.30
39.09	35.35
40.10	36.37
41.10	37.39
42.11	38.34
43.11	39.31
44.11	40.27
45.11	41.21
46.10	42.16
47.09	43.09
48.08	44.03
49.07	44.93
50.06	45.85
51.05	46.78
52.03	47.70
53.02	48.85
54.00	49.64
54.99	50.51
55.98	51.47
56.96	52.44
57.95	53.41
58.94	54.45
59.94	55.49
60.94	56.59
61.94	57.77
62.85	59.25
63.98	60.41
65.02	62.04
66.07	63.95
67.14	66.38
68.21	69.88
69.03	72.51
69.58	77.10
70.10	84.73
70.57	97.87
71.02	119.1
71.53	131.9
72.22	134.6
73.13	134.9
74.14	135.0
75.37	134.5
76.39	134.3
Series 5	
72.02	135.4
73.02	135.3
74.04	134.8
75.08	134.7
76.13	134.3
77.19	134.1
78.27	133.9
79.36	133.6
80.46	133.3
81.57	133.0
82.69	132.8
83.83	132.6
84.98	132.5
Series 6	
89.19	132.1
90.39	131.6
91.57	131.6
92.55	131.4
97.61	130.4
98.82	130.2
100.05	130.1
101.28	130.2
102.51	130.0
103.76	129.9
105.00	129.8
106.26	129.7
108.78	129.6
110.06	129.3
111.34	128.9
112.62	129.1
113.91	129.0
115.21	129.0
116.51	129.1
117.82	128.9
119.14	128.9
120.46	128.8
123.13	128.5
Series 7	
69.86	77.65
70.81	133.8
71.49	138.8
72.35	135.3
73.22	135.1
74.10	134.8
75.00	134.4
75.92	134.2
76.84	134.1
77.78	133.7
78.73	133.6
79.70	133.4
Series 8	
110.16	129.3
111.45	129.4
112.75	129.3
114.05	129.1
115.36	129.2
116.68	127.0
118.00	128.9
119.33	128.6
120.66	128.8
122.00	128.6
123.35	129.0
124.70	128.8
126.06	128.4
127.43	128.4
128.80	128.6
130.18	128.5
131.56	128.5
132.95	128.5
134.35	128.6
135.76	128.3
137.16	128.4
138.58	128.5
140.00	128.3
141.43	128.4
142.87	128.3
144.31	128.7
145.76	128.6
Series 9	
141.24	128.5
143.83	128.6
146.45	128.6
149.09	128.8
151.76	128.9
154.46	129.1
157.17	129.1

Table 5-1. Continued.

T_{av} / K	C_s / $JK^{-1}mol^{-1}$	T_{av} / K	C_s / $JK^{-1}mol^{-1}$	T_{av} / K	C_s / $JK^{-1}mol^{-1}$	T_{av} / K	C_s / $JK^{-1}mol^{-1}$
159.91	129.4	194.64	132.7	231.46	138.8	269.01	147.4
162.69	129.4	197.68	133.1	234.56	139.5	272.15	148.2
165.46	129.7	200.72	133.5	237.67	140.1	275.29	148.8
168.28	129.9	203.77	134.0	240.79	140.6	278.42	149.7
171.11	130.1	206.82	134.4	243.91	141.4	281.55	150.6
173.97	130.4	209.88	134.8	247.04	142.1	284.68	151.6
176.86	130.6	212.94	135.4	250.17	142.6	287.81	152.3
179.76	131.0	216.01	135.9	253.31	143.4	290.94	153.1
182.69	131.3	219.09	136.4	256.45	144.2	294.07	154.1
185.65	131.6	222.17	137.0	259.59	144.9	297.20	155.0
188.62	132.0	225.26	137.6	262.73	145.6	300.33	155.9
191.62	132.2	228.35	138.1	265.78	146.5	303.45	156.7

5-4-2 Enthalpy Relaxation Phenomenon in VQ and LQ Samples

In Fig. 5-4, the configurational enthalpies evaluated by the method described in Section 5-2-1 are shown as a function of temperature. The total enthalpy of the VQ glass relaxed below T_g is more than 1 kJ mol^{-1} while that of the LQ glass is about 0.15 kJ mol^{-1}. Accordingly, the enthalpy of the VQ sample is much higher than that of the LQ sample at low temperature. This indicates that a highly strained local structure is frozen in the VQ glass.

The LQ sample does not show any significant enthalpy relaxation compared to the VQ sample at low temperature. Therefore, comparison of the relaxation process between the VQ and LQ samples is possible to make only at one temperature just below the glass transition point. Figure 5-5 shows plots of the configurational enthalpies against temperature for the VQ and LQ samples. The solid line represents the equilibrium and extrapolated enthalpy values. It is remarkable that the VQ sample possesses higher enthalpy than the LQ sample even around T_g.

Time dependence of the configurational enthalpy is shown in Fig. 5-6. ΔH_C denotes the enthalpy departure from the equilibrium value. Applications of the KWW function to the ΔH_C vs. t curve of the LQ and VQ samples are also shown as solid curves in this figure. Both values of β (0.84 for VQ and 0.45 for LQ samples) are clearly smaller than unity and they are definitely different from each other. The deviation from unity shows non-exponentiality of the relaxation function, which is one of the universal character of the structural relaxation. The difference of β between the LQ and VQ samples is an important information

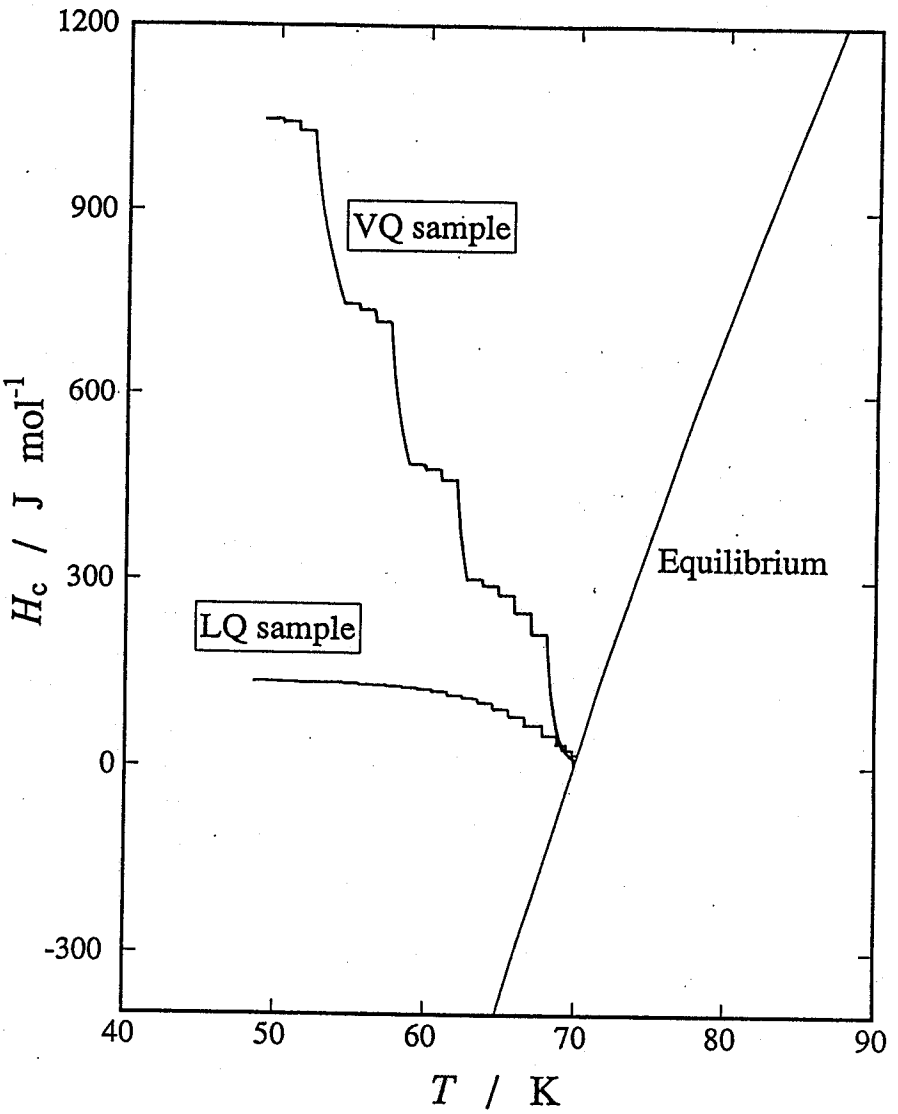

Fig. 5-4. The configurational enthalpy vs temperature diagram for the VQ and LQ samples in the whole temperature range.

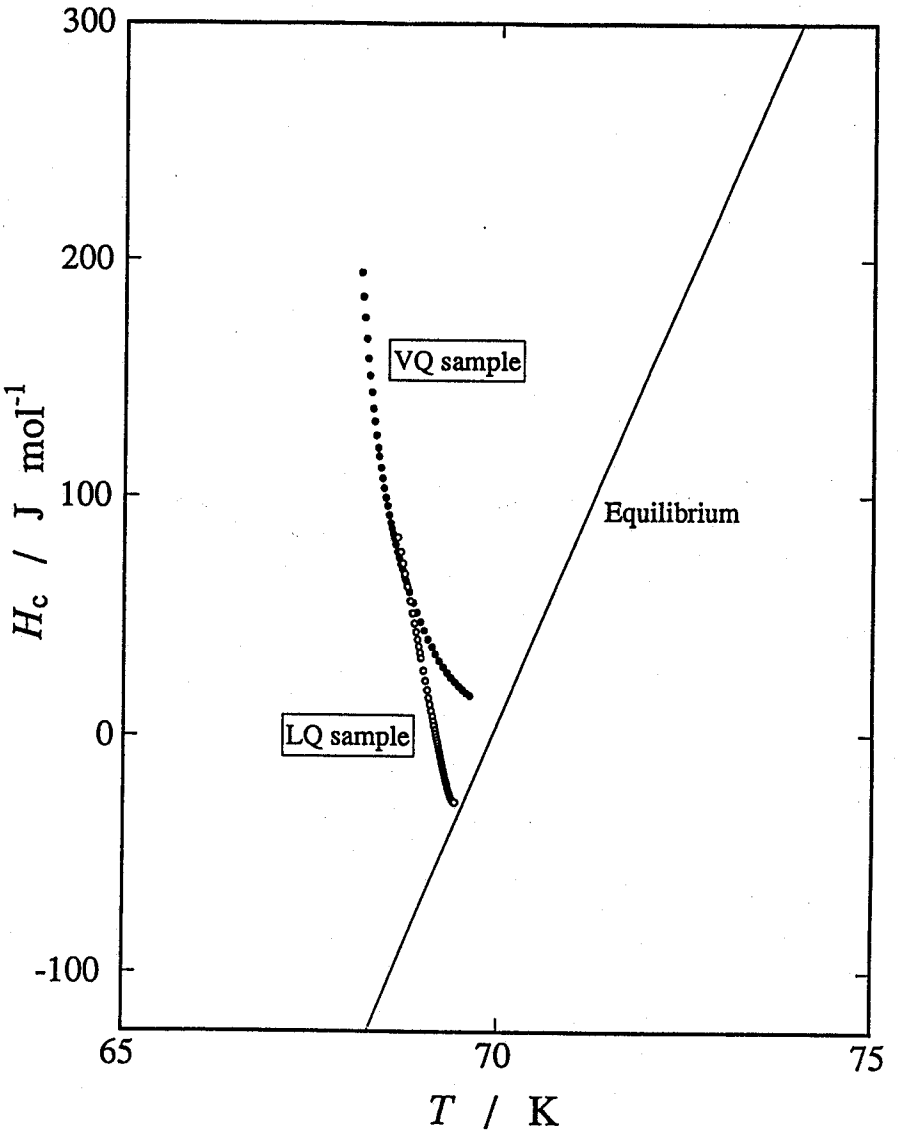

Fig. 5-5. The configurational enthalpy vs temperature diagram for the VQ and LQ samples around 69 K.

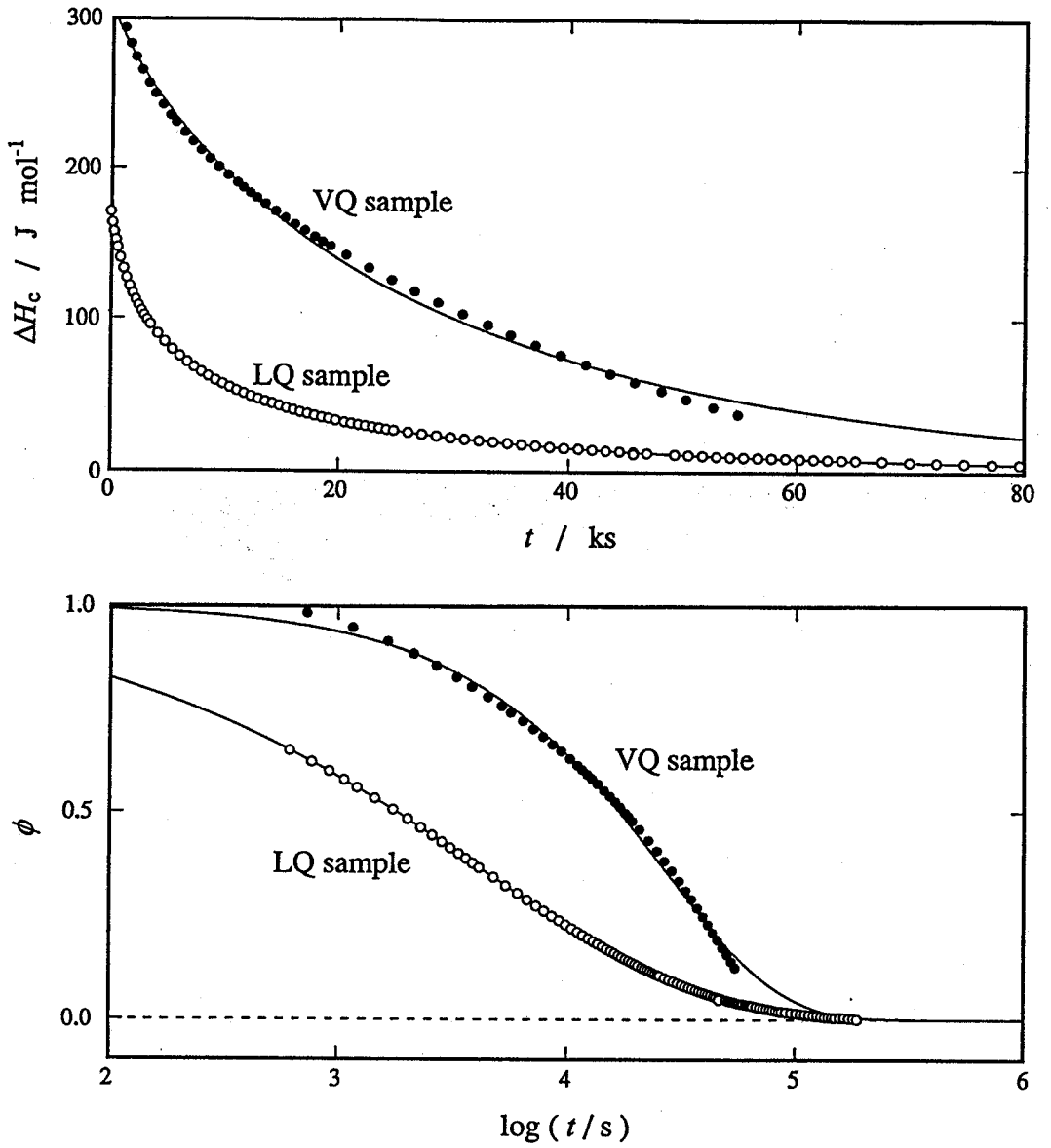

Fig. 5-6. Time dependence of configurational enthalpy of the VQ and LQ samples observed around 69 K. The solid lines indicate the best fit curve of the KWW type relaxation function.

which is revealed for the first time by the present study. This difference would be caused by the difference between the microscopic structures of the two samples. Unfortunately, it is not possible to discuss further, because the KWW function is an empirical function and the physical meaning of β is not clear.

5-4-3 Application of the Adam-Gibbs Theory

AG plots for the VQ sample at various temperatures are shown in Fig. 5-7. Every plot shows good linearity and their slopes slightly tend to decrease with temperature. These results are in good agreement with the case of butyronitrile.

As shown in Eq. 5-6, the slope of the AG plot is proportional to the two parameters s_c^* and $\Delta\mu$, both being related to the microscopic structure of liquid. The quantity s_c^*, the configurational entropy of the smallest cooperative unit, would be rather insensitive to the changes of the size of the cooperative unit and the external parameters (*e.g.* temperature). The order of magnitude of the entropy s_c^* can be estimated by regarding the cooperative rearrangement of the molecules as an overall reorientation of the cooperative unit in which orientation of each molecule is nearly fixed. As the medium order develops, each cluster of the unit grows its size keeping the shape, and the relative molecular configurations inside the cluster are essentially unchanged. It is this constant entropy s_c^* with ever-increasing size of the cooperative unit that brings about a decrease of the configurational entropy of the system. On the other hand, the quantity $\Delta\mu$, the molar activation free energy of the cooperative rearrangement, may be influenced by various

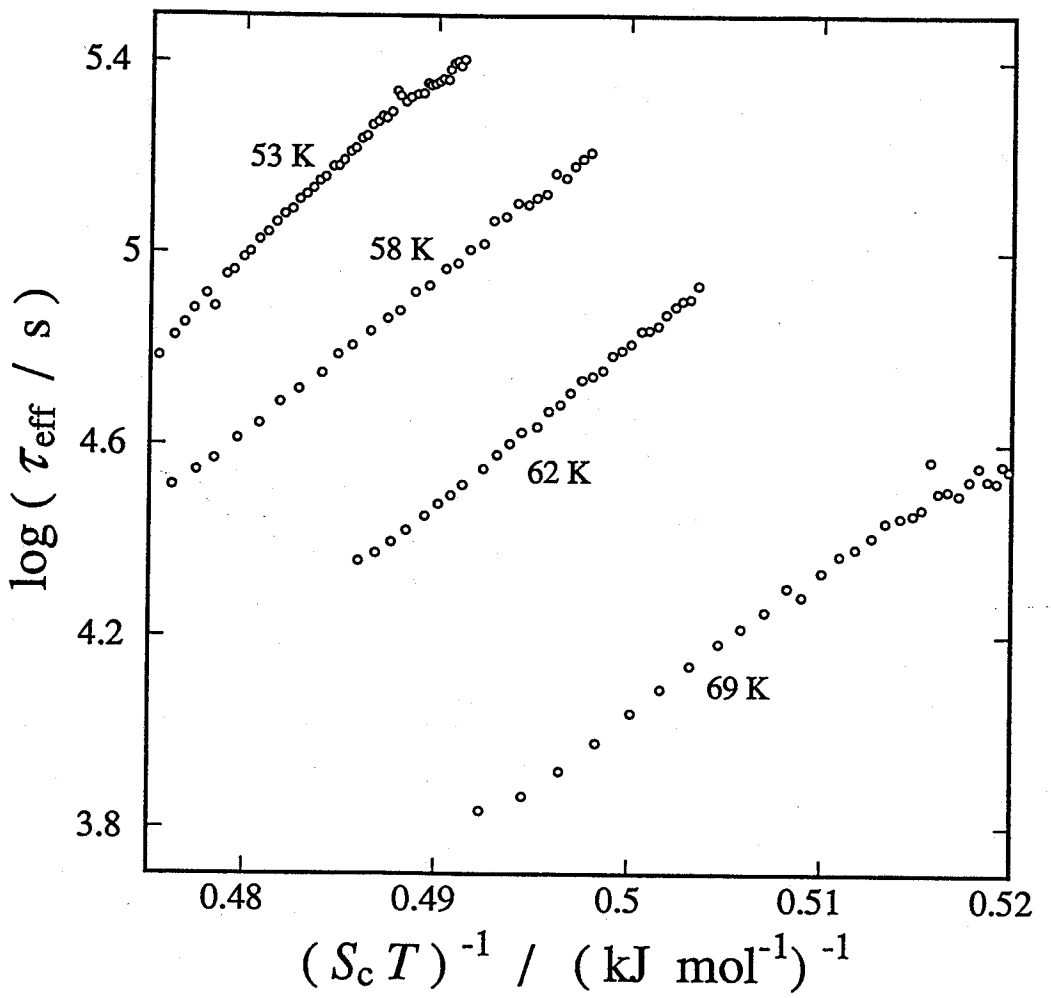

Fig. 5-7. The Adam-Gibbs plot for the enthalpy relaxation of the VQ samples at several temperatures.

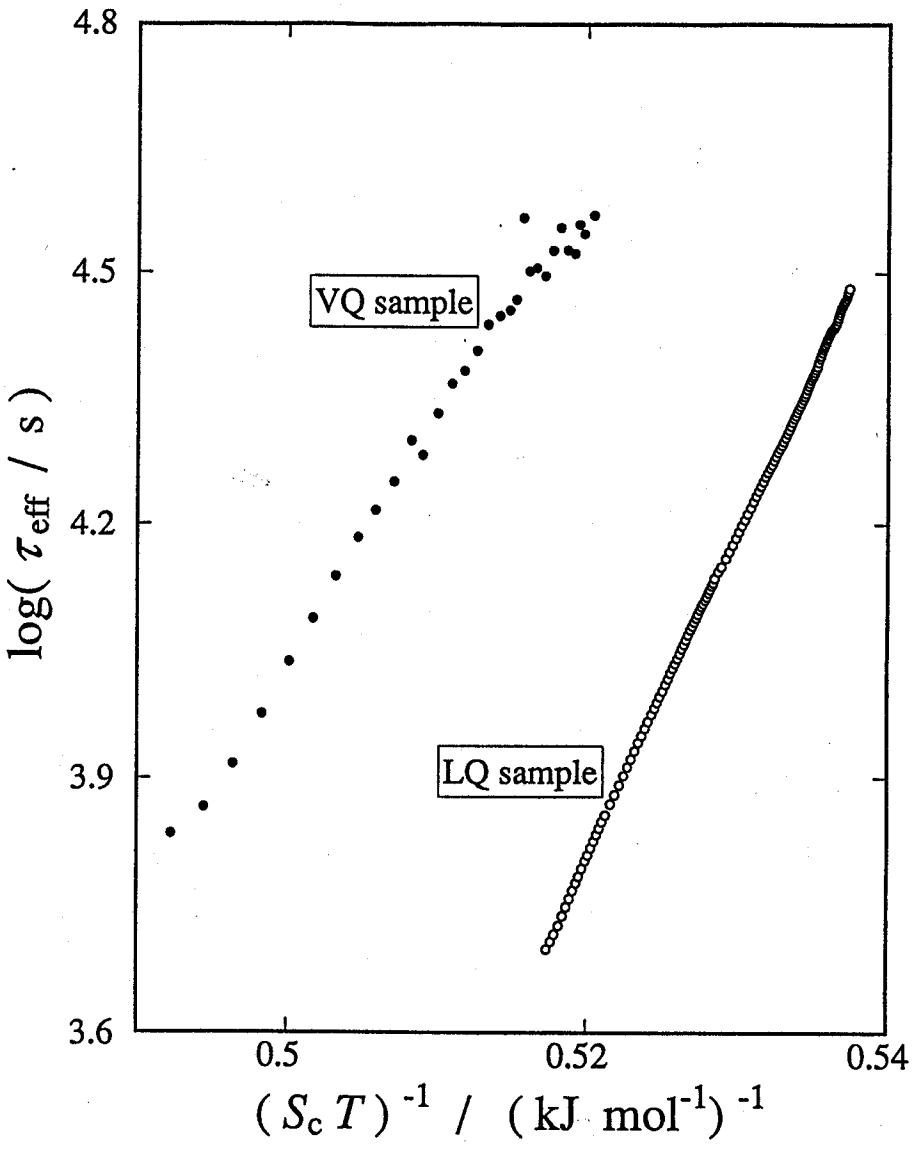

Fig. 5-8. The Adam-Gibbs plot of the enthalpy relaxation processes observed for the VQ and LQ samples around 69 K.

environments in which the molecule is located. It is decomposed into the following form.

$$\Delta\mu = \Delta U + p\Delta V - T\Delta S. \qquad (5\text{-}9)$$

The decrease of the slope with increasing temperature can be explained by the decrease in the third term since ΔS should be positive.

Figure 5-8 gives the comparison of the AG plots between the VQ and LQ glasses observed in almost the same temperature region. Both data can be well reproduced by straight lines, confirming the validity of the application of the AG equation. It was found that the slope of the VQ sample is smaller than that of the LQ sample. According to the above discussion, the effect due to the difference in the external parameters p and T is not significant in this case. As shown in Fig. 5-8, the VQ glass has larger configurational enthalpy and resulting larger local molecular strain and smaller density than the LQ glass. Though the magnitude of a total thermodynamic quantity does not always influence the corresponding activation value, it is not difficult to image that the VQ glass has larger activation enthalpy and then the larger activation free energy $\Delta\mu$ than the LQ sample.

Thus the difference in the structural relaxation between the VQ and LQ glasses was found for the first time and the qualitative discussion on the basis of the AG equation was successful. A more microscopic and qualitative treatments, *e.g.*, using appropriate intermolecular interaction including the knowledge of the molecular shape, would make the next step toward the better

understanding of the structural relaxation.

References to Chapter 5

[1] J. Bigot, *Summer School on Amorphous Metals*, p. 1, Edited by H. Matyja and P. G. Zieliński, World Scientific, Singapore (1986).

[2] M. Harmelin, A. Naudon, J. M. Frigerio and J. Rivory, *Proc. 5th Int. Conf. Rapidly Quenched Metals*, Wuerzburg, 1, 659 (1985).

[3] H. Hikawa, M. Oguni and H. Suga, *J. Non-cryst. Solids*, 101 90 (1988).

[4] M. Oguni, H. Hikawa and H. Suga, *Thermochim. Acta*, 158, 143 (1990).

[5] Kohlrausch, *Ann. Phys. (Leipzig)*, 12, 393 (1847).

[6] G. Williams and D. C. Watts, *Trans. Faraday Soc.*, 66, 80 (1970).

[7] K. L. Ngai, R. W. Rendell, A. K. Rajagopal and S. Teitler, *Dynamic Aspects of Structural Change in Liquids and Glasses*, p. 150, Edited by C. A. Angell and M. Goldstein, N. Y. Acad. Sci., New York (1986).

[8] R. G. Palmer, D. L. Stein, E. Abrahams and P. W. Anderson, *Phys. Rev. Lett.*, 53, 958 (1984).

[9] J. H. Gibbs and E. A. Dimarzio, *J. Chem. Phys.*, 28,373 (1958); E. A. Dimarzio and J. H. Gibbs, *J. Chem. Phys.*, 28, 807 (1958).

[10] J. H. Gibbs, *Modern Aspects of the Vitreous States*, Vol. 1 p. 152, Edited by J. D. Mackinzie, Butterworth, London (1960).

[11] G. Adam, J. H. Gibbs, *J. Chem. Phys.*, 43, 139 (1965).

[12] A. J. Kovacs, J. J. Aklonis, J. M. Hutchinson and A. R. Ramos, *J. Polym. Sci. Polym. Phys. Ed.*, 17, 1097 (1979).

[13] S. Brawer, *Relaxation in Viscous Liquids and Glasses*, Am. Ceram. Soc. Inc., Columbus (1985)

[14] A. Q. Tool and C. G. Eichlin, *J. Am. Ceram. Soc.*, 54, 491 (1931).

[15] W. Kauzmann, *Chem. Rev.*, 43, 219 (1948).

[16] S. S. Todd, G. D. Oliver and H. M. Huffman, *J. Am. Chem. Soc.*, 69, 1519 (1947).

Chapter 6

CALORIMETRIC STUDY OF ENTHALPY RELAXATION IN 1-BUTENE
EXOTHERMIC AND ENDOTHERMIC RELAXATION PROCESSES

6-1 Introduction

The significant non-linearity of relaxation process in vapor-deposited sample was mainly caused by the large departure from the equilibrium state relative to liquid-quenched sample as described in the previous chapter. Even in the liquid-quenched sample, however, the non-linearity is an essential property of the relaxation of the glass. The strong coupling between molecular motions in the supercooled liquid leads to an essential deviation from the linear response in various dynamic properties. The non-linearity is typically observed as an *asymmetric* relaxation behavior, that is, the rate of the recovery of any physical property toward the equilibrium state is not symmetrical for two initial states with opposite sign and essentially the same departure of the property from the equilibrium. This phenomenon has been observed for the volume recovery experiments of various kinds of glass after the abrupt temperature change around the glass transition temperature [1-4]. Quantitative analysis of them has also been made by Kovacs *et al* [5], although their theory included some physically ambiguous parameters as pointed out by Rendell *et al* [6]. Any other experiment on the asymmetric relaxation of the glass has not been done as far as we are concerned.

On the other hand, the entropy theory potentially predicts the asymmetric relaxation behavior, because the exothermic process is an *entropy-decreasing* process in contrast to the endothermic process as an *entropy-increasing* one. According to the Adam-Gibbs theory [7], opposite departure of the initial state corresponding to different configurational entropy would make some effects on the time dependence of the relaxation time.

In the present chapter, the characterization of the asymmetric nature of enthalpy relaxation processes was studied by means of adiabatic calorimetry. The enthalpy is an important thermodynamic quantity as well as the volume. Nevertheless, asymmetric nature has not been examined for the enthalpy relaxation so far. The adiabatic calorimetry is the most precise experimental technique to detect directly the quasi-isothermal enthalpy relaxation process. Moreover, this would be the only technique to elucidate the entropic aspect of the asymmetry that has rarely been investigated. The examination of the entropy theory will be discussed in this chapter.

The sample used here is 1-butene whose thermodynamic study has already been carried out by Aston *et al* [8]. They reported that 1-butene is such a good glass-former that it hardly crystallizes just above T_g. Therefore, we can detect the endothermic relaxation at relatively high temperature without disturbance by crystallization for a long time.

6-2 Experimental

A commercial sample of 1-butene, which was claimed to be more than 99 mol %, was purchased from Tokyo Kasei Kogyo Co. Ltd.

and purified by a vacuum distillation. The purity of the sample was determined to be 99.73 mol % by the fractional melting method as described later. Since 1-butene has rather high vapor pressure, the calorimeter cell for high pressure experiment was used as described in Chapter 2. The purified sample of 50.816 g (≙ 0.10069 mol) was introduced into the cell by vacuum distillation with helium gas of 2×10^{-4} mol to facilitate thermal contact between the cell and the sample. The BS II calorimeter was used for the measurements of the heat capacity and the enthalpy relaxation.

6-3 Results and Discussion

6-3-1 Heat Capacity and Standard Thermodynamic Functions

Prior to the comparison of relaxation processes, brief description of presence of the stable crystalline phase which was discovered in the course of the heat capacity measurement is given here. Realization of the stable phase is important because the absolute entropy of crystal is required to derive the absolute configurational entropy of the liquid.

Two crystalline samples were prepared by different means of annealing. The first sample (CR1) was crystallized by annealing the undercooled liquid between 65 and 85 K for 3 days, with repeated heating-and-cooling cycles. The second (CR2) was obtained by further annealing the CR1 sample for 9 days between 85 and 87.5 K and cooling very slowly (0.2 - 10 mK min^{-1}) down to 80 K. The heat capacity measurements of both samples were performed after confirming that no exothermic effect due to the crystallization was observed.

Figure 6-1 shows the heat capacities of the CR1 and CR2 samples around the melting point. In the CR1 sample, a small endothermic peak appeared about 2 K below the main peak of the fusion. An exothermic effect was observed just above the first peak, overlapping the steeply rising peak due to the main fusion. These complicated phenomena can be interpreted by considering the Gibbs energy diagram shown in Fig. 6-2. The arrow shows the path through which the CR1 sample went. The metastable phase M melts at its fusion point T_{fus}^{M} (the first peak), and then crystallizes into the stable phase S with the exothermic effect. Finally, the stable phase melts at T_{fus}^{S} (the main peak). Taking the enthalpies of the two peaks into consideration, the sample CR1 should be a mixture of a minor part of the metastable crystal and a major part of the stable crystal.

On the other hand, the CR2 sample exhibited only a large endothermic peak at T_{fus}^{S} (= 87.8 K). This guarantees that the CR2 sample was composed of a single phase without involving any trace of the metastable crystal. The enthalpy of fusion was determined to be 3.959 kJ mol^{-1}. The value reported by Aston *et al.* [8] was 3.847 kJ mol^{-1}, which was about 3 % smaller than the present value. The difference is obviously beyond the accuracies of both data. They did not mention the existence of the metastable phase. Their sample was crystallized by annealing only for 2 days above 72 K, and the purity of their sample (99.5 %) was not different much from ours (99.78 %). These facts suggest that they measured possibly the heat capacity of a mixture of the stable and metastable crystals as in the case of our CR1 sample.

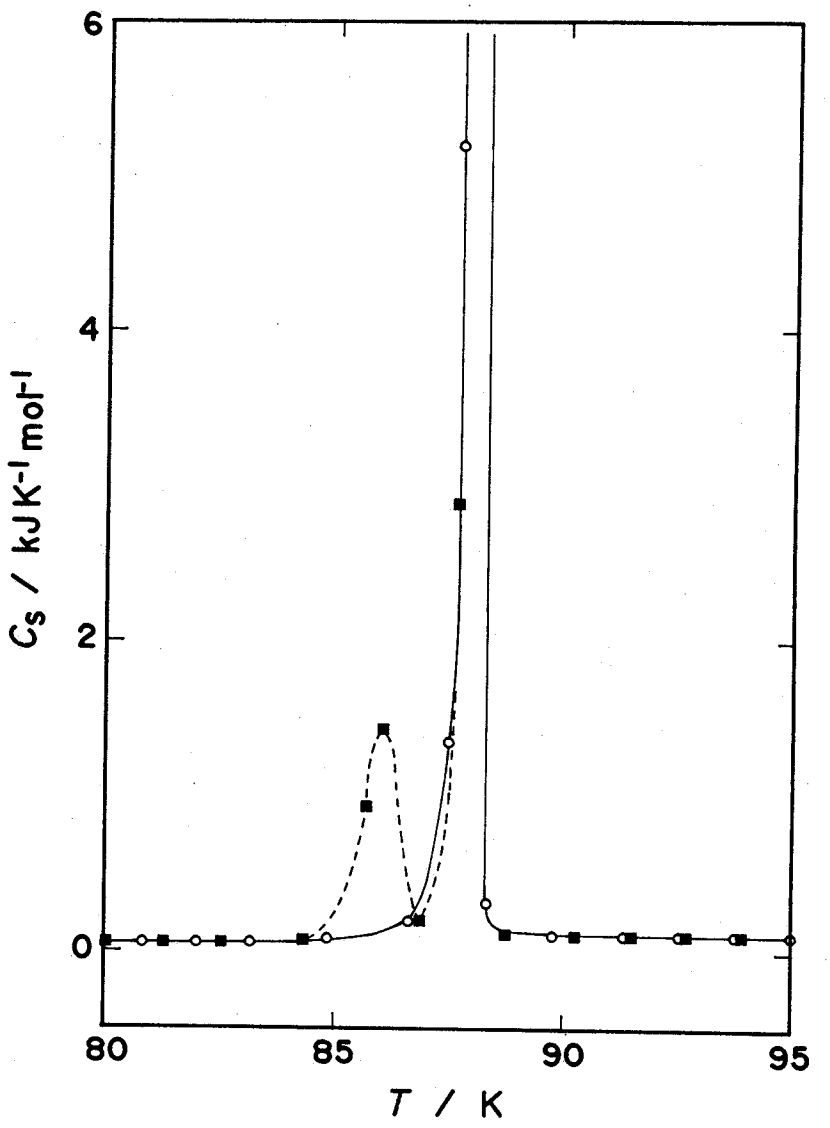

Fig. 6-1. Observed heat capacity data around the fusion point of 1-butene for CR1 (broken curve) and CR2 (solid curve) samples. The heat capacity of CR1 has a subpeak just below the main peak of fusion.

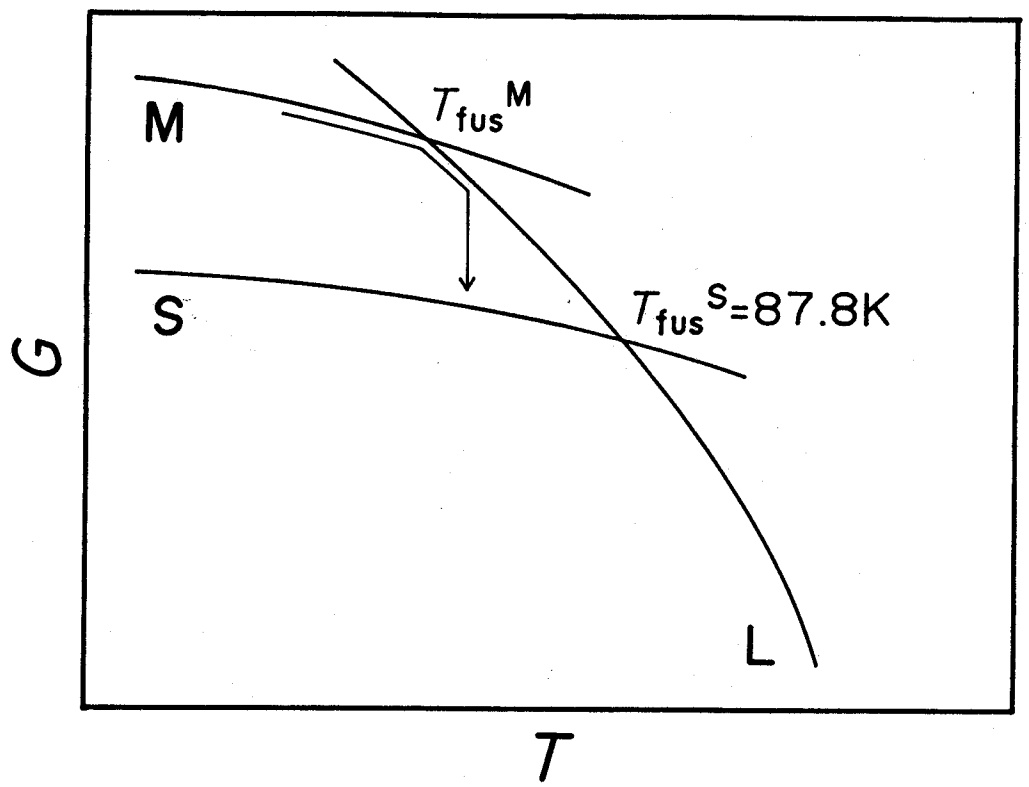

Fig. 6-2. Conceptual drawing of Gibbs energy around the fusion point of 1-butene. Existence of a metastable crystalline phase is proposed to explain the experimental results. The arrow represents a supposed pathway for the metastable phase to undergo on heating.

For the determination of the temperature of fusion and the purity of the sample, a fractional melting experiment was carried out. The equilibrium temperatures $T(f)$ were observed at several fractions f of the sample already fused at the temperature. The equilibrium temperature was determined as the temperature at the time of two hours after each energy supply. These data are summarized in Table 6-1, along with the values of hypothetical temperature of fusion for pure 1-butene and the mole fraction of impurities based on the analysis of the liquid-soluble, solid-insoluble impurity scheme.

Molar heat capacities of the stable crystal (CR2), glass and liquid of 1-butene were tabulated in Table 6-2. For the temperature range above 200 K, the vaporization effect of the sample into the dead space of the calorimetric cell was corrected for by using the vapor pressure data given by Aston *et al* [8]. Heat capacities under the saturated pressure, C_s, were plotted against temperature in Fig. 6-3. Heat capacity jump due to the glass transition was observed at around 60 K, which agreed well with that reported by Aston *et al*. The heat capacity above the glass transition temperature amounts to almost twice of the value of the crystal at the same temperature. Unusually large increase in the heat capacity at the glass transition means that the present material belongs to *fragile liquid* according to the classification proposed by Angell *et al* [9]. Weak van der Waals force acting on the molecules leads to a high configurational degeneracy and a rapid degradation of the short- or medium-range order in the liquid as the temperature is raised. Asymmetrization of molecule due to the double bond at one molecular end will enhance

Table 6-1. Fraction of melt and equilibrium temperature.

f	$T(f)$ / K
0.0682	87.3296
0.1671	87.6296
0.2759	87.7116
0.3866	87.7511
0.4981	87.7730
0.6100	87.7861
0.7222	87.7937
0.8346	87.7981
0.9466	87.8102

Hypothetical melting point of pure sample

T^* = 87.8724 K

Mole fraction of impurity

x = 0.0022

Table 6-2. Molar heat capacity under the saturated vapor-pressure of 1-butene.

T_{av} / K	C_s / J K^{-1} mol^{-1}	T_{av} / K	C_s / J K^{-1} mol^{-1}	T_{av} / K	C_s / J K^{-1} mol^{-1}
Crystal		50.84	37.26	8.29	1.572
6.01	.1608	52.02	38.11	9.04	1.973
6.53	.2256	53.19	38.95	9.81	2.474
7.11	.3069	54.36	39.76	10.55	2.956
7.62	.4056	55.52	40.53	11.28	3.560
8.12	.5156	56.68	41.30	12.02	4.150
9.26	.8338	57.86	42.05	12.81	4.768
9.68	.9770	59.00	42.78	13.23	5.070
11.25	1.648	60.46	43.71	13.88	5.729
11.58	1.807	61.79	44.50	14.46	6.267
11.96	2.012	63.00	45.28	15.12	6.901
12.39	2.251	64.19	45.97	15.83	7.593
12.86	2.530	65.39	46.58	16.64	8.413
13.41	2.874	66.58	47.30	17.53	9.322
14.08	3.318	67.77	47.96	18.41	10.25
14.85	3.870	68.95	48.58	19.29	11.18
15.64	4.467	70.14	49.23	20.16	12.14
16.42	5.080	71.32	49.87	21.03	13.09
17.17	5.713	72.53	50.47	21.89	14.02
17.93	6.370	73.71	51.07	22.74	14.94
18.70	7.076	74.90	51.63	23.58	15.84
19.50	7.822	76.08	52.19	24.58	16.89
20.29	8.591	77.26	52.74	25.61	17.96
21.08	9.365	78.45	53.28	26.62	19.01
21.88	10.18	79.64	53.90	27.62	20.07
22.71	11.03	80.82	54.75	28.60	21.21
23.55	11.89	82.01	56.13	29.57	22.34
24.41	12.76	83.18	59.71	30.60	23.18
25.36	13.72	84.85	85.89	31.70	24.28
26.37	14.76	86.63	198.0	32.78	25.37
27.35	15.77			33.84	26.46
28.33	16.88	T_{fus} = 87.807 K		34.88	27.48
30.32	18.96			35.95	28.52
31.38	20.05	Liquid		37.03	29.53
32.46	21.16	89.77	109.0	38.10	30.58
33.56	22.29	91.33	108.8	39.19	31.57
34.67	23.38	92.54	108.6	40.29	32.57
35.79	24.53	93.76	108.5	41.38	33.56
36.91	25.61	94.99	108.3	42.47	34.56
38.05	26.65	96.22	108.2	43.57	35.59
39.18	27.69	97.46	108.0	44.67	36.60
40.32	28.70	98.70	107.8	45.77	37.48
41.47	29.71	99.95	107.7	46.86	38.57
42.61	30.70			47.96	39.71
43.76	31.63	Glass & Liquid		49.05	40.80
44.91	32.59	5.10	.3195	50.14	42.00
46.08	33.59	5.67	.4609	51.24	43.13
47.27	34.54	6.10	.5837	52.33	44.41
48.46	35.46	6.74	.8058	53.43	45.80
49.65	36.37	7.57	1.194	54.54	47.47

Table 6-2. Continued.

T_{av} / K	C_s / J K^{-1} mol^{-1}	T_{av} / K	C_s / J K^{-1} mol^{-1}	T_{av} / K	C_s / J K^{-1} mol^{-1}
55.65	49.57	97.20	107.8	182.61	108.4
56.77	52.55	98.46	107.7	186.00	108.7
57.88	57.84	99.73	107.7	189.41	109.1
58.79	69.02	101.00	107.6	192.82	109.5
59.48	103.1	102.28	107.5	196.23	109.8
60.17	114.5	103.57	107.3	199.65	110.2
60.87	115.9	104.87	107.3	203.07	110.6
61.73	115.7	106.17	107.2	206.49	111.1
62.75	115.5	107.47	107.1	209.91	111.5
63.78	115.3	108.79	107.0	213.34	111.9
64.83	114.8	110.11	106.9	216.77	112.4
65.88	114.4	111.43	106.9	220.21	113.0
67.00	114.2	112.77	106.8	223.65	113.6
68.21	113.7	114.11	106.7	227.10	114.1
69.43	113.3	115.45	106.6	230.54	114.7
70.65	113.0	116.80	106.5	234.00	115.3
71.86	112.6	118.16	106.4	237.45	115.9
72.44	112.5	120.41	106.4	240.91	116.4
73.65	112.1	123.43	106.3	244.38	117.1
74.87	111.8	126.47	106.3	247.84	117.7
76.08	111.5	129.52	106.2	251.31	118.4
77.29	111.3	132.59	106.2	254.77	119.0
78.51	111.0	135.68	106.1	258.24	119.7
79.73	110.7	138.79	106.2	261.70	120.4
80.95	110.5	141.91	106.2	265.17	121.1
82.17	110.2	145.06	106.3	268.64	121.6
83.72	109.8	148.22	106.3	272.10	122.5
84.91	109.7	151.40	106.4	275.57	123.4
86.11	109.5	154.60	106.6	279.04	124.2
87.32	109.3	157.83	106.7	282.50	124.9
88.53	109.2	161.07	106.9	285.97	125.8
89.75	109.0	162.69	106.9	289.43	126.6
90.98	108.8	165.96	107.1	292.89	127.6
92.21	108.7	169.25	107.3	296.36	128.4
93.45	108.5	172.56	107.6	299.83	129.3
94.69	108.2	175.89	107.9		
95.94	108.0	179.24	108.1		

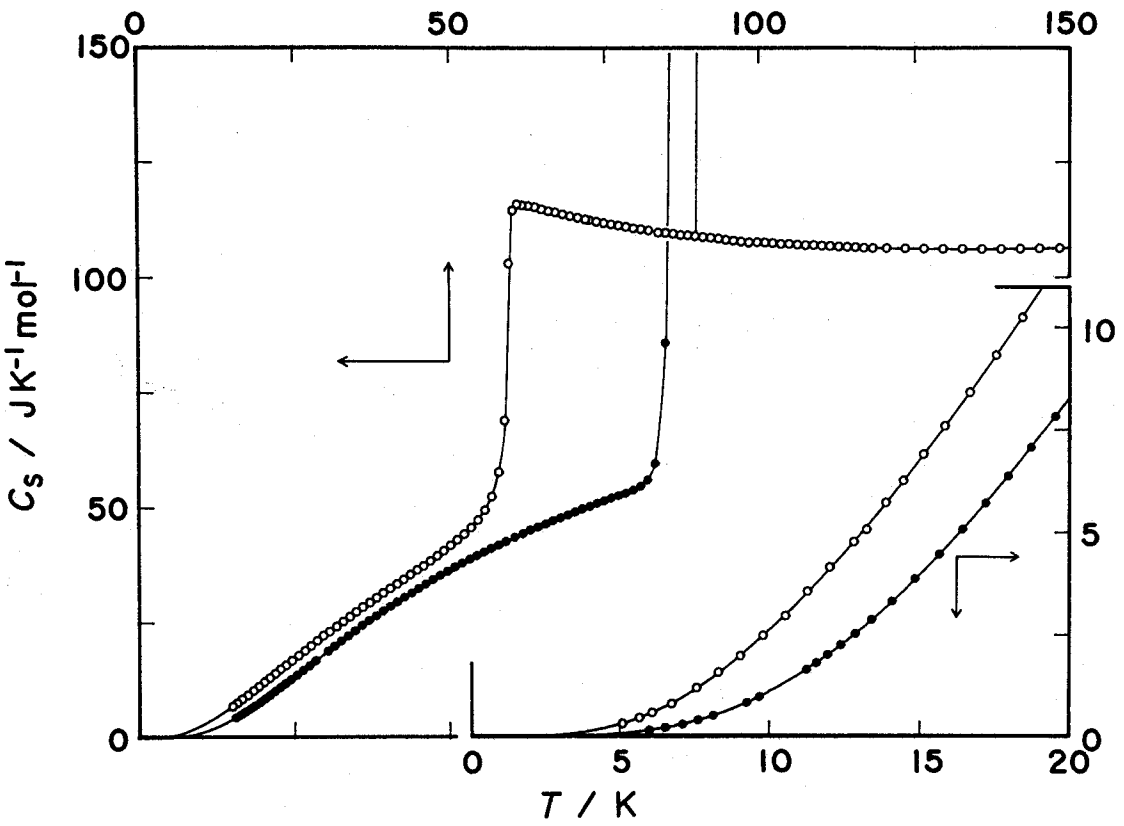

Fig. 6-3. Molar heat capacities of 1-butene. Open circles show those of glassy and liquid samples, and solid ones of crystalline sample. Optimized curves are drawn as solid curves by which the standard thermodynamic functions were evaluated.

the configurational degeneracy of 1-butene compared to n-butane.

Standard thermodynamic functions at rounded temperatures were evaluated from the heat capacity data, and are summarized in Table 6-3. On calculating these quantities, the heat capacities were fitted to some polynomial functions. The extrapolation down to 0 K was performed by using odd-order polynomials from 3 to 11 for crystalline and from 3 to 13 for glassy samples, respectively. The actual functional form of each polynomial is as follows.

$$C_S/\mathrm{J\ K^{-1}mol^{-1}} = 3.58162\times10^{-4}(T/\mathrm{K})^3 + 1.35398\times10^{-5}(T/\mathrm{K})^5 - 8.02854\times10^{-8}(T/\mathrm{K})^7 + 2.09736\times10^{-10}(T/\mathrm{K})^9 - 2.14756\times10^{-13}(T/\mathrm{K})^{11}$$

for the crystal, and

$$C_S/\mathrm{J\ K^{-1}mol^{-1}} = 1.81589\times10^{-3}(T/\mathrm{K})^3 + 3.52671\times10^{-5}(T/\mathrm{K})^5 - 4.69896\times10^{-7}(T/\mathrm{K})^7 + 2.56407\times10^{-9}(T/\mathrm{K})^9 - 6.62360\times10^{-12}(T/\mathrm{K})^{11} + 6.61863\times10^{15}(T/\mathrm{K})^{13}$$

for the glass.

The third-law entropy of 1-butene at 298.15 K in the ideal gas state was evaluated to be 306.8 J K^{-1} mol^{-1}. Table 6-4 shows the actual calculation of the entropy. The spectroscopic entropy was 305.6 J K^{-1} mol^{-1} [10] and 306.2 J K^{-1} mol^{-1} [9]. The difference between the two spectroscopic data arises from ambiguity in the estimation of the barrier height for internal rotation of the methyl group around the C-C axis. Taking the error of the measurement into consideration, it is safely concluded that the

Table 6-3. Standard thermodynamic functions of 1-butene at rounded temperatures.

$\frac{T}{K}$	$\frac{C_p}{R}$	$\frac{H-H(0,cr)}{RT}$	$\frac{S-S(0,cr)}{R}$	$\frac{G-G(0,cr)}{RT}$
Crystal				
0	0	0	0	0
10	0.1320	0.0281	0.0357	-0.0080
20	0.9995	0.2678	0.3532	-0.0854
30	2.237	0.7153	0.9892	-0.2739
40	3.419	1.248	1.800	-0.5518
50	4.404	1.783	2.672	-0.8881
60	5.223	2.291	3.549	-1.259
70	5.914	2.760	4.408	-1.648
75	6.215	2.981	4.826	-1.846
Melting Point 87.81 K		$\Delta_{fus}H_m$ = 3958.6 J mol^{-1}		
		$\Delta_{fus}S_m$ = 45.09 J K^{-1}mol^{-1}		
Glass & Liquid				
10	0.3141	23.37	1.640	21.73
20	1.439	12.10	2.174	9.928
30	2.714	8.762	3.001	5.761
40	3.887	7.400	3.945	3.454
50	5.027	6.808	4.932	1.876
55	5.805	6.678	5.444	1.234
Glass Transition at 60 K				
70	13.61	7.771	8.241	-0.4698
80	13.31	8.481	10.04	-1.556
90	13.10	9.005	11.59	-2.587
100	12.95	9.407	12.96	-3.557
110	12.86	9.726	14.19	-4.468
120	12.80	9.982	15.31	-5.327
130	12.77	10.20	16.33	-6.134
140	12.77	10.38	17.28	-6.894
150	12.80	10.55	18.16	-7.615
160	12.85	10.69	18.99	-8.301
170	12.92	10.82	19.77	-8.952
180	13.01	10.94	20.51	-9.574
190	13.12	11.05	21.22	-10.17
200	13.26	11.15	21.89	-10.74
210	13.42	11.26	22.54	-11.28
220	13.59	11.36	23.17	-11.81
230	13.78	11.46	23.78	-12.32
240	13.99	11.56	24.37	-12.81
250	14.21	11.66	24.94	-13.28
260	14.44	11.77	25.51	-13.74
270	14.69	11.87	26.06	-14.19
280	14.95	11.98	26.59	-14.62
290	15.24	12.08	27.13	-15.04
298.15	15.51	12.17	27.55	-15.38
300	15.57	12.19	27.65	-15.45

Table 6-4. Evaluation of entropy of 1-butene in the ideal gas state.

T / K	S / J K^{-1}mol^{-1}	
	Present Study	J. G. Aston et al.[a]
0 - 20	2.937	2.987
20 - 87.8	45.77	45.89
Fusion at 87.8 K	44.97	43.81
87.8 - 266.91	121.56	121.11
Third-law entropy at the normal boiling point 266.91 K	215.24	213.80
Entropy of vaporization at 266.91 K	82.11 J K^{-1}mol^{-1} [a]	
Gas imperfection correction at 266.91 K	0.59 J K^{-1}mol^{-1} [a]	
Entropy of ideal gas 266.91 - 298.15 K	8.84 J K^{-1}mol^{-1} [b]	
Third-law entropy at 298.15 K	306.78 ± 0.5	305.34 ± 0.88
Spectroscopic entropy at 298.15 K	305.6 J K^{-1}mol^{-1} [c]	
	306.2 J K^{-1}mol^{-1} [a]	

a) Ref. [8]. b) Evaluated from the heat capacity of the ideal gas state given in Ref. [10]. c) Ref. [10].

stable crystal is the completely ordered phase. Based on these facts, the glassy state of 1-butene was found to retain a residual entropy amounting to 12.76 J $K^{-1}mol^{-1}$. The molar entropy of various states of 1-butene is plotted in Fig. 6-4 as a function of temperature.

6-3-2 Enthalpy Relaxation and the KWW Type Relaxation Function

The enthalpy relaxation around the glass transition was measured by two different manners of the temperature jump method. In *RC* series, the equilibrium liquid at 90 K was rapidly cooled (1 K min^{-1}) down to 57 K and the temperature drift rate due to structural relaxation was observed under the adiabatic condition. On the other hand, in *RH* series, the sample was equilibrated by annealing at lower temperature than T_g (between 63 and 55 K for a week and at 54.8 K for 21 hours), and then was rapidly heated up to the same temperature region as that in RC series. The initial equilibration process is necessary in order to erase the previous thermal history (memory effect). The samples in the RC and RH series should have larger and smaller enthalpies than that in the equilibrium state at 58 K, respectively. The experiment aims at clarification of non-linear nature of the enthalpy relaxation rates starting from the positive and negative excess enthalpies towards almost the same equilibrium liquid.

An exothermic temperature drift was observed in the RC series and an endothermic one in the RH series. These are both caused by the configurational enthalpy relaxation towards the equilibrium state. Figure 6-5 shows the reduced enthalpy relaxation function ϕ defined in the previous chapter. As the func-

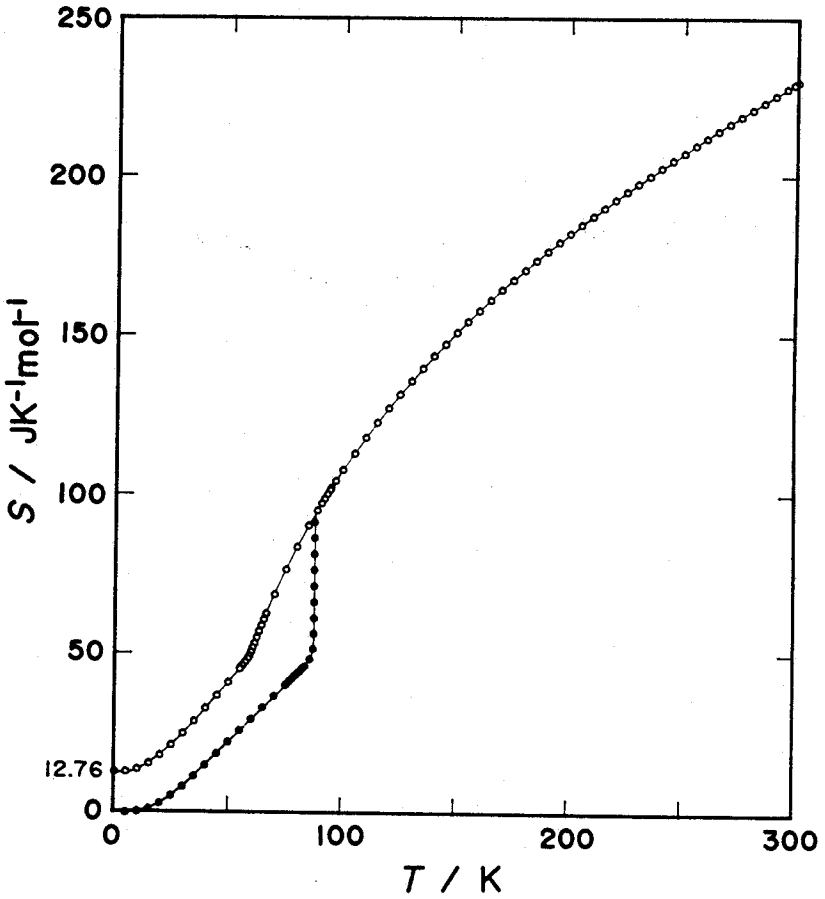

Fig. 6-4. Molar entropy of crystalline (solid circles), and glassy and liquid (open circles) 1-butene.

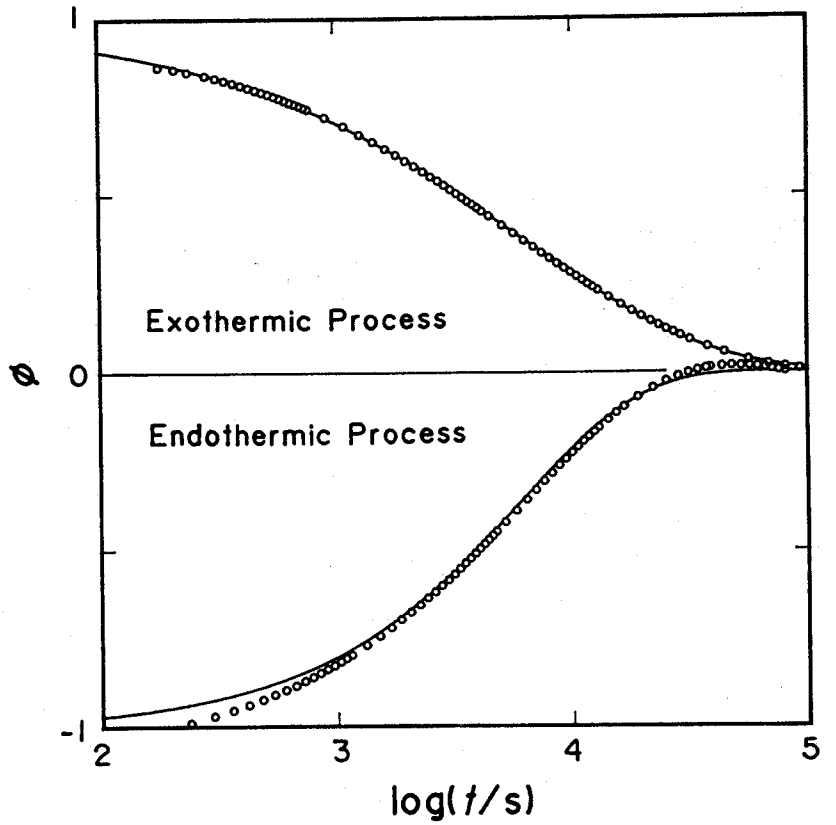

Fig. 6-5. Time dependence of the enthalpy relaxation function for the exothermic (upper) and endothermic (lower) processes of 1-butene.

tion is defined by denominating the absolute value of the enthalpy difference at the origin of time. $\phi(t)$ changes from 1 to 0 for the positive departure and from -1 to 0 for the negative departure experiment as the relaxation proceeds. The quality of the data is based on the high temperature resolution and the high temperature stability of the calorimetric cell under a good adiabatic condition. A correction due to natural heat leakage was done in the analysis of the relaxation rate. It is clearly shown that the relaxation process was quite asymmetric with respect to the sign of the initial departure. This is the first case that the asymmetry was explicitly shown in the enthalpy relaxation process.

Solid curves in Fig. 6-5 show the those optimized to the KWW function. The best fit values of τ_{KWW} and β are tabulated in Table 6-5. The KWW function successfully reproduced the exothermic relaxation consistent with the previous results, but did not for the endothermic process. In addition, the best fit values of β is definitely different from each other. In an ideal experiment of infinitesimal departure, the parameters determined from both sides should be coincident. The parameter will be an intrinsic property of the equilibrium structure. The initial departures of the present sample from the equilibrium state is too large to guarantee the correct application of the KWW function with uniquely determined parameter values. Some phenomenological models describing the asymmetric and non-linear relaxations near the glass transition were proposed by Moynihan *et al.* [12] and Kovacs *et al* [5]. However, their model functions involve parameters whose physical meanings are not clear as noted

Table 6-5. Best fit parameters of the KWW function.

	$\frac{\tau_{KWW}}{ks}$	β
Exothermic process (RC series)	6.52	0.56
Endothermic process (RH series)	5.96	0.84

in Section 6-1. Hence, in the next section, the analysis of the present data in terms of the Adam-Gibbs theory will be described. Their theory implicitly accounts for the asymmetric and non-exponential relaxation through the change in configurational entropy of the system during the enthalpy recovery process.

6-3-3 Analysis in Terms of the Adam-Gibbs Equation

Figures 6-6 and 6-7 show the plots of effective relaxation times τ_{eff} based on the Adam-Gibbs equation. The values τ_{eff} and S_c were calculated by using the equations described in the previous Chapter. Each point should lie on a straight line if the AG equation is valid. A good linearity is shown for the exothermic process, whereas not for the endothermic one. What is more strange is that the slope is negative for the endothermic one, because the slope of the plot corresponding to the product $\Delta\mu s_c^*/k_B$ has to be positive.

The temperature dependence of structural relaxation times for fragile liquids can be usually described by the Vogel-Tammann-Fulcher (VTF) equation [12].

$$\tau = \tau_V \cdot \exp\left[E_0 / (T - T_2) \right] \qquad \cdots (6\text{-}1)$$

where τ_V, E_0 and T_2 are temperature-independent constants which vary from material to material. The equation describes well the non-Arrhenius behavior of the effective relaxation time which is observed frequently in the fragile liquids. It predicts also that the relaxation time becomes infinity at T_2. The AG equation reproduces likely the non-Arrhenius temperature dependence of

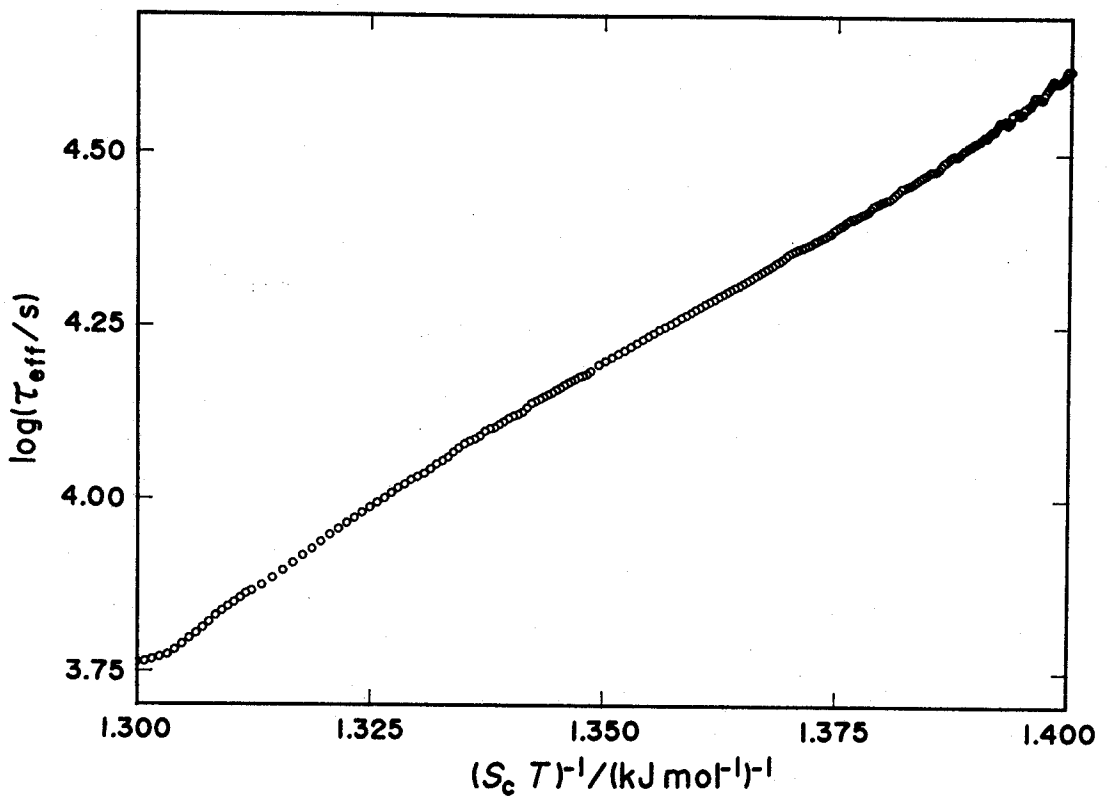

Fig. 6-6. $\log(\tau_{eff})$ vs. $(S_c T)^{-1}$ plot for the exothermic process of 1-butene.

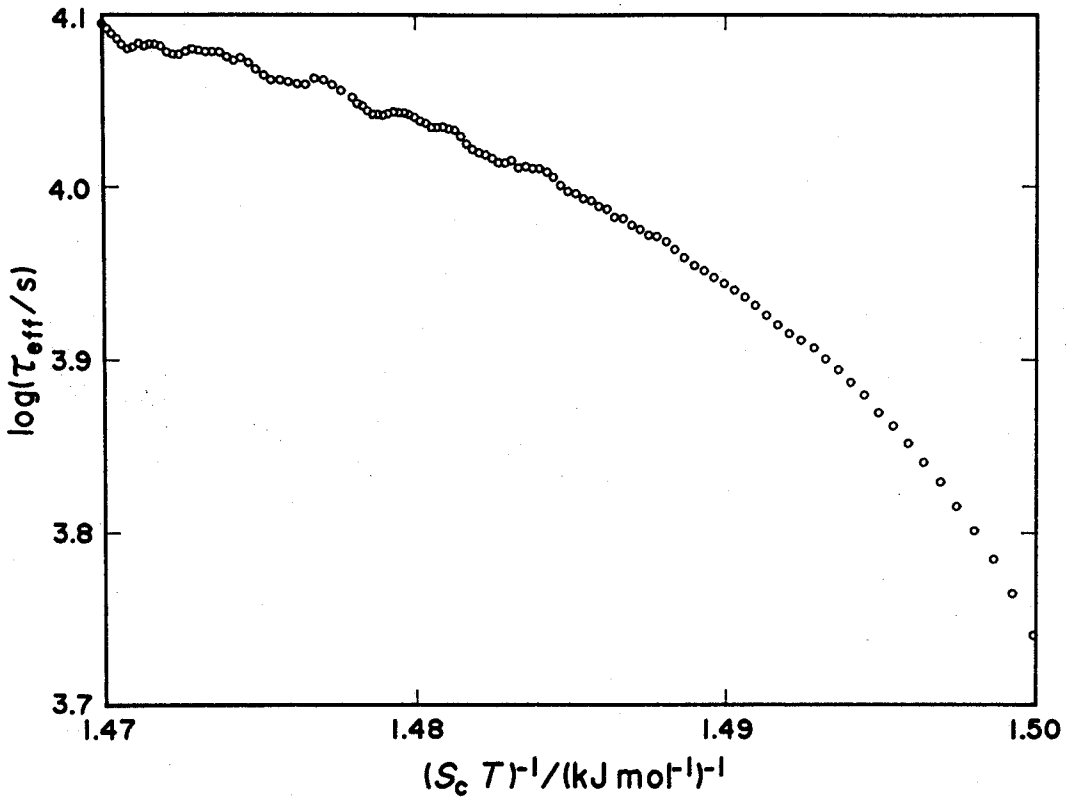

Fig. 6-7. $\log(\tau_{eff})$ vs. $(S_c T)^{-1}$ plot for the endothermic process of 1-butene.

linear response data. The AG equation is successful to describe the ever-decreasing rate of structural relaxation by correlating the relaxation time with the ever-decreasing entropy as the temperature is lowered along the equilibrium line. The theory also takes into account ingeniously the cooperative nature of molecular rearrangement in the glass transition region. It predicts again that the relaxation time becomes infinity at the temperature T_K at which the configurational entropy is zero. It was suggested [7,13] that the VTF and AG equations take the same functional form with $T_K = T_2$, if a hyperbolic expression for the temperature dependence of the configurational heat capacity is assumed. This expression for the excess heat capacity and the coincidence of T_K and T_2 values are consistent with some experimental observations [13,14,15]. The AG equation was also successful in describing quantitatively the volume [16] and enthalpy [17] relaxation data of glasses located far from equilibrium.

In the present experiment, the enthalpy relaxation data for the exothermic direction were faithfully reproduced by the AG equation. For the relaxation of opposite direction, however, the direct application to the experimental data produces a physically unreasonable results with negative value of $\Delta\mu s_c^*$. This situation imposes a limitation of applicability of the AG equation to entropy-decreasing structural relaxation process. Some extensions of the AG theory, such as taking the distribution of relaxation times into consideration, is highly desiderative in order that the theory is made applicable for both positive and negative departure regime.

References to Chapter 6

[1] S. Brawer, *Relaxation in Viscous Liquids and Glasses*, Am. Ceram. Soc. Inc., Columbus (1985)

[2] R. O. Davies and G. O. Jones, *Adv. Phys. (Phil. Mag. Suppl.)*, 2, 370 (1953).

[3] H. N. Ritland, *J. Am. Ceram. Soc.*, 37, 370 (1954); *ibid*, 39, 403 (1956).

[4] J. M. Hutchinson and A. J. Kovacs, *J. Polym. Sci. Polym. Phys. Ed.*, 14, 1575 (1975).

[5] A. J. Kovacs, J. J. Aklonis, J. M. Hutchinson and A. R. Ramos, *J. Polym. Sci. Polym. Phys. Ed.*, 17, 1097 (1979).

[6] R. W. Rendell, K. L. Ngai, G. R. Fong and J. J. AKlonis, *Mocromolecules*, 20, 1070 (1987).

[7] G. Adam and J. H. Gibbs, *J. Chem. Phys.*, 43, 139 (1965)

[8] J. G. Aston, H. L. Fink, A. B. Bestul, E. L. Pace and G. J. Szasz, *J. Am. Chem. Soc.*, 68, 52 (1946).

[9] C. A. Angell, *J. Non-cryst. Solids*, 73, 1 (1985).

[10] F. D. Rossini, K. S. Pitzer, R. L. Arnett, R. M. Braun and G. C. Pimentel, *Selected Values of Physical and Thermodynamic Properties of Hydrocarbons*, Carnegie Press, Pittsburgh (1953).

[11] C. T. Moynihan, P. B. Macedo, C. J. Montrose, P. K. Gupta, M. A. DeBolt, J. F. Dill, B. E. Dom, P. W. Drake, A. J. Easteal, P. B. Elterman, R. P. Moeller, H. Sasabe and A. Wilder, *Ann. N. Y. Acad. Sci.*, 279, 15 (1976).

[12] H. Vogel, *Phys. Z.*, 22, 645 (1921); G. Tammann and G. Husse, *Z. Anorg. Allgem. Chem.*, 156, 245 (1926).

[13] M. Goldstein and R. Simha eds., *The Glass Transition and the*

Nature of the Glassy State (Ann. N. Y. Acad. Sci.), 279, 53 (1976).

[14] C. A. Angell and D. L. Smith, *J. Phys. Chem.*, 86, 3845 (1982).

[15] C. Alba, L. E. Busse, D. L. List and C. A. Angell, *J. Chem. Phys.*, 92, 617 (1990).

[16] G. W. Scherer, *J. Am. Ceram. Soc.*, 67, 504 (1984); 69, 374 (1986).

[17] M. Oguni, H. Hikawa and H. Suga, *Thermochim. Acta*, 158, 143 (1990).

Chapter 7

CONCLUDING REMARKS

In the present thesis, the thermodynamic study of glass transition was carried out from the interest of kinematics in viscous liquids and glasses. The glassy state has two thermodynamic characters; *i.e.*, the metastability against the stable crystal and the non-equilibrium nature against the equilibrium liquid. Both characters vividly appeared in the simple hydrocarbons. The significance of the configurational enthalpy was clarified from the various types of glass transition and enthalpy relaxation phenomena.

The metastability was typically observed as a crystallization as described in Chapter 3. It was the first time that the crystallization was found below T_g for the molecular glasses. It was confirmed that the glass transition phenomenon is the process competing with the crystallization not only in the cooling experiment (vitrification) but also in the heating experiment (devitrification).

In Chapter 4, the composition dependence of the glass transition temperature in binary mixtures of hydrocarbon disclosed that the configurational entropy plays an important role even in the mixture and that the excess configurational entropy of mixing is not negligible. The configurational part of the excess entropy is insignificant at high temperature but should become important in the undercooled liquid where the molecular correlation is

highly developed. The excess configurational entropy will be a valuable parameter in future to understand the molecular motion in the mixture, if its direct measurement becomes possible.

The enthalpy relaxation around the glass transition region was observed by an adiabatic calorimeter employed as a time-domain spectrometer. The experiment on the vapor-deposited 1-pentene (Chapter 5) confirmed that the anomalously excess enthalpy far below the glass transition temperature is a universal phenomenon for the glasses produced at an extremely high cooling rate such as vapor vapor-deposition. The enthalpy relaxation process of the vapor-quenched glass was compared with that of liquid-quenched sample in the same temperature region. Both relaxations could be analyzed by means of the entropy theory (Adam-Gibbs theory). Comparison of the parameters included in the Adam-Gibbs equation showed some difference in the microscopic structures between the two glassy state. The configurational entropy was confirmed again to be an important physical quantity and the related entropy theory was recognized to be hopeful to understand the structural relaxation phenomena of the viscous liquids and glasses. It is noteworthy that the configurational entropy is a measure of the molecular correlation in the wide range from a pair to fairly large size of cluster. The present diffraction techniques in liquids provide information only for a short-range molecular correlation.

The limitation of the entropy theory was also disclosed in this study. The two glassy states of 1-butene with higher and lower enthalpies than the equilibrium value were prepared at the same temperature region (Chapter 6). The application of the

Adam-Gibbs theory was done for both recovery processes to the equilibrium state but resulted in failure in describing the behavior of the entropy increasing (endothermic) process. This result suggests an existence of some parameter governing the relaxation phenomenon other than the configurational entropy. This parameter would be significant near the equilibrium state where the effect of the configurational entropy becomes relatively small. The development of the modified entropy theory including the new parameters is a subject of future study.

As emphasized in Chapter 1, the sample material should be as simple as possible for the purpose of investigation of the basic nature of the structural relaxation. So far, a small number of experimental work has been done for such simple molecular compounds. The present samples, the straight-chain hydrocarbons, are one of the most simple substances for which the glass transition can be observed by the thermodynamic techniques at the present stage. The present results will hopefully provoke new theoretical and computer simulation studies. The next target of the experimental study is the vitreous argon which was recently prepared for the first time. In the present stage of experimental technique, however, many practical difficulties must be overcome in order to employ vitreous argon as a calorimetric sample.

In these days, the main stream of the investigation on the liquid dynamics is carried out by using the spectroscopic technique. However, the present study showed the applicability of rather classical technique, calorimetry. In addition, it is known that the very slow dynamics in the glass transition region

is essentially different from that in the higher temperature region. The classical thermodynamic study is the only method to detect such a slow dynamics. In this sense, the calorimetric study will enhance the role in the study of non-equilibrium state at present and in the future.